JUL 10 1936

UNITED STATES DEPARTMENT OF COMMERCE

Journal of Research

of the

National Bureau of Standards

Vol. 16, No. 6 June 1936

CONTENTS

RP	TITLE AND AUTHOR	Page
889.	Calculation of the concentration and dissociation constant of each acid group in a mixture from the pH titration curve of the mixture. J. O. Burton and S. F. Acree..... [Price 5c]	525
890.	Thermal expansion of copper-beryllium alloys. Peter Hidnert [Price 5c]	529
891.	A rapid method for the determination of silica in portland cement. Edwin E. Maczkowske..... [Price 5c]	549
892.	Note on the thermal mutarotation of *d*-galactose, *l*-arabinose, and *d*-talose. Horace S. Isbell and W. W. Pigman..... [Price 5c]	553
893.	Determination of sulphuric anhydride in portland cement by means of the Wagner turbidimeter. Robert B. Rudy..... [Price 5c]	555
894.	An alternating-current magnetic comparator, and the testing of tool-resisting prison bars. Raymond L. Sanford..... [Price 5c]	563
895.	Dissociation constants of malonic acid in its sodium-salt solutions at 25° C from electrometric titration measurements. J. O. Burton, Walter J. Hamer, and S. F. Acree..... [Price 5c]	575
896.	Tests of eight large H-shaped columns fabricated from carbon-manganese steel. Ambrose H. Stang, Herbert L. Whittemore, and Leroy R. Sweetman..... [Price 5c]	595
897.	Tests of steel chord members for the Bayonne Bridge. Ambrose H. Stang, Herbert L. Whittemore, and Leroy R. Sweetman..... [Price 5c]	627
898.	Third spectrum of xenon. C. J. Humphreys..... [Price 5c]	639
	Index to Volume 16 (January to June 1936) Research Papers 857 to 898.....	649

The articles listed above may be purchased separately (see cover page II) at the prices indicated in the table of contents

A monthly periodical of pure and applied science published by our National Government

Journal of Research

of the

National Bureau of Standards

The January 1936 issue of the Journal of Research of the National Bureau of Standards began the sixteenth semiannual volume of this periodical. Fundamental researches in progress in the Bureau's laboratories are reported in this JOURNAL. If you are interested in new developments in science and technology, you should receive the JOURNAL. If you are not already a subscriber you are invited to send in your subscription.

Technical News Bulletin

This is a monthly publication containing short articles reporting progress of work in the Bureau laboratories, abstracts of papers which appear in the Journal of Research, accounts of scientific and technical meetings in which the Bureau has taken part, a list of all publications by members of the staff, and other items within the Bureau's fields. The BULLETIN is designed primarily to give a general and timely review of the activities of the Bureau in brief form. It is a prompt and reliable source of official information. If you have not already subscribed for the BULLETIN, you are invited to do so.

ANNUAL SUBSCRIPTION	Price	
	United States, Canada, Cuba, Mexico, Newfoundland, Republic of Panama	Other countries
Journal of Research of the National Bureau of Standards:		
12 monthly issues (2 volumes), paper covers	$2.50	$3.25
Bound volume (½ year, 1 volume), blue buckram . . .	3.00	3.50
Technical News Bulletin, 12 monthly issues	.50	.70

Research Papers, reprinted individual articles appearing in the Journal of Research, are available from the Superintendent of Documents shortly after appearance of monthly issue of the JOURNAL.

Address orders only to
Superintendent of Documents, U. S. Government Printing Office,
Washington, D. C.

UNITED STATES DEPARTMENT OF COMMERCE
DANIEL C. ROPER, Secretary
NATIONAL BUREAU OF STANDARDS
LYMAN J. BRIGGS, Director

✦

Journal of Research

of the

National Bureau of Standards

✦

Volume 16, Number 6
June 1936

UNITED STATES
GOVERNMENT PRINTING OFFICE
WASHINGTON : 1936

For sale by the Superintendent of Documents, Washington, D. C. - - - - - Price 25 cents
$2.50 per year on subscription

The prices of the separate Research Papers appearing in this JOURNAL are given on the front cover page. If 100 or more copies of any separate are ordered, a discount of 25 percent is allowed. Those who desire copies of separate Research Papers should send their orders and remittances without delay to the Superintendent of Documents, U. S. Government Printing Office, Washington, D. C. This will aid him to determine the number of copies to be printed for sale. Research Papers are not printed from electrotypes, and usually no more reprints can be had when the first and only printing is exhausted.

U. S. Department of Commerce National Bureau of Standards
RESEARCH PAPER RP889

Part of Journal of Research of the National Bureau of Standards, Volume 16, June 1936

CALCULATION OF THE CONCENTRATION AND DISSOCIATION CONSTANT OF EACH ACID GROUP IN A MIXTURE FROM THE pH TITRATION CURVE OF THE MIXTURE

By J. O. Burton and S. F. Acree

ABSTRACT

Experimental methods and equations are given for calculating the concentration and dissociation constant of each acid or base in a mixture by use of its complex pH titration curve. The principle is illustrated by means of experimental data for malonic acid.

This problem is important as an aid in determining the nature of the acids and bases in plant and animal fibers, fruits, culture media, pulp, paper, and products derived from them.

CONTENTS

	Page
I. Introduction	525
II. Application of equations	526
1. Dissociation constant of first acid	528
2. Concentrations and dissociation constants of the other acids	528
III. References	528

I. INTRODUCTION

The plot of the pH values against the mole fractions of neutralization of a given concentration of any acid or base at a given temperature is called its pH titration curve, a mixture of acids or bases giving a corresponding complex pH titration curve. Both liquids and solids may give such curves.

In earlier articles [1] [1] mathematical equations and graphical methods were described by the use of which a complex pH titration curve for a mixture of acids or bases can be resolved into the individual pH curve for each acid or base. In the same way the individual pH curves can be integrated into the total or complex pH curve for any known mixture of acids or bases within experimental errors.

General equations for calculating the values of the two dissociation constants, K_1 and K_2, from the pH titration curves for dibasic acids were then developed [2], and when applied to malonic acid gave

$$K_1=2.06\times10^{-3} \text{ and } K_2=2.94\times10^{-6}.$$

The purpose of this article is to present an extension of the use of these equations for the calculation of the concentration and the dissociation constant of each acid or base in a mixture, and to illustrate the principle with data for malonic acid. This problem is important

[1] The numbers in brackets refer to the literature references given on p. 528.

in determining the nature of the acids and bases in plant and animal fibers, fruits, culture media, pulp, paper, and products derived from them.

Whether the solution contains only one mono- or n-basic acid, H_nAn, or n different monobasic acids, or a mixture of mono- and polybasic acids, we may call the total equivalent concentration of acid $[H_nAn]$ and let a represent the fraction of $[H_nAn]$ which corresponds to the strongest acid group. If the acid is a single polybasic one, the salts formed in sequence on addition of NaOH are $NaH_{n-1}An$, $Na_2H_{n-2}An$, etc., whereas a mixture of monobasic acids in any proportions forms, in succession, the salts represented by NaAn, NaAn′, NaAn″, etc. A logical application of the law of mass action leads to no confusion in the calculation of the value of a for each successively weaker acid in any of these mixtures, and hence we may point out the general principles by discussing the particular application of the law to malonic acid, for which the data are available [2].

II. APPLICATION OF EQUATIONS

Equation 1 gives the values of the primary dissociation constant, K_1, of a polybasic acid when $[H_nAn]$ is the *equivalent* concentration of *total* acid, determined by titration with standard alkali, a is the fraction corresponding to the strongest or primary acid group, $[H^+]$ is the hydrogen-ion concentration, α_1 is the degree of ionization of the primary salt, and $[NaH_{n-1}An]$, $[Na_2H_{n-2}An]$, etc., are the *molar* concentrations of the salts. As no assumption of the basicity of the acid is involved this equation applies also to the strongest acid in a mixture.

$$K_1=\frac{[H^+](\alpha_1[NaH_{n-1}An]+[H^+])}{a[H_nAn]-[NaH_{n-1}An]-[Na_2H_{n-2}An]\text{ - - - }[H^+]}. \tag{1}$$

The parenthesis does not represent activities and is used here for simplicity. These symbols can be replaced by activities [2] to secure the thermodynamic-activity constant instead of the classical dissociation constant, K_1. Since the values of a are obtained from a series of simultaneous equations discussed below and the ionic strength remains nearly constant, thus giving an approximately constant value [2] for the activity-coefficient product, $f_H f_{H_{n-1}An}$, either the classical or the thermodynamic method may be employed. The former is used here because of its simplicity and direct adaptability to a simple analytical treatment of mixed acids.

Let u represent the numerator of equation 1 at any given pH or $[H^+]$ and v all the denominator except a $[H_nAn]$. No values of $[H^+]$ need be considered which cause formation of secondary salt, and calculations are thereby simplified. $[NaH_{n-1}An]$ is then equivalent to the alkali added to give each $[H^+]$ value, correction being made for the dilution of the acid solution by the alkali.

We then have a series of simultaneous equations in a and K_1 for all values of $[H^+]$, which we may write

$$K_1=\frac{u}{a[H_nAn]-v}=\frac{u'}{a[H_nAn]'-v'}. \tag{2}$$

When solved for a we get

$$a=\frac{u'v-uv'}{u'[H_nAn]-u[H_nAn]'}. \tag{3}$$

This equation is simplified when $[H_nAn]$ is kept constant experimentally by adding different mole fractions of alkali to fixed volumes of acid and diluting with pure water to a chosen value of $[H_nAn]$, instead of changing it to $[H_nAn]'$ by addition of successive portions of alkali to one volume of acid to change the $[H^+]$ values, as was done in the work [2] on malonic acid, given in table 1. Smaller deviations are found for a by adopting mathematical artifices [3] such as comparison of equation 2 for any one value of $[H^+]$ against the summation equations for all values of $[H^+]$. When two simultaneous equations of the series (2) involve values of $[H^+]$ which are close together, small experimental errors in u, u', v, v', etc., may produce large percentage deviations in the numerator and denominator of equation 3 and hence in a. The smallest errors in a are, therefore, obtained when wide differences in $[H^+]$ are used in equation 3. The summation method was used with the values of $[H^+]$ and NaOH found in the earlier article [2] on malonic acid (0.1 M), and some of the results for a are given in table 1. It is seen that the average value of a, 0.484, is very close to the theoretical value, 0.5, for the dibasic malonic acid. In other words, if a for the strongest acid group is found by this method to be approximately 0.5 for an unknown pure acid, it is a dibasic acid; if a is found to be approximately 0.33 or 0.25, it is a tribasic or tetrabasic acid, respectively. This emf method for determining the basicity of any acid supplements data on the number of its salts and esters and on its structural formula.

TABLE 1.—*Calculated values of a and K_1 for 0.1 M malonic acid*[1]

Equivalents of NaOH	Equivalent concentration Na salt	$a[H_nAn]$+ Na salt (equivalents)	$[H^+]\times10^3$	α_1	a	$K_1\times10^3$ from equation 2	$K_1\times10^3$ from equation 1	
0.1294	0.011461	0.088621	7.9433	0.927	0.491	2.18	2.13	(2.06)
.2059	.017090	.083029	6.0255	.911	.476	2.33	2.17	(2.06)
.3667	.026873	.073314	3.3113	.891	.509	2.03	2.09	(2.04)
.5279	.034624	.065617	1.8621	.878	.467	2.42	2.06	(1.99)
.6891	.040902	.059382	.9550	.868	.464	2.62	1.99	(2.00)
.7697	.043614	.056690	.64565	.865	.490	2.19	1.99	(1.97)
.8100	.044880	.055432	.51286	.863	.494	2.15	2.01	(2.00)
Average					.484	2.27±0.16	2.06±0.06	(2.02)±0.03

[1] The values in parentheses are those obtained after the emf has been corrected for liquid junction potential and interionic attraction between ions of unlike sign [2]. The values of a in column 6 vary, owing primarily to the fact that they were obtained without the use of activity coefficients. However, the conclusions as to the significance of the magnitude of a remain unchanged. Since the important point of this paper is the determination of the type of an acid in an unknown, the liquid-junction potentials are not considered as was done [2] earlier. Accurate corrections with an unknown are not possible, but they are generally very small when saturated potassium chloride is employed for the solution of the reference calomel electrode.

Equations 2 and 3 are valuable in estimating the concentration of a solution of a single, weak monobasic acid HAn instead of relying upon a colorimetric, electrometric, or differential electrometric end point involving rapidly changing pH values. In this case $a=1$ and the value of $[H_nAn]$, that is, [HAn] is sought. If [HAn] is kept constant and equal to $(u'v-uv')/(u'-u)$ from equation 3, its value can be determined by measuring out the standard solution of NaOH by weight, and using precision methods for evaluating $[H^+]$ in a linear accurate pH titration curve without even reaching the end point. Even when $[HAn]'$ is the known x fraction of [HAn] at any $[H^+]$, from equation 3 [HAn] is equal to $(u'v-uv')/(u'-xu)$, and can be found accurately by taking its average for several values of $[H^+]$. Then K_1 can be calculated for the weak acid from equation 1.

1. DISSOCIATION CONSTANT OF FIRST ACID

The various simultaneous equations 2 used to determine a can also be solved for K_1 in this treatment. We may, however, simply substitute the value found for a at the given $[H^+]$, or preferably the average value of a, in the corresponding equation 2 and solve for K_1. The results of the first method are given in column 7 of table 1 and are to be compared with values of K_1 obtained from equation 1. We note that, in general, K_1 from equation 2 rises as a decreases. The average value of K_1 obtained from equation 2 is slightly higher than that from equation 1, because the average a for the $[H^+]$ values chosen is slightly less than the theoretical value 0.5. When 0.5 is used for a in equation 2, the values of K_1 obtained are very close to those from equation 1. If the value $K_1=2.06\times10^{-3}$ is employed, the a values are, respectively, 0.513, 0.520, 0.505, 0.500, 0.499, 0.501, and 0.498, and their average is 0.505.

2. CONCENTRATIONS AND DISSOCIATION CONSTANTS OF THE OTHER ACIDS

It is clear, then, that within the experimental errors both the mole fraction and the dissociation constant of the strongest acid group in a mixture can be calculated by this method. The equations can then be applied as follows to successive portions of the pH curve to calculate in turn the concentration and dissociation constant of each successively weaker acid. The values of K_1 obtained for successive additions of standard alkali show a sharp increase upon formation of the second salt, whose concentration can then be calculated as previously described [2]. By use of the values of $[H^+]$ and the concentrations of secondary salt found for the overlapping pH titration curves of the first and second acids, and for that portion of the pH curve for the second acid not overlapping those for the first and third acids, the magnitude of K_2 and a for the second acid can be calculated as above for the first acid. These values of K_2 and a remain constant until formation of the salt of the third acid, for which K_3 and a can then be calculated.

It should also be pointed out that in those portions of the pH curve involving overlapping of the individual pH curves for two acids undergoing simultaneous neutralization, the denominator of equation 1 is related to the amount of added alkali in two different ways, depending on whether a mixture of monobasic acids or a polybasic acid is concerned. This method is therefore useful as a means of analysis of mixed acids, whether mono- or polybasic.

The authors wish to express their appreciation to Dr. Walter J. Hamer for helpful criticism in the preparation of this paper.

III. REFERENCES

[1] Mellon, Avery, Slagle, and Acree, J. Infect. Diseases 29, **1**, 75 (1921).
[2] J. O. Burton, W. J. Hamer, and S. F. Acree, J. Research NBS **16**, 575 (1936) RP895.
[3] E. K. Marshall and S. F. Acree, J. Phys. Chem. **19**, 589 (1915); W. A. Taylor and S. F. Acree, J. Phys. Chem. **20**, 365 (1916).

Washington, April 18, 1936.

U. S. Department of Commerce National Bureau of Standards

RESEARCH PAPER RP890

Part of Journal of Research of the National Bureau of Standards, Volume 16, June 1936

THERMAL EXPANSION OF COPPER-BERYLLIUM ALLOYS

By Peter Hidnert

ABSTRACT

Measurements were made on the linear thermal expansion of 12 samples of copper-beryllium alloys at various temperatures between 20 and 300 ° C, in order to determine the effects of chemical composition and treatments on the expansion of these alloys, which have come into industrial use during the past few years.

Table 1 gives the chemical composition and the treatment of each sample. The observations obtained on heating and cooling are shown in figures 9 to 13. The expansion curves of the quenched samples show critical regions which presumably were caused by changes in the structures of the alloys. Deformation or cold-work after quenching facilitates and accelerates these changes. Stabilization of copper-beryllium alloys may be accomplished either by cold-working or by tempering.

There is no simple relation between the coefficients of expansion, chemical composition, and heat treatment of the copper-beryllium alloys investigated. Figure 14 indicates the effects of beryllium content, cold-work, and heat treatment on the coefficients of expansion of these alloys. Table 2 gives the ranges of the coefficients of expansion. The coefficients of expansion of the copper-beryllium alloys do not differ from the corresponding value for copper by more than 8 percent of the latter value, whereas the differences indicated in figure 8 for the hardness, tensile strength, elongation, and reduction of area are considerably greater. For example, the tensile strength of copper-beryllium alloys may be more than 4 times as great as the tensile strength of copper.

CONTENTS

		Page
I.	Introduction	529
II.	Previous determinations	530
III.	Materials investigated	532
IV.	Apparatus	533
V.	Results	533
VI.	Summary	547
VII.	References	548

I. INTRODUCTION

Data on the linear thermal expansion of beryllium and aluminum-beryllium alloys were published by Hidnert and Sweeney [1] [1] in 1927. Data on the linear thermal expansion of another series of beryllium alloys, namely copper-beryllium alloys, are presented at the present time. This investigation was undertaken in order to determine the effects of chemical composition and treatments on the expansion of

[1] The numbers in brackets here and elsewhere in the text refer to the literature references at the end of this paper.

these alloys, which have come into industrial use during the past few years. Important applications of copper-beryllium alloys have been indicated by Illig [2], Davis [3], and in an anonymous article [4].

As it is known that various properties of copper-beryllium alloys (up to about 3 percent of beryllium) are subject to aging phenomena, it was assumed that the thermal expansion might be likewise affected. Consequently samples of each composition, in various conditions of heat treatment, were investigated. The beryllium contents ranged from 1.3 to 3.0 percent, for the results already obtained on other properties of the alloys indicated that this range included the useful alloys.

II. PREVIOUS DETERMINATIONS

Masing and Dahl [5] published a curve showing the linear thermal expansion of a quenched copper-beryllium alloy containing 2.5 percent of beryllium. This curve is reproduced in figure 1. They stated that owing to the heating, a decrease in length of about 0.24 percent took place, as is indicated by the distance between the intersection points of the heating and cooling curves with the ordinate axis. On reheating the same rod of copper-beryllium alloy to 500° C, they found that the expansion curve followed almost a straight line and after cooling an additional shortening of 0.01 percent took place. They concluded as follows: "Due to aging, a shortening of about 0.25 percent results with the 2.5-percent alloy. This shortening occurs in the temperature range above that for age hardening and therefore is not an age-hardening effect like the increase in hardness, but is simply due to the disintegration of the α-solid solution."

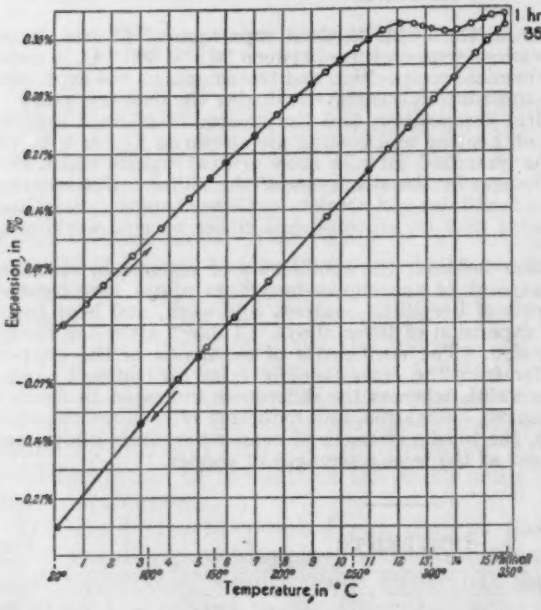

FIGURE 1.—*Linear thermal expansion of a quenched copper-beryllium alloy containing 2.5 percent of beryllium (Masing and Dahl [5]).*

Figures 2 and 3 show the differential dilatometric curves obtained by Haas and Uno [6] on a copper-beryllium alloy containing 2.5 percent of beryllium. Figure 2 shows six curves for various heat treatments. They stated that precipitation of γ crystals begins at about 220° C in the alloy air-cooled from 800° C, agglomeration starts at 400° C, and at approximately 500° C the transformation from γ into β takes place. Curve 4 for the alloy aged at 200° C shows slight anomalies, for during the aging the precipitation occurred.

In the alloy aged at 300° C, the precipitation and agglomeration of the γ constituent took place, as is evident from curve 5. They further

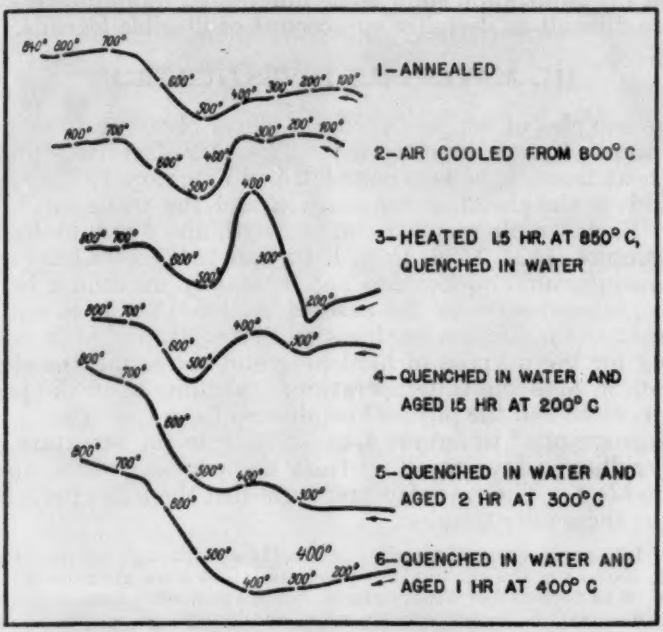
1—ANNEALED
2—AIR COOLED FROM 800° C
3—HEATED 1.5 HR. AT 850° C, QUENCHED IN WATER
4—QUENCHED IN WATER AND AGED 15 HR AT 200° C
5—QUENCHED IN WATER AND AGED 2 HR AT 300°C
6—QUENCHED IN WATER AND AGED 1 HR AT 400° C

FIGURE 2.—*Dilatometric curves of a copper-beryllium alloy containing 2.5 percent of beryllium (Haas and Uno* [6]).

stated that neither an expansion nor contraction effect of the γ crystals can be observed in curve 6 for the alloy aged at 400° C.

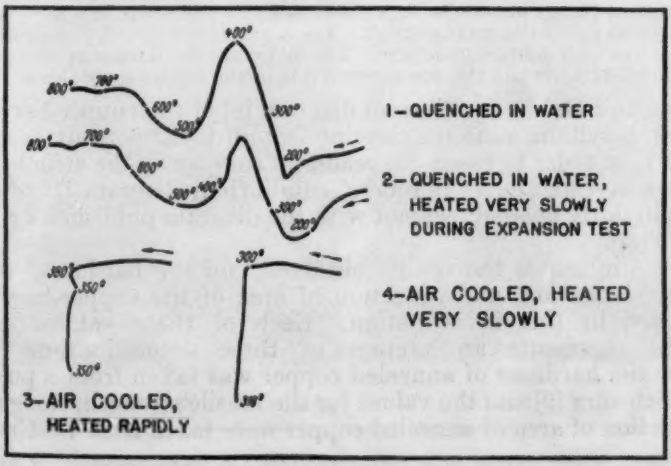
1—QUENCHED IN WATER
2—QUENCHED IN WATER, HEATED VERY SLOWLY DURING EXPANSION TEST
4—AIR COOLED, HEATED VERY SLOWLY
3—AIR COOLED, HEATED RAPIDLY

FIGURE 3.—*Temperature displacement of the hardening effect with various heating rates on a copper-beryllium alloy containing 2.5 percent of beryllium (Haas and Uno* [6]).

Figure 3 shows that slow heating causes the maximum of the differential expansion curve to shift to a lower temperature.

Borchers [7] used the dilatometric method in an investigation of the equilibrium diagram of the copper-beryllium alloys. Figures 10 and 11 of his publication show some differential dilatometric curves, which are difficult to decipher on account of illegible legends.

III. MATERIALS INVESTIGATED

Twelve samples of copper-beryllium alloys obtained from a commercial source,[2] were investigated. The manufacturing processes and the heat treatments were completed in February 1933. Table 1 (sec. V) gives the chemical composition and the treatment of each sample. Each sample was 300 mm in length and 6 mm in diameter.

Five samples (1534, 1536, 1538, 1540, and 1542) were heat treated by the manufacturer to develop approximately maximum hardness and strength, although in the case of sample 1536 it is not quite certain that the maximum hardness and strength had been reached. The aging for the purpose of hardening and increasing the strength varies both in time and in temperature, depending upon the percentage of beryllium and the physical condition of the specimen.

The micrographs [3] in figures 4 to 6 illustrate the structure of the copper-beryllium alloys resulting from the various treatments indicated in table 1. The manufacturer furnished the following information about these micrographs:

(a) The 1.33-percent-beryllium alloy is mostly α, although micrograph 1536, in figure 4, shows a slight amount of γ precipitation at some grain boundaries.

(b) The 2.14-percent-beryllium alloy, when properly homogenized and quenched from 800° C, should contain no β, but in commercial practice a little of the β constituent is found, as shown in figure 5. The precipitation of $\alpha+\beta$ at the grain boundaries is shown distinctly in micrograph 1540, figure 5.

(c) The 3.03-percent-beryllium alloy, when homogenized at 800° C and quenched, contains α and β grains, as shown in micrograph 1541, figure 6. The solid white areas are the β, the darker and cross-hatched areas the α. After heat treatment of this alloy the structure appears as shown in figure 6, micrographs 1542, 1542(a), and 1542(b), at 75, 500, and 1,000 diameters, respectively. The heat treatment brings about decomposition of the white areas into $\alpha+\gamma$ usually in a more or less pearlitic arrangement. The α grains also break down into $\alpha+\gamma$ but with a less well defined structure. The latter are the darker areas shown in micrograph 1542(b), while the decomposed β is in the lighter gray shade.

Masing and Dahl's equilibrium diagram [8] of the copper-beryllium alloys for beryllium contents ranging from 0 to 12 percent, is shown in figure 7, in order to assist the reader in comparing the structures of the alloys investigated. Borchers' equilibrium diagram [7] of these alloys is in fairly good agreement with the diagram published by Masing and Dahl.

Figure 8 indicates the results obtained [4] on the hardness,[5] tensile strength, elongation, and reduction of area of the copper-beryllium alloys used in this investigation. Each of these values (except hardness) represents an average of three determinations. The value for the hardness of annealed copper was taken from a publication by Schwarz [9] and the values for the tensile strength, elongation, and reduction of area of annealed copper were taken from BS Circular 73 [10].

[2] American Brass Co.
[3] Micrographs by American Brass Co.
[4] By the American Brass Co., in February 1933.
[5] Rockwell B hardness (100-kg load with 1/16-inch ball).

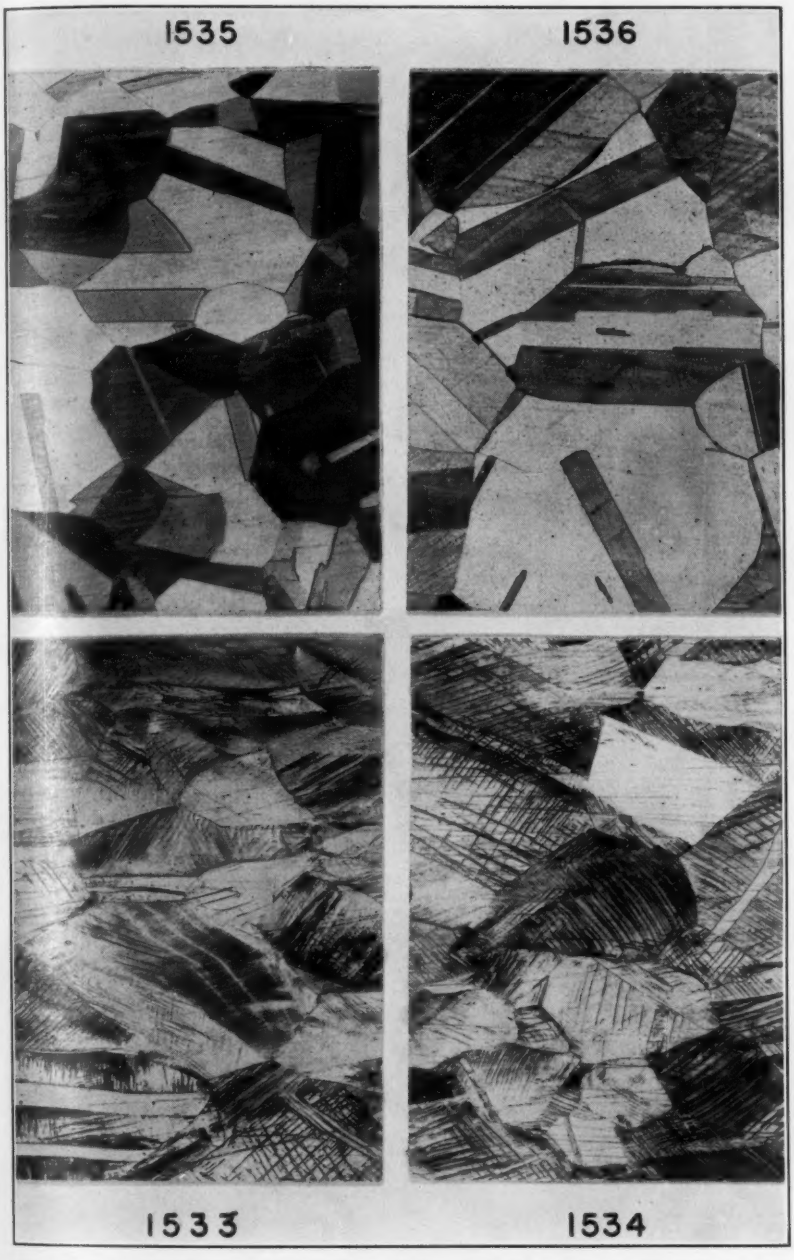

FIGURE 4.—*Microstructure of copper-beryllium alloy (copper 98.54, beryllium 1.33 silicon 0.02, iron 0.03 percent), ×75.*

Sample 1535—quenched from 800° C. Sample 1536—quenched from 800° C and aged 5 hours at 350° C. Sample 1533—quenched from 800° C and hard-drawn (30 percent reduction). Sample 1534—quenched from 800° C, hard-drawn and aged 5 hours at 325° C.

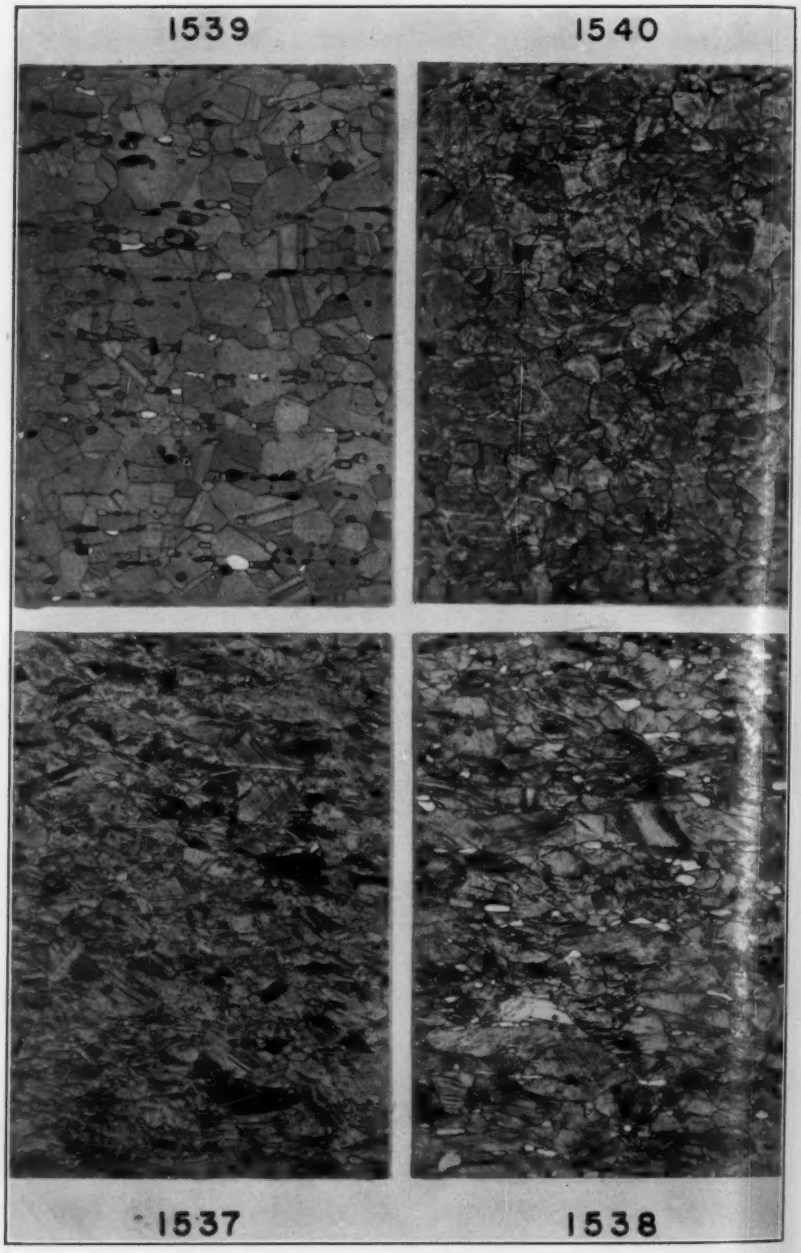

FIGURE 5.—*Microstructure of copper-beryllium alloy (copper 97.78, beryllium 2.14, silicon 0.02, iron 0.06 percent),* $\times 75$.

Sample 1539—quenched from 800° C. Sample 1540—quenched from 800° C and aged 2½ hours at 300° C. Sample 1537—quenched from 800° C and hard-drawn (30 percent reduction). Sample 1538—quenched from 800° C, hard-drawn and aged 2 hours at 275° C.

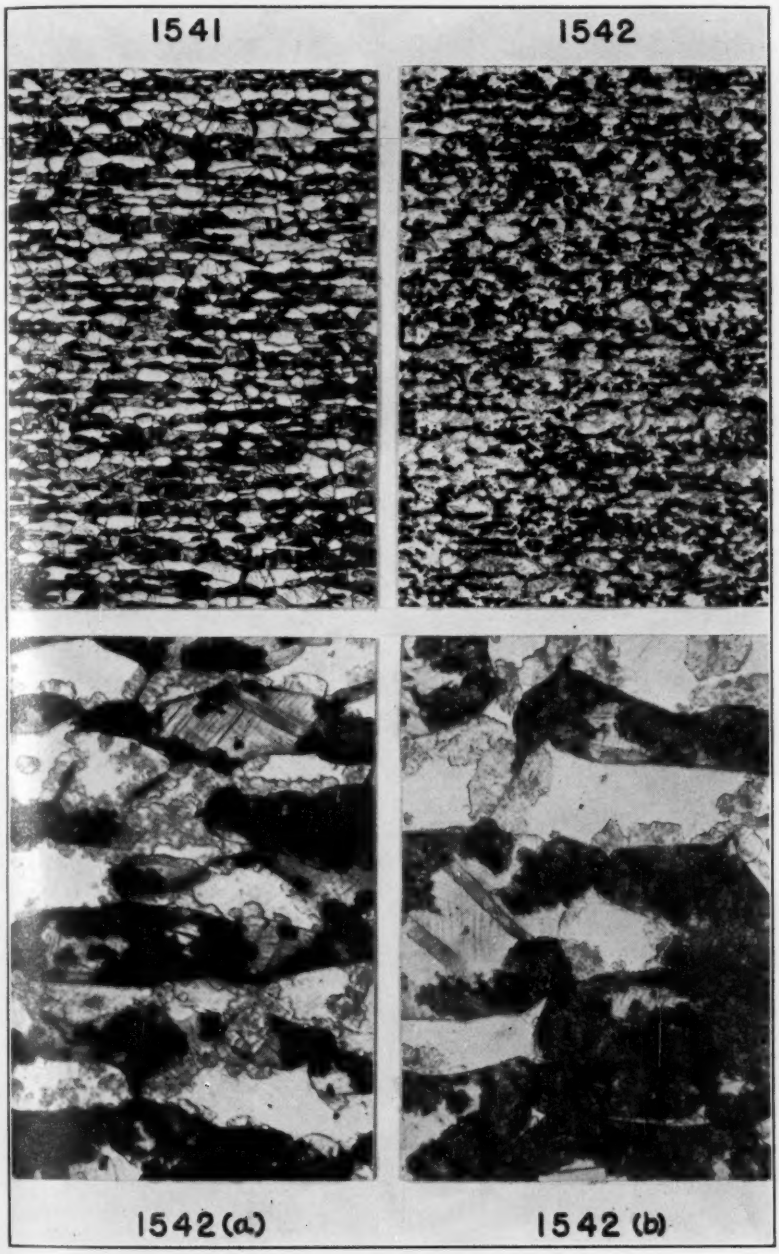

FIGURE 6.—*Microstructure of copper-beryllium alloy (copper 96.98, beryllium 3.03, silicon 0.02, iron 0.03 percent).*

Sample 1541—quenched from 800° C and hard-drawn (20 percent reduction), ×75. Sample 1542—quenched from 800° C, hard-drawn and aged 1¾ hours at 300° C, ×75. Sample 1542 (a)—same treatment as 1542, ×500. Sample 1542 (b)—same treatment as 1542, ×1,000.

UNIV. OF MICH.

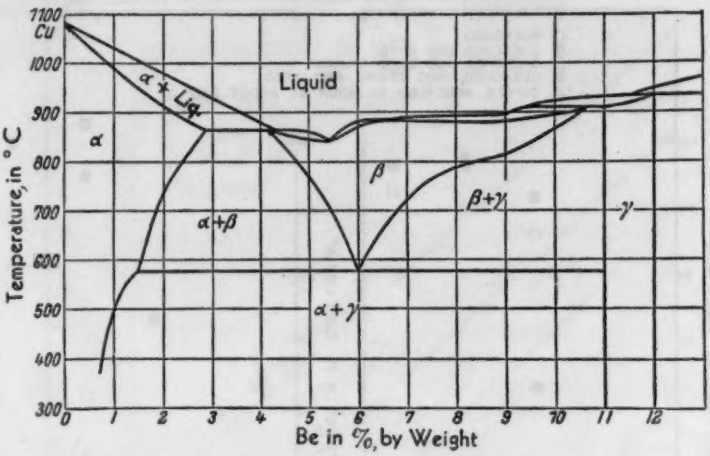

FIGURE 7.—*Equilibrium diagram of copper-beryllium alloys (Masing and Dahl* [8])

IV. APPARATUS

All samples except 1541A were investigated in the stretched-wire bath furnace described in BS Scientific Papers S410 and S524. The air furnace described in BS Scientific Paper S524 was used for sample 1541A.

The stretched-wire thermal-expansion apparatus referred to herein was originally designed and used by Dr. Arthur W. Gray, formerly of this Bureau, and was described by him in the Journal of the Washington Academy of Sciences, vol. II, no. 10, p. 248, 1912, and in the Bulletin of the Bureau of Standards, vol. 10, Scientific Paper S219, 451, (1914). The apparatus has been modified and improved by subsequent workers, and, in its later forms, has been described, in detail and by reference, in a large number of scientific papers by W. Souder, P. Hidnert, L. W. Schad, and other research workers at the National Bureau of Standards. Among these papers the following may be mentioned as of particular value in describing the apparatus: Scientific Papers S352, S433, and S524, by W. Souder and P. Hidnert, and S410 by P. Hidnert.

V. RESULTS

Observations were made on the linear thermal expansion of the copper-beryllium alloys at various temperatures between 20 and 300° C. The results obtained on heating and cooling are shown in figures 9 to 13. Each expansion curve is plotted from a different origin in order to display the individual characteristics of each curve. The numbers adjoining the observations on each curve that showed critical regions, represent the time, in hours, from the time of the initial observation.

Two or more tests were made on each sample except 1541A, on which only one test was made. The results obtained on the first heating apply for the samples having the treatments indicated in table 1, but the results obtained in the second and third tests apply

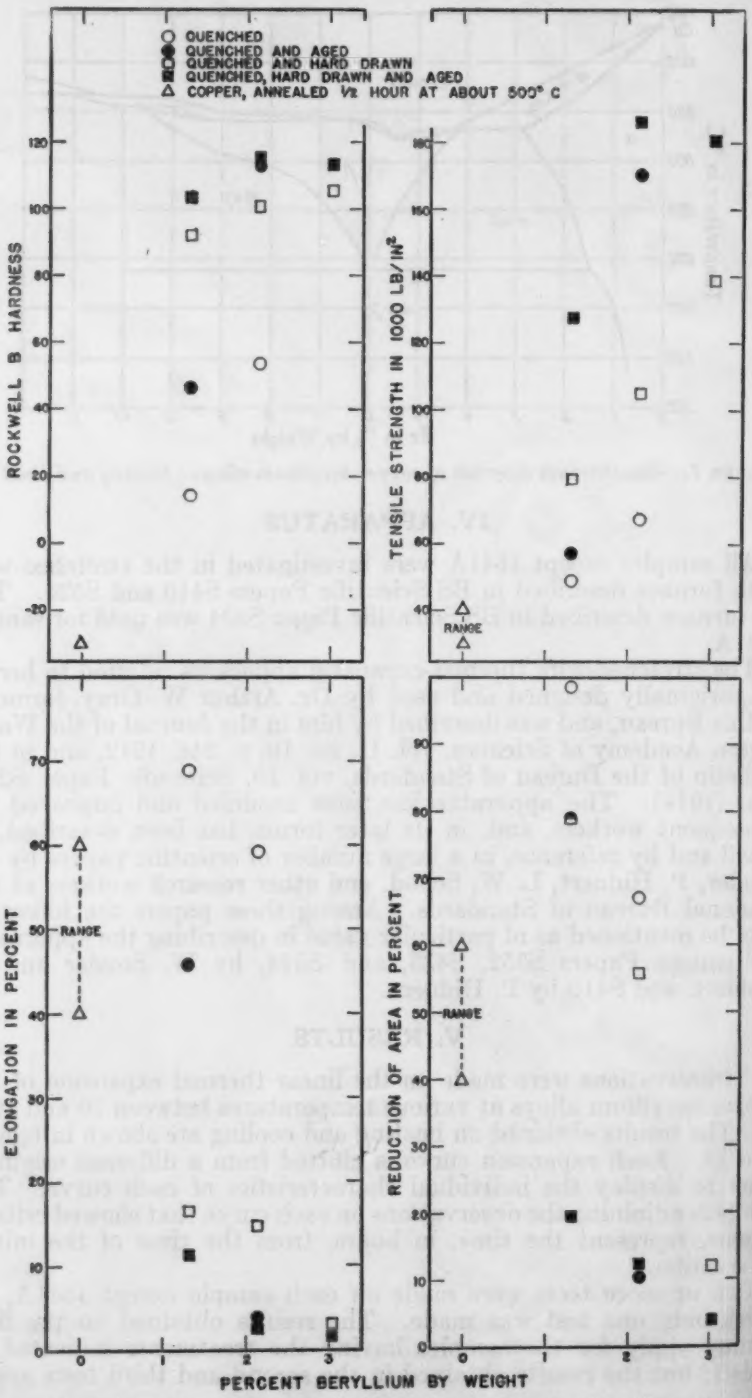

FIGURE 8.—*Hardness, tensile strength, elongation, and reduction of area of copper-beryllium alloys used in the investigation on thermal expansion.*

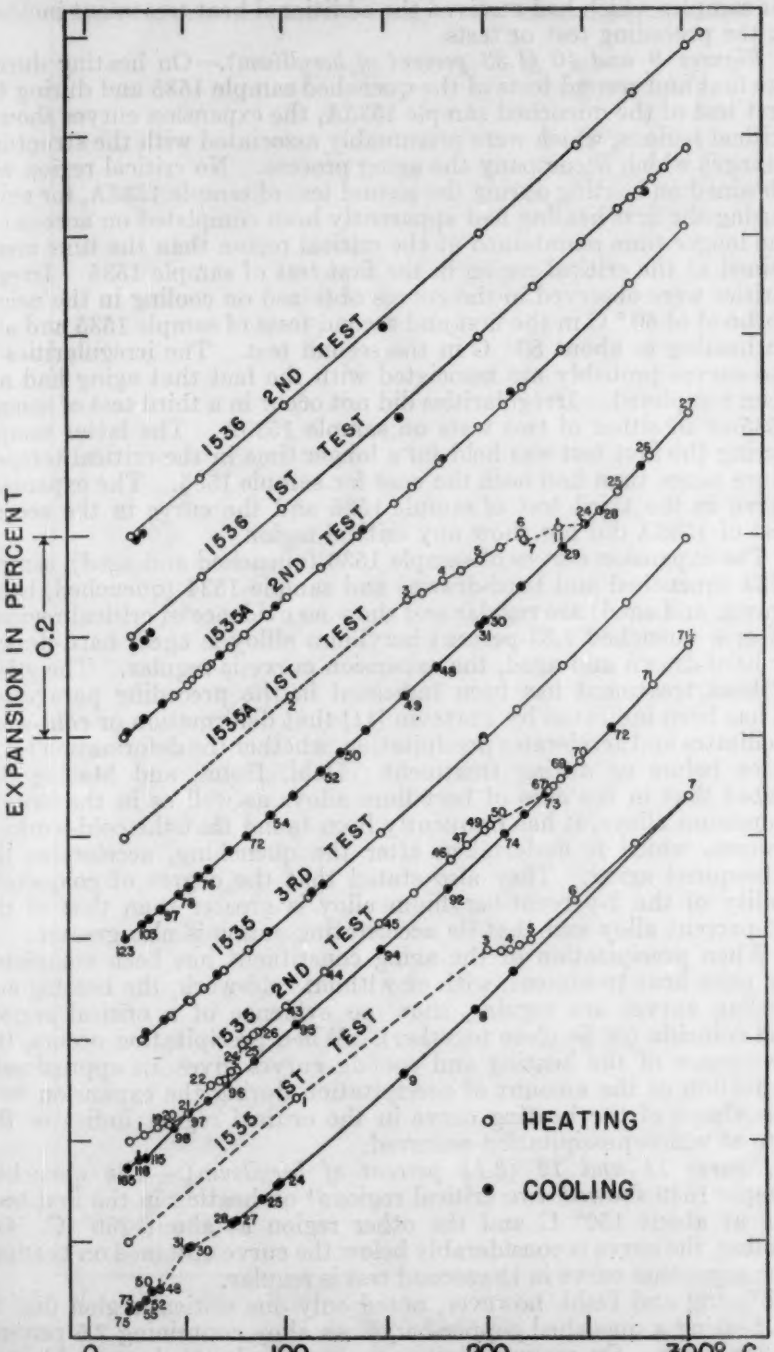

FIGURE 9.—*Linear expansion of 3 samples of Cu-Be alloy (1.33% Be).*

Samples 1535 and 1535A—Heated for ½ hour at 800° C and quenched; sample 1536—same treatment as sample 1535 and aged for 5 hours at 350° C.

NOTE.—Each number adjoining an observation indicates the time, in hours, from the time of the initial observation. A tagged symbol indicates more than one observation.

for samples which had received the additional heat treatment incident to the preceding test or tests.

Figures 9 and 10 (1.33 percent of beryllium).—On heating during the first and second tests of the quenched sample 1535 and during the first test of the quenched sample 1535A, the expansion curves showed critical regions, which were presumably associated with the structural changes which accompany the aging process. No critical region was obtained on heating during the second test of sample 1535A, for aging during the first heating had apparently been completed on account of the longer time maintained at the critical region than the time maintained at the critical region in the first test of sample 1535. Irregularities were observed in the curves obtained on cooling in the neighborhood of 50° C in the first and second tests of sample 1535 and also on heating to about 80° C in the second test. The irregularities in the curves probably are associated with the fact that aging had not been completed. Irregularities did not occur in a third test of sample 1535 or in either of two tests on sample 1535A. The latter sample during the first test was held for a longer time in the critical temperature range than had been the case for sample 1535. The expansion curve in the third test of sample 1535 and the curve in the second test of 1535A did not show any critical region.

The expansion curves of sample 1536 (quenched and aged), sample 1533 (quenched and hard-drawn) and sample 1534 (quenched, hard-drawn, and aged) are regular and show no evidence of critical regions. After a quenched 1.33-percent beryllium allloy is aged, hard-drawn, or hard-drawn and aged, the expansion curve is regular. The effect of heat treatment has been indicated in the preceding paragraph. It has been indicated by Portevin [11] that deformation or cold-work facilitates and accelerates precipitation, whether the deformation takes place before or during treatment. Dahl, Holm, and Masing [12] stated that in the case of beryllium alloys as well as in the case of aluminum alloys, it has frequently been found that the cold-working process, which is undertaken after the quenching, accelerates the subsequent aging. They also stated that the degree of cold-workability of the 2-percent-beryllium alloy is greater than that of the 2.5-percent alloy and that its accelerating action is also greater.

When precipitation of the aging constituent has been completed by prior heat treatment, with or without cold-work, the heating and cooling curves are regular, show no evidence of a critical region, and coincide (or lie close together). When precipitation occurs, the divergence of the heating and cooling curves gives an approximate indication of the amount of precipitation during the expansion test. The shape of the heating curve in the critical region indicates the rate at which precipitation occurred.

Figures 11 and 12 (2.14 percent of beryllium).—The quenched sample 1539 showed two critical regions [6] on heating in the first test, one at about 150° C and the other region at about 250° C. On cooling, the curve is considerably below the curve obtained on heating. The expansion curve in the second test is regular.

Masing and Dahl, however, noted only one critical region (fig. 1) on heating a quenched copper-beryllium alloy containing 2.5 percent of beryllium. On cooling, their curve was similar to the one obtained in the present investigation.

[6] The two critical regions were verified on a duplicate sample.

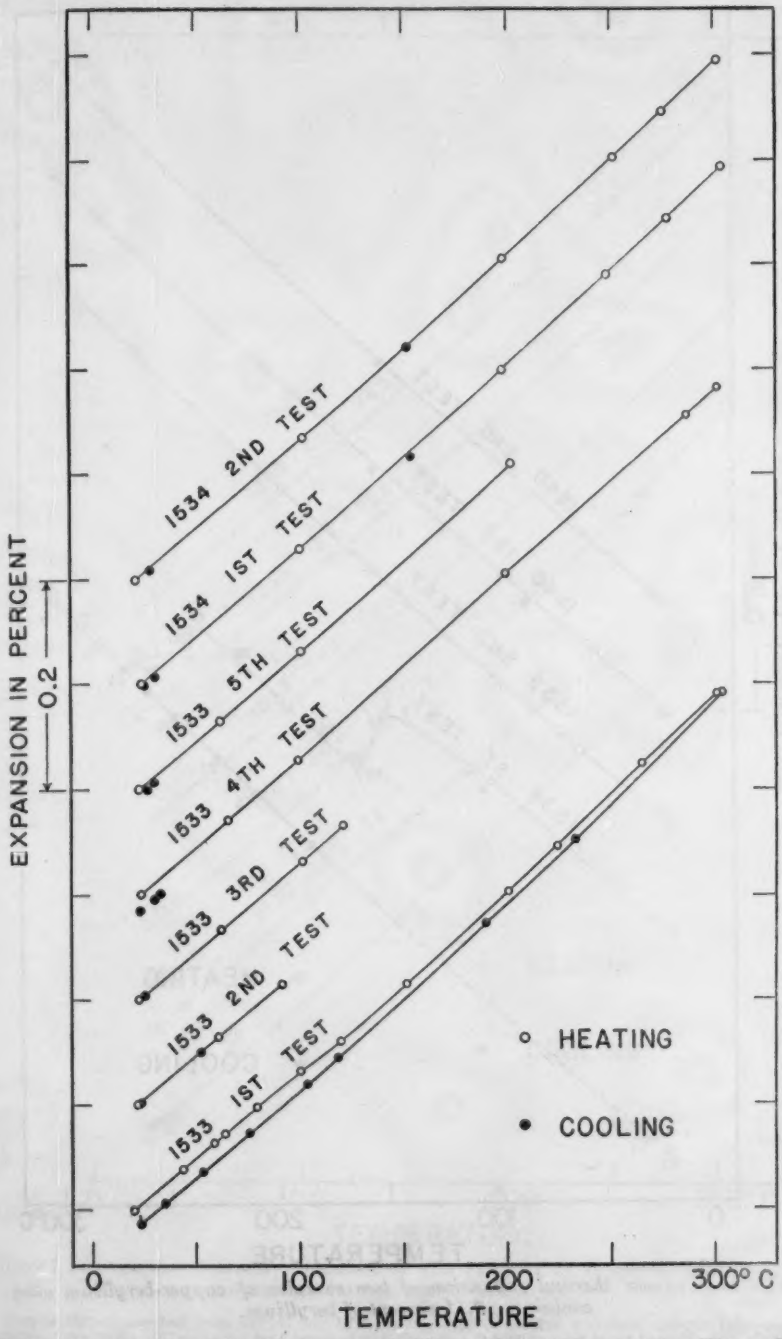

FIGURE 10.—*Linear thermal expansion of two samples of copper-beryllium alloy containing 1.33 percent of beryllium.*

Sample 1533—Quenched from 800° C and hard-drawn, with 30 percent reduction; sample 1534—same treatment as sample 1533 and aged for 5 hours at 325° C.
The tagged symbol indicates more than one observation.

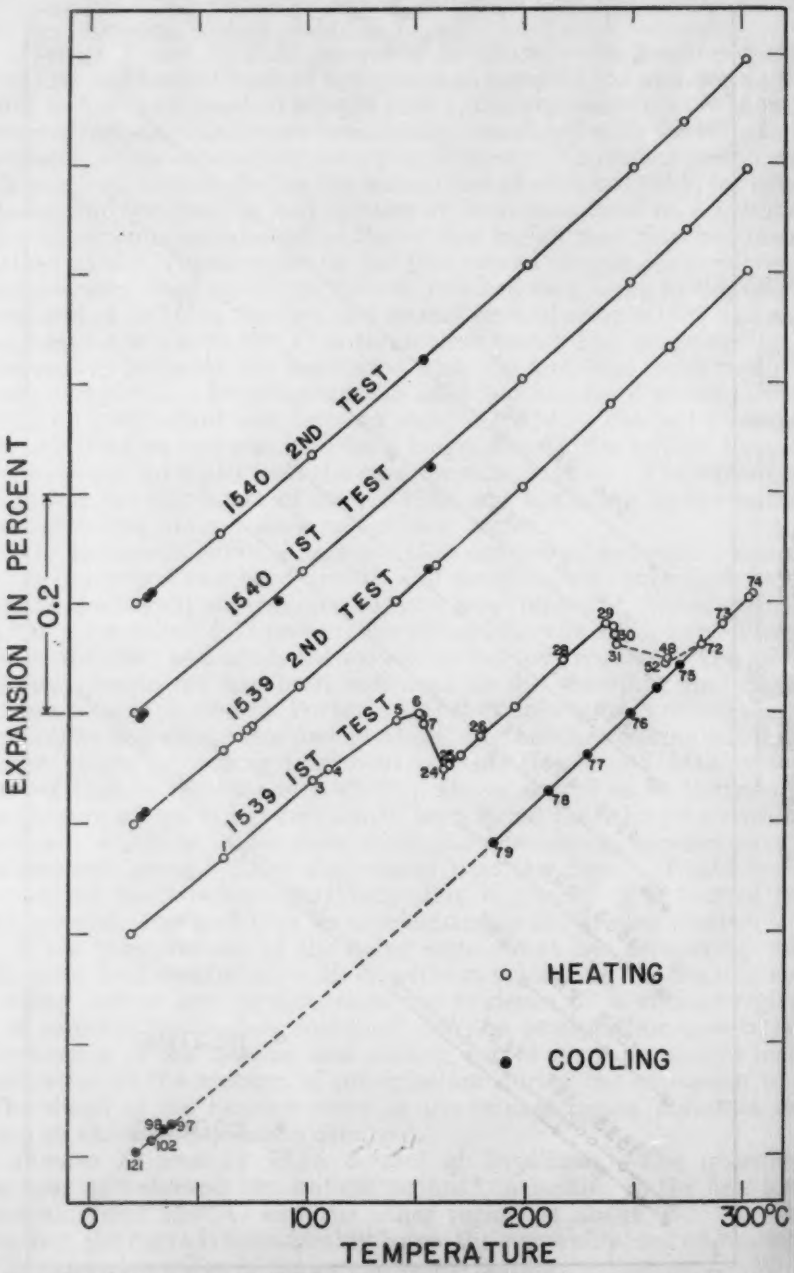

FIGURE 11.—*Linear thermal expansion of two samples of copper-beryllium alloy containing 2.14 percent of beryllium.*

Sample 1539—Heated for ½ hour at 800° C and quenched; sample 1540—same treatment as sample 1539 and aged for 2½ hours at 300° C.

NOTE.—Each number adjoining an observation in the first test of sample 1539, indicates the time, in hours, from the time of the initial observation.

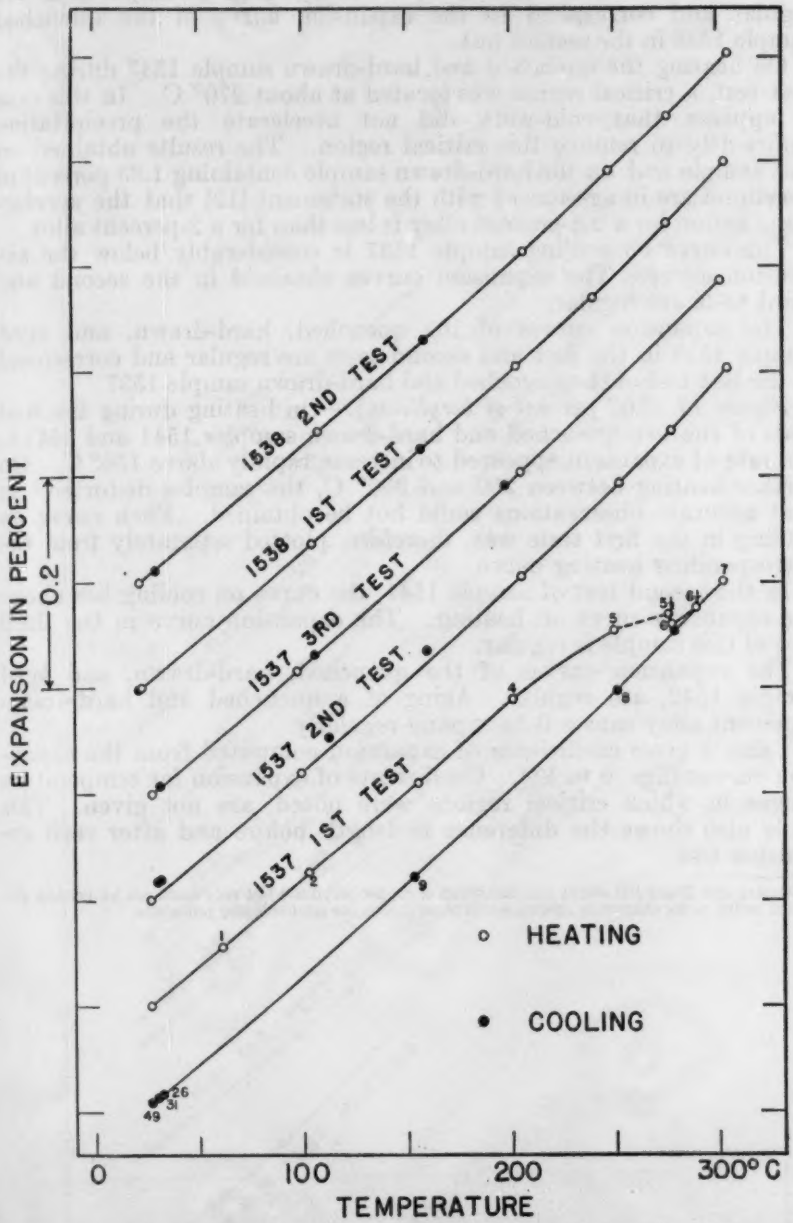

FIGURE 12.—*Linear thermal expansion of two samples of copper-beryllium alloy containing 2.14 percent of beryllium.*

Sample 1537—Quenched from 800° C and hard-drawn, with 30-percent reduction; sample 1538—same treatment as sample 1537 and aged for 2 hours at 275° C.

NOTE.—Each number adjoining an observation in the first test of sample 1537, indicates the time, in hours, from the time of the initial observation.

66929—36——2

The expansion curves of the quenched and aged sample 1540 are regular and correspond to the expansion curve of the quenched sample 1539 in the second test.

On heating the quenched and hard-drawn sample 1537 during the first test, a critical region was located at about 270° C. In this case it appears that cold-work did not accelerate the precipitation sufficiently to remove this critical region. The results obtained on this sample and on the hard-drawn sample containing 1.33 percent of beryllium are in agreement with the statement [12] that the accelerating action for a 2.5-percent alloy is less than for a 2-percent alloy.

The curve on cooling sample 1537 is considerably below the expansion curve. The expansion curves obtained in the second and third tests are regular.

The expansion curves of the quenched, hard-drawn, and aged sample 1538 in the first and second tests are regular and correspond to the last test of the quenched and hard-drawn sample 1537.

Figure 13 (3.03 percent of beryllium).—On heating during the first tests of the two quenched and hard-drawn samples 1541 and 1541A, the rate of expansion appeared to increase rapidly above 150° C. On further heating between 200 and 300° C, the samples distorted,[7] so that accurate observations could not be obtained. Each curve on cooling in the first tests was, therefore, plotted separately from the corresponding heating curve.

In the second test of sample 1541, the curve on cooling lies above the expansion curve on heating. The expansion curve in the third test of this sample is regular.

The expansion curves of the quenched, hard-drawn, and aged sample 1542, are regular. Aging of a quenched and hard-drawn 3-percent alloy causes it to expand regularly.

Table 1 gives coefficients of expansion computed from the expansion curves (figs. 9 to 13). Coefficients of expansion for temperature ranges in which critical regions were noted, are not given. This table also shows the difference in length before and after each expansion test.

[7] Masing and Haase [13] stated that distortion of copper-beryllium test rods could not be entirely prevented owing to the changes in volume which occur during the age-hardening procedure.

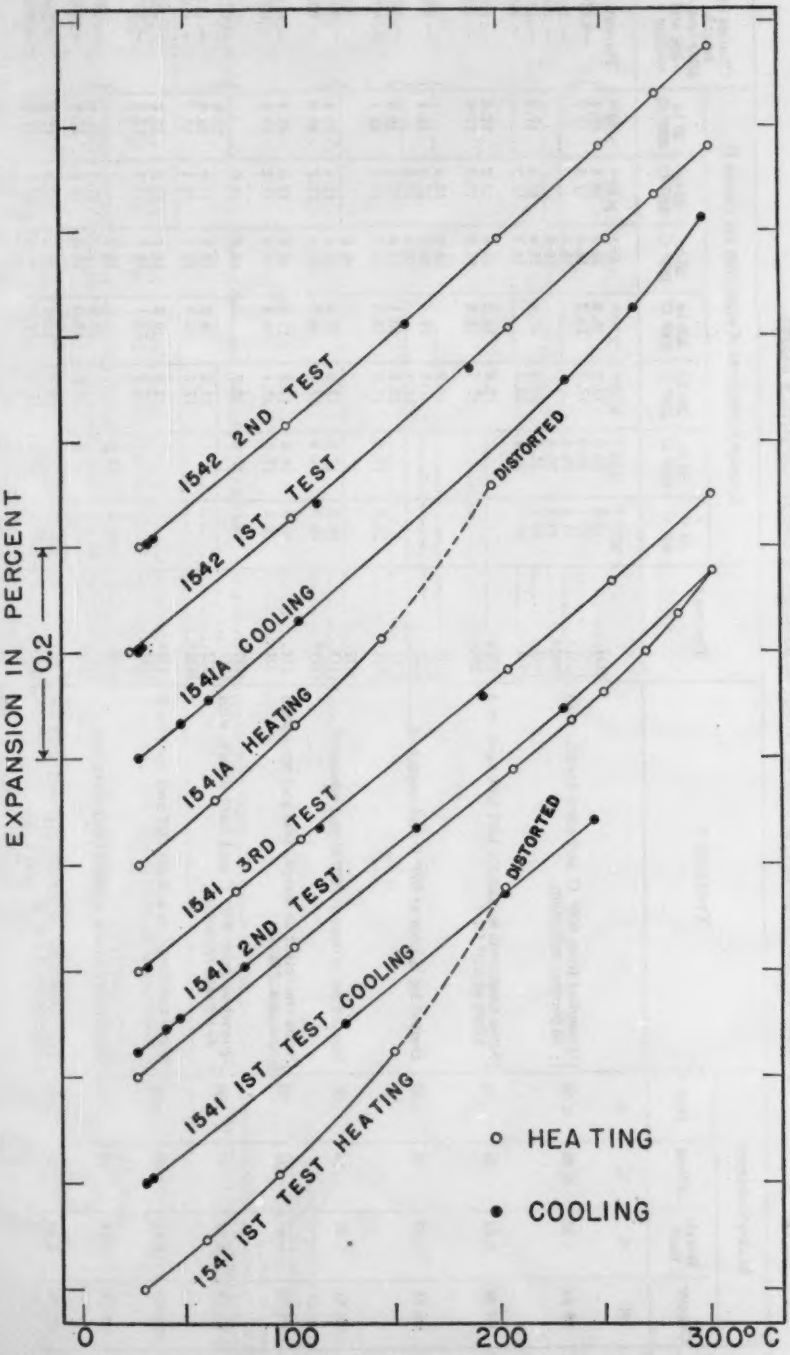

FIGURE 13.—*Linear expansion of 3 samples of* Cu-Be *alloy (1.33%* Be).

Samples 1541 and 1541A—Quenched from 800° C and hard-drawn, with 20 percent reduction; sample 1542—same treatment as sample 1541 and aged for 1¾ hours at 300° C.

NOTE.—The curves obtained on cooling in the first tests of samples 1541 and 1541A are not continuations of the corresponding curves obtained on heating.

TABLE 1.—*Average coefficients of linear expansion of copper-beryllium alloys*

Sample	Maker's analysis				Treatment [a]	Test no. [b]	Average coefficients of expansion per degree C							Change in length after heating and cooling [a]
	Copper	Beryllium	Silicon	Iron			20 to 60° C	60 to 100° C	100 to 200° C	200 to 300° C	20 to 100° C	20 to 200° C	20 to 300° C	
	%	%	%	%			×10⁻⁶	×10⁻⁶	×10⁻⁶	×10⁻⁶	×10⁻⁶	×10⁻⁶	×10⁻⁶	*Percent*
1533	98.54	1.33	0.02	0.03	Quenched from 800° C and hard-drawn with 30 percent reduction.	1H	16.6	16.5	17.0	18.6	16.5	16.8	17.4	−0.019
						1C	16.7	16.6	17.7	19.2	16.6	17.2	17.9	
						2H[d]	16.4	16.4			16.4			−.000
						3H[d]	16.8	16.5			16.6			−.000
						4H	16.7	17.1	17.6	17.4	16.9	17.3	17.3	−.015
						5H[d]	16.6	16.8	17.6		16.7	17.2		−.004
1534	98.54	1.33	.02	.03	Same treatment as sample 1533 and aged for 5 hours at 325° C.	1H[d]			17.6	18.2	16.8	17.2	17.6	−.004
						2H[d]			17.7	18.3	16.8	17.3	17.6	−.002
1535	98.54	1.33	.02	.03	Heated for ½ hour at 800° C and quenched	1H			15.2		16.8	15.9		−.069
						1C			17.6	19.7	16.6	17.2	18.1	
						2H			17.4		16.9	17.2		−.025
						2C			17.8	20.1	16.6	17.3	18.3	
						3H[d]	16.3	17.1	17.6	19.6	16.7	17.2	18.1	+.003
1535A [c]	98.54	1.33	.02	.03	Heated for ½ hour at 800° C and quenched	1H					16.8			−.101
						1C	16.6	17.0	17.9	20.2	16.8	17.4	18.4	
						2H[d]	16.6	17.4	17.6	19.3	17.0	17.3	18.0	+.003
1536	98.54	1.33	.02	.03	Same treatment as sample 1535 and aged for 5 hours at 350° C.	1H	16.6	16.8	17.3	17.9	16.7	17.0	17.4	−.012
						2H	16.6	17.0	17.4	18.1	16.8	17.2	17.5	−.007
1537	97.78	2.14	.02	.06	Quenched from 800° C and hard-drawn with 30-percent reduction.	1H	16.1	17.0	16.7		16.6	16.6		−.092
						1C							17.8	
						2H			17.4	19.7	16.5	17.0	18.0	+.012
						3H[d]			17.5	18.9	16.6	17.1	17.7	+.002
1538	97.78	2.14	.02	.06	Same treatment as sample 1537 and aged for 2 hours at 275° C.	1H[d]			17.2	19.3	16.7	17.0	17.8	.000
						2H[d]			17.2	19.1	16.7	17.0	17.7	−.001
1539	97.78	2.14	.02	.06	Heated for ½ hour at 800° C and quenched	1H	16.2	17.0			16.6			−.202
						1C				18.9		17.1	17.8	
						2H[d]	16.3	16.8	17.5	19.0	16.5	17 1	17.8	+.002
1540	97.78	2.14	.02	.06	Same treatment as sample 1539 and aged for 2½ hours at 300° C.	1H[d]			17.3	18.3	16.6	17.0	17.5	−.008
						2H[d]	16.4	16.9	17.3	18.6	16.6	17.0	17.6	−.002

1541	96.98	3.03	.02	.03	Quenched from 800° C and hard-drawn with 20-percent reduction.	1H	15.9	17.9			16.9				
						1C			15.9		15.4	15.7			
						2H			15.9	19.2	16.4	16.1	17.2		+.024
						2C	15.7	15.8			15.7		16.4		
						3H[d]	16.0	15.8	16.0	17.0	15.9	16.0	16.4		−.003
1541A[f]	96.98	3.03	.02	.03	Quenched from 800° C and hard-drawn with 20-percent reduction.	1H	16.4	18.2			17.3				
						1C	16.3	17.1			16.7		18.9		
1542	96.98	3.03	.02	.03	Same treatment as sample 1541 and aged for 1¼ hours at 300° C.	1H[d]			17.3	17.9	16.3	16.9	17.3		−.006
						2H[d]			17.4	18.1	16.3	16.9	17.4		−.003

[a] By American Brass Co.
[b] H indicates heating and C cooling.
[c] Determined from the expansion curve on heating and the contraction curve (or observations) on cooling. The plus (+) sign indicates an increase in length and the minus (−) sign a decrease in length.
[d] Observations on cooling close to expansion curve on heating.
[e] Cut from same rod as sample 1535.
[f] Cut from same rod as sample 1541.

Figure 14 indicates the coefficients of expansion [8] of the copper-beryllium alloys for three temperature ranges. Values for copper [14] are included. This figure shows the effects of beryllium content,

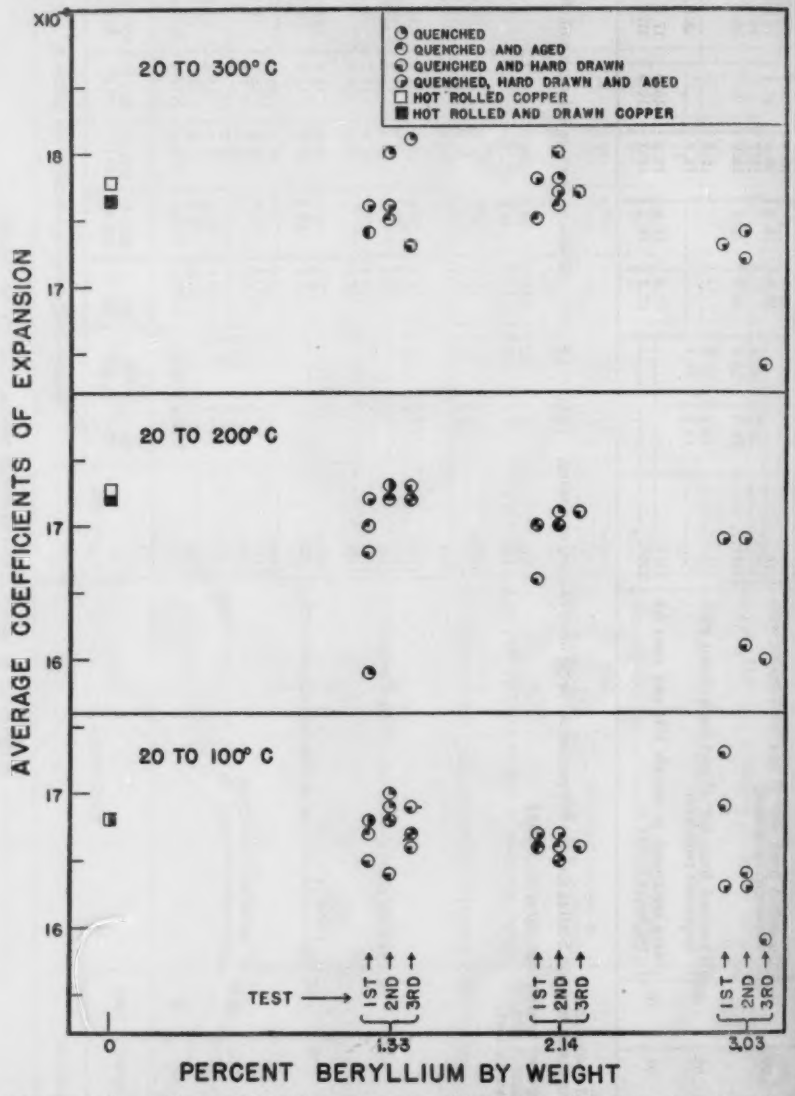

FIGURE 14.—*Effects of beryllium content, cold-work, and heat treatment on the coefficients of expansion of copper-beryllium alloys.*

NOTE.—A tagged symbol indicates a value obtained in a fourth or fifth test.

cold-work, heat treatment, etc., on the coefficients of expansion of these alloys. There is no simple relation between the coefficients of expansion, chemical composition, heat treatment, etc. The differences in the coefficients of expansion between the first and succeeding

[8] On heating.

tests are attributed to changes in the alloys on account of the heat treatments incident to the tests.

Table 2 gives the ranges of the coefficients of expansion indicated in figure 14. The coefficients of expansion of the copper-beryllium alloys do not differ from the corresponding value for copper by more than 8 percent of the latter value, whereas the differences indicated for the hardness, tensile strength, elongation, and reduction of area (fig. 8) are considerably greater. For example, the tensile strength of copper-beryllium alloys may be more than four times as great as the tensile strength of copper.

TABLE 2.—*Ranges of coefficients of expansion of copper-beryllium alloys* [a]

Beryllium content	Average coefficients of expansion [b] per degree C		
	20 to 100° C	20 to 200° C	20 to 300° C
Percent	×10⁻⁶	×10⁻⁶	×10⁻⁶
0.00	16.8 (2)	17.2 to 17.3 (2)	17.6 to 17.8 (2)
1.33	16.4 to 17.0 (14)	15.9 to 17.3 (11)	17.3 to 18.1 (8)
2.14	16.5 to 16.7 (9)	16.6 to 17.1 (8)	17.5 to 18.0 (7)
3.03	15.9 to 17.3 (6)	16.0 to 16.9 (4)	16.4 to 17.4 (4)

[a] This table does not include coefficients of expansion for temperature ranges in which critical regions were observed (fig. 9 to 13).
[b] Each number in parenthesis represents the number of determinations.

Table 3 gives several coefficients of expansion computed from the expansion curve obtained by Masing and Dahl (fig. 1) on a quenched copper-beryllium alloy containing 2.5 percent of beryllium. The coefficient obtained for the range from 300 to 20° C on cooling, is in satisfactory agreement with the corresponding coefficient obtained in the present investigation on the quenched alloy containing 2.14 percent of beryllium. However, the coefficient of expansion for the range from 20 to 100° C on heating is appreciably lower than the corresponding coefficient for the quenched 2.14-percent alloy of the present investigation.

TABLE 3.—*Coefficients of expansion of a quenched copper-beryllium alloy containing 2.5 percent of beryllium*

[Computed [a] from data by Masing and Dahl [5]]

Temperature range	Average coefficient of expansion per degree C
°C	×10⁻⁶
20 to 100	14.2
100 to 200	15.4
20 to 200	14.9
300 to 20	[b] 18.2

[a] By Hidnert.
[b] From curve on cooling.

Table 4 shows the length changes, the densities before and after the expansion tests, and the volume changes of the samples of copper-beryllium alloys. The changes in length, density, and volume noted for both the quenched and the hard-drawn samples are somewhat larger than the small changes noted for the aged alloys. The changes

in length, volume, and density of a quenched copper-beryllium alloy depend upon the temperature and the time of aging. Masing and Dahl [5] obtained a volume change of 0.60 percent on a quenched copper-beryllium alloy containing 2.5 percent of beryllium, after

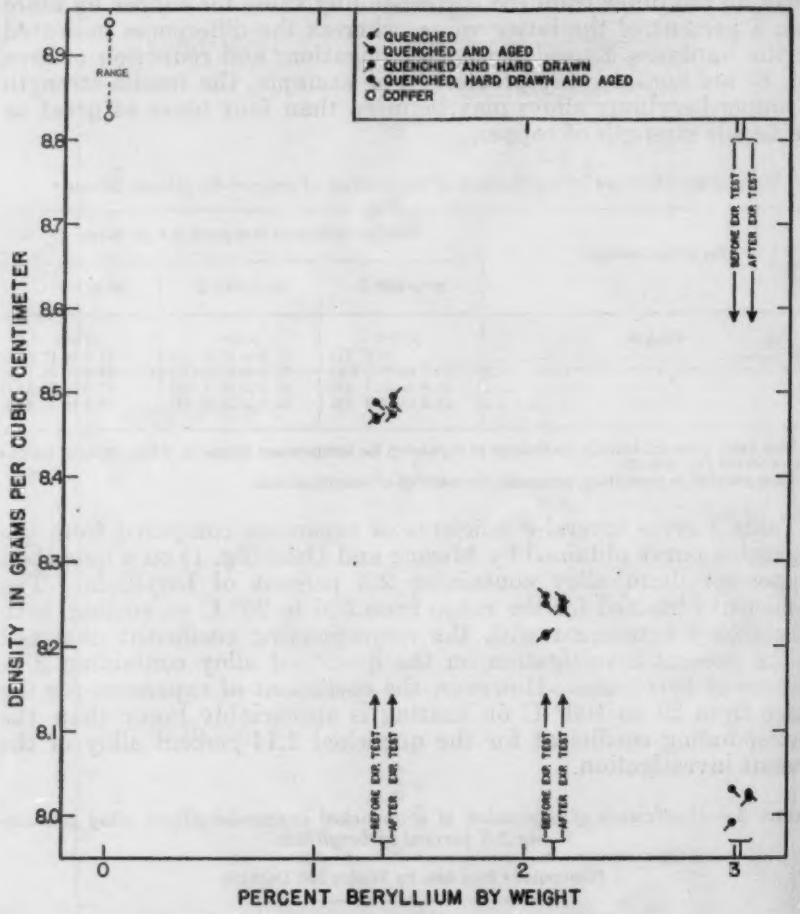

FIGURE 15.—*Density of copper-beryllium alloys.*

heating 78 hours at 250° C. They concluded that the change in volume is determined only by the quantity of γ crystals separated out and not by the form of the precipitate, as is the case with the hardness and electrical conductivity.

Figure 15 shows the densities of the samples indicated in table 4. The range of densities for copper, taken from BS Circular 73 [15], is included in the figure. The data show that the density of copper-beryllium alloys decreases with increase of beryllium.

TABLE 4.—*Changes in length, density, and volume of copper-beryllium alloys*

Sample	Beryllium content	Treatment	Change in length [a]	Density at 25° C		Change in volume [d]
				Before expansion tests [b]	After expansion tests [c]	
	Percent		*Percent*	g/cm³	g/cm³	*Percent*
1535	1.33	Quenched	[e]−0.09	8.468	8.492	−0.28
1535A	1.33	Quenched	−.10	8.466	8.492	−.30
1536	1.33	Quenched and aged	−.02	8.472	8.474	−.03
1533	1.33	Quenched and hard-drawn	−.04	8.471	8.475	−.05
1534	1.33	Quenched, hard-drawn, and aged	−.01	8.488	8.485	+.04
1539	2.14	Quenched	−.20	8.212	8.246	−.41
1540	2.14	Quenched and aged	−.01	8.260	8.254	+.07
1537	2.14	Quenched and hard-drawn	−.08	8.213	8.246	−.40
1538	2.14	Quenched, hard-drawn, and aged	−.00	8.250	8.243	+.09
1541	3.03	Quenched and hard-drawn	[f]	7.991	8.020	−.36
1542	3.03	Quenched, hard-drawn, and aged	−.01	8.031	8.025	+.07

[a] Each value is the algebraic sum of the changes in length (noted in the last column of table 1) for each sample.
[b] Density determined by W. S. Clabaugh of this Bureau.
[c] Density determined by L. J. Clark of this Bureau.
[d] Computed from the density before and after the expansion tests. The plus (+) sign indicates an increase in volume and the minus (−) sign a decrease in volume.
[e] At end of second expansion test.
[f] Distortion occurred during the first expansion test.

VI. SUMMARY

1. Data have been obtained on the linear thermal expansion of copper-beryllium alloys of three compositions and various heat treatments.

2. The expansion curves of quenched copper-beryllium alloys containing 1.33 and 2.14 percent of beryllium, showed critical regions which may be associated with structural changes accompanying aging.

3. Stabilization of copper-beryllium alloys may be accomplished either by tempering or by cold-working.

4. There is no simple relation between the coefficients of expansion, chemical composition, and heat treatment of the copper-beryllium alloys investigated. Figure 14 indicates the effects of beryllium content, cold-work, and heat treatment on the coefficients of expansion of these alloys.

5. Table 2 gives the ranges of the coefficients of expansion obtained on heating. The coefficients of expansion of the copper-beryllium alloys do not differ from the corresponding value for copper by more than 8 percent of the latter value, whereas the differences for the hardness, tensile strength, elongation, and reduction of area (fig. 8) are considerably greater. For example, the tensile strength of copper-beryllium alloys may be more than four times as great as the tensile strength of copper.

6. The changes in length, density, and volume noted for both the quenched and the hard-drawn alloys are somewhat larger than the small changes noted for the aged alloys (table 4). The changes in length, volume, and density of quenched copper-beryllium alloys depend upon the temperature and the time of aging.

7. The density of copper-beryllium alloys decreases with increase of beryllium (fig. 15).

The author expresses his appreciation to the American Brass Co., Waterbury, Conn., for their cooperation in this investigation. Acknowledgment is also due to the following members of the staff

of the National Bureau of Standards: H. W. Bearce, W. Souder, H. S. Rawdon, and J. G. Thompson for valuable suggestions and to J. Burks for assistance during part of this investigation.

VII. REFERENCES

[1] Hidnert and Sweeney, BS Sci. Pap. **22**, 533 (1927) S565.
[2] Illig, Wiss. Veröff. Siemens-Konzern **8**, Heft 1, 3 (1929). English translation by Richard Rimbach and A. J. Michel, Beryllium, Its Production and Application, p. 11 (The Chemical Catalog Co., Inc., New York, N. Y., 1932).
[3] Davis, Machine Design **5**, 23 (March 1933).
[4] Anonymous, The Engineer **5**, 624 (1933).
[5] Masing and Dahl, Wiss. Veröff, Siemens-Konzern **8**, Heft 1, 126 (1929). See English translation in reference [2], p. 164. See also Dahl and Haase, Z. Metallk. **20**, 433 (1928).
[6] Haas and Uno, Z. Metallk. **22**, 154 (1930).
[7] Borchers, Metallwirtschaft **11**, 317, 329 (Jan. to June 1932).
[8] Masing and Dahl, Wiss. Veröff, Siemens-Konzern **8**, Heft 1, 94 (1929).
[9] Schwarz, Z. Metallk. **22**, 198 (1930).
[10] BS Circular 73, 2d ed., p. 33 (Nov. 1922).
[11] Portevin, Metal Ind. (London), **42**, p. 491, 521, 543 (1933).
[12] Dahl, Holm, and Masing, Wiss. Veröff, Siemens-Konzern **8**, Heft 1, 154 (1929).
[13] Masing and Haase, Wiss. Veröff, Siemens-Konzern **8**, Heft 1, 142 (1929).
[14] Hidnert, BS Sci. Pap. **17**, 91 (1922) S410.
[15] BS Circular 73, 2d ed., p. 38 (Nov. 1922).

WASHINGTON, April 18, 1936.

U. S. DEPARTMENT OF COMMERCE NATIONAL BUREAU OF STANDARDS

RESEARCH PAPER RP891

Part of Journal of Research of the National Bureau of Standards, Volume 16, June 1936

A RAPID METHOD FOR THE DETERMINATION OF SILICA IN PORTLAND CEMENT

By Edwin E. Maczkowske

ABSTRACT

If ammonium chloride is mixed with portland cement before the cement is dissolved in hydrochloric acid, and the solution is then digested on the steam bath for 30 minutes, an accurate determination of silica can be made without the customary double evaporation of the solution. The results of the determination of silica in several brands of cement by this modified method are tabulated and compared with the results obtained by the standard method.

CONTENTS

	Page
I. Introduction	549
II. Recommended procedure for the rapid determination of silica in portland cement	550
III. Discussion of the method	551

I. INTRODUCTION

In the course of some work with a silicate of soda (waterglass), it was observed that ammonium chloride, in the presence of hydrochloric acid, facilitated the precipitation of the silicic acid in a thick jellylike mass. This effect of ammonium chloride suggested its possible use to shorten the time required for the determination of silica in materials such as portland cement. Preliminary results indicated that mixing solid ammonium chloride with the cement before it is decomposed with hydrochloric acid makes it possible to dispense entirely with the tedious double evaporation of the solution.

A review of the literature shows that a number of investigators have used ammonium chloride in somewhat similar ways. One of the earliest of these to use ammonium chloride in analyzing silicates decomposable by acids was Barta,[1] who found that the addition of solid ammonium chloride to the solution containing the silicic acid markedly increased the speed of filtration. Shigeynki Shinkai [2] observed that when ammonium chloride was added to a silicate hydrosol the latter was transformed into a hydrogel. This observation applied not only to pure silicates, but also to silicates containing Al_2O_3, Fe_2O_3, CaO, and MgO.

After the present work was begun, a paper by Zaitzev [3] appeared which describes the use of ammonium chloride in the analysis of

[1] R. Barta, Rev. matériaux construction trav. publics **166**, 156 (1923).
[2] Shigeynki Shinkai, J. Soc. Chem. Ind., Japan **29**, 303–5 (1926).
[3] M. I. Zaitzev, Zavodskaya Lab. **3**, 492–4 (1934).

cement. Zaitzev's method differs from the procedure that was developed in this laboratory, and is described in the next section, since he took a different weight of sample for analysis, and used different quantities of ammonium chloride and acid, and especially since he digested the solution on a steam bath for only 10 minutes.

II. RECOMMENDED PROCEDURE FOR THE RAPID DETERMINATION OF SILICA IN PORTLAND CEMENT

Mix thoroughly 0.500 g of cement and an approximately equal weight of ammonium chloride crystals in a 50-ml Pyrex beaker, cover the beaker with a watchglass, and add cautiously 5 ml of hydrochloric acid (sp gr 1.18) from a pipette, allowing the acid to run down the lip of the covered beaker.

After the chemical action has subsided, lift the cover slightly and stir the mixture with a glass rod, replace the cover and set the beaker on the steam bath for 30 minutes. During this time of digestion stir the contents occasionally and break up any remaining lumps to facilitate complete solution of the cement.

Fit a 9-cm quantitative filter paper of medium fineness to a funnel, place a small quantity of macerated filter paper, about the size of a large pea, in the bottom of the cone, and wash the filter thus prepared once or twice with hot water. Transfer the jelly-like mass of silicic acid as completely as possible, without dilution, to the filter and allow the hydrochloric acid solution to drain through.

Loosen adhering particles in the beaker by means of a small rubber policeman and wash them on to the filter with hot water; finally wipe the inside of the beaker thoroughly with a small piece of filter paper and place this in the filter. Wash with small portions of hot water, allowing each portion to run through completely, until the volume of the filtrate is about 125 ml. Complete the determination by the standard procedure.

III. DISCUSSION OF THE METHOD

To compare the results of this modified procedure with the conventional one, seven samples of cement of varying silica content were analyzed by the two methods. Three determinations by each method were made on each sample, and these triplicate determinations were made at different times.

The procedure used for checking the ammonium chloride method was a double dehydration with hydrochloric acid and with a filtration between dehydrations. Platinum dishes were used for evaporation and dehydration. Evaporations were made on the steam bath and the residues were dried for 1 hour at 115 to 120° C. in an electric oven.

By following the procedure used in standard methods, it is possible to recover, from the R_2O_3-group precipitate, silica which may have escaped into the acid filtrate as a soluble silicate. In the present study the silica recovery was not made in all the samples used. However, determinations on a few samples showed that the amount of silica passing into the acid filtrate was small, and of the same order of magnitude in the two methods, varying from 0.2 to 0.9 mg.

The results obtained from the determinations of silica on seven samples of portland cement by two analysts are shown in table 1.

TABLE 1.—*Comparison of results obtained by the rapid and standard methods*

[SiO_2 IN 0.500-g SAMPLES OF PORTLAND CEMENTS]

Analyst	Cement	Experiment	Crude SiO_2		Residue after HF treatment		Refined SiO_2	
			Rapid method	Standard method	Rapid method	Standard method	Rapid method	Standard method
			g	g	g	g	g	g
1	A	1	0.1066	0.1071	0.0007	0.0009	0.1059	0.1062
		2	.1064	.1070	.0004	.0008	.1060	.1062
		3	.1068	.1067	.0008	.0005	.1060	.1062
Average value							.1060	.1062
1	B	1	.1192	.1198	.0005	.0008	.1187	.1190
		2	.1188	.1200	.0004	.0009	.1184	.1191
		3	.1198	.1193	.0009	.0006	.1189	.1187
Average value							.1187	.1189
1	C	1	.1105	.1100	.0013	.0009	.1092	.1091
		2	.1098	.1103	.0008	.0012	.1090	.1091
		3	.1101	.1096	.0012	.0005	.1089	.1091
Average value							.1090	.1091
1	D	1	.1008	.1015	.0004	.0010	.1004	.1005
		2	.1007	.1017	.0003	.0008	.1004	.1009
		3	.1010	.1009	.0006	.0006	.1004	.1003
Average value							.1004	.1006
1	E	1	.1004	.1002	.0006	.0007	.0998	.0995
		2	.1007	.1009	.0006	.0008	.1001	.1001
		3	.1008	.1006	.0006	.0004	.1002	.1002
Average value							.1000	.0999
1	F	1	.1076	.1072	.0006	.0008	.1070	.1064
		2	.1074	.1078	.0005	.0008	.1069	.1070
		3	.1073	.1075	.0004	.0005	.1069	.1070
Average value							.1069	.1068
2	G	1	.1029	.1031	.0009	.0008	.1020	.1023
		2	.1033	.1037	.0008	.0008	.1025	.1029
		3	.1030	.1027	.0008	.0006	.1022	.1021
		4	.1031	.1035	.0008	.0008	.1023	.1027
		5	.1031	.1029	.0009	.0007	.1022	.1022
		6	.1032	.1035	.0009	.0007	.1023	.1028
Average value							.1023	.1026

Table 2 shows the results of a further series of experiments, in which four operators used the rapid procedure in comparison with the standard procedure, on a single sample of cement.

TABLE 2.—*Determinations on the same sample by different analysts with the rapid method*

[SiO_2 IN A 0.500-g SAMPLE OF PORTLAND CEMENT NO. A]

Experiment	Analyst 1		Analyst 2		Analyst 3		Analyst 4	
	[1] SiO_2	Deviation from standard average value	SiO_2	Deviation from standard average value	SiO_2	Deviation from standard average value	SiO_2	Deviation from standard average value
	g	g	g	g	g	g	g	g
1	0.1059	−0.0003	0.1058	−0.0004	0.1058	−0.0004	0.1058	−0.0004
2	.1060	−.0002	.1056	−.0006	.1058	−.0004	.1060	−.0002
3	.1060	−.0002	.1057	−.0005	.1059	−.0003	.1057	−.0005
Average value	.1060	−.0002	.1057	−.0005	.1058	−.0004	.1058	−.0004

[1] The average result obtained by the standard method = 0.1062 g.

Table 3 shows the effect of the time of digestion on the amount of silica recovered from a sample of portland cement by the rapid method. While 5 to 10 minutes' digestion on the bath, as suggested by Zaitzev, may be satisfactory with most cements, our experience has shown that 30 minutes' digestion is necessary to completely decompose the silicates in some samples.

TABLE 3.—*Effect of time of digestion on the amount of silica recovered by the rapid method as compared with the standard method*

[SiO_2 IN A 0.500-g SAMPLE OF CEMENT]

Sample	10 minutes on steam bath		15 minutes on steam bath		30 minutes on steam bath		Double dehydration
	SiO_2	Deviation from standard average value	SiO_2	Deviation from standard average value	SiO_2	Deviation from standard average value	SiO_2
	g	g	g	g	g	g	g
A	0.1050	−0.0012	0.1056	−0.0006	0.1060	−0.0002	0.1062
B	.1174	−.0015	.1178	−.0011	.1187	−.0002	.1189
C	.1083	−.0007	.1085	−.0005	.1090	.0000	.1090
D	.0996	−.0010	.1001	−.0005	.1004	−.0002	.1006

The principal advantage of this modified procedure for the determination of silica in cement is that an analysis can be carried to the stage of igniting the silica in about an hour, instead of 1 day, thus expediting not only the determination of silica, but also the preparation of the solution for the determination of other constituents. There may also be a gain in accuracy.

Although the present study of the effect of ammonium chloride on the determination of silica has been limited to the analysis of portland cement, there appears to be no reason why its use cannot be extended to other siliceous materials which are decomposed by acids in preparation for analysis.

WASHINGTON, April 18, 1936.

U. S. Department of Commerce National Bureau of Standards

RESEARCH PAPER RP892

Part of Journal of Research of the National Bureau of Standards, Volume 16, June 1936

NOTE ON THE THERMAL MUTAROTATION OF *d*-GALACTOSE, *l*-ARABINOSE, AND *d*-TALOSE

By Horace S. Isbell and W. W. Pigman

It has been found that on changing the temperature of aqueous solutions of galactose, arabinose, and talose, mutarotations occur which give maximum values similar to the mutarotations of ribose,[1] and β-glucoheptose.[2] The first stage of these mutarotations, hereafter called thermal mutarotations, is found to be largely due to a change in the concentration of the labile constituents whose presence was discovered by Riiber and Minsaas.[3] The later slow change presumably corresponds to a disturbance in the equilibrium of the α- and β-normal isomers such as that previously noted by Hudson.[4]

In order to compare the thermal mutarotations with the ordinary mutarotations new measurements on the above compounds were made at 0 and 20° C. The results obtained with 4-percent aqueous solutions are expressed by the following equations:

α-*d*-Galactose:

$$[\alpha]_D^{20} = 64.9 \times 10^{-0.00803t} + 5.6 \times 10^{-0.079t} + 80.2.$$
$$[\alpha]_D^{0} = 66.3 \times 10^{-0.00093t} + 2.7 \times 10^{-0.0119t} + 84.0.$$

$$\text{Thermal mutarotation} = 0.9 \times 10^{-0.00107t} - 3.0 \times 10^{-0.0132t} + 84.0.$$

(25.0⟶0.3° C).

α-*l*-Arabinose:

$$[\alpha]_D^{20} = 77.3 \times 10^{-0.030t} + 8.8 \times 10^{-0.138t} + 104.5.$$
$$[\alpha]_D^{0} = 78.9 \times 10^{-0.00362t} + 5.9 \times 10^{-0.0217t} + 109.2.$$

$$\text{Thermal mutarotation} = 1.6 \times 10^{-0.00364t} - 4.9 \times 10^{-0.0271t} + 109.2.$$

(25.2⟶0.2° C).

α-*d*-Talose:

$$[\alpha]_D^{20} = 9.3 \times 10^{-0.0263t} + 37.9 \times 10^{-0.126t} + 20.8.$$
$$[\alpha]_D^{0.1} = 9.8 \times 10^{-0.00362t} + 27.5 \times 10^{-0.0255t} + 25.2.$$

$$\text{Thermal mutarotation} = 0.15 \times 10^{-0.0036t} - 5.0 \times 10^{-0.0289t} + 25.2.$$

(25.8⟶0.1° C).

[1] Phelps, Isbell, and Pigman, J. Am. Chem. Soc. **56**, 747 (1934).
[2] Isbell, J. Am. Chem. Soc. **56**, 2789 (1934).
[3] Ber. deut. Chem. Ges. **59**, 2266 (1926).
[4] J. Am. Chem. Soc. **31**, 80 (1909).

The thermal mutarotations were obtained by cooling the aqueous solutions rapidly from 25 to 0 ° C, measuring the optical rotations at various times, t, after the temperature change. The ordinary mutarotations of α-d-galactose and α-l-arabinose are in approximate agreement with those of Lowry and Smith [5] and Riiber and Sørensen,[6] while heretofore the mutarotations of α-d-talose had not been previously reported in equation form. The exponents representing the velocity constants for the reactions comprising the thermal mutarotations agree approximately with the corresponding constants for the ordinary mutarotations.

Inasmuch as the rapid reactions comprise a large part of the thermal mutarotations, the equilibrium proportions of the labile constituents vary markedly with temperature, indicating that the heat of reaction is considerable. The proportions of the α- and β-modifications change to a lesser degree, and hence the heat of interconversion is smaller.

Assuming that the changes during mutarotation are due to two simultaneous reactions, application of the Arrhenius equation,

$$ln\frac{k_1}{k_2}=\frac{Q}{R}\left(\frac{1}{T_2}-\frac{1}{T_1}\right)$$

to the exponents representing the rate of change for the rapid reactions at 0 and 20° C gives values for Q corresponding to 15,040, 14,700, and 12,750 calories per mole for α-d-galactose, α-l-arabinose, and α-d-talose; application of the same equation to the slow reactions gives values corresponding to 17,130, 16,800, and 15,820. The mean heat of activation, Q, for the substances corresponding to the rapid change in mutarotation is therefore less than the mean heat of activation for the slow change which comprises the interconversion of the α- and β-normal sugars.

WASHINGTON, April 28, 1936.

---

[5] J. Phys. Chem. **33**, 9 (1929).
[6] Kgl. Norske Videnskab. Selskabs, Skrifter, no. 7, 50 (1933).

U. S. DEPARTMENT OF COMMERCE NATIONAL BUREAU OF STANDARDS

RESEARCH PAPER RP893

Part of Journal of Research of the National Bureau of Standards, Volume 16, June 1936

DETERMINATION OF SULPHURIC ANHYDRIDE IN PORTLAND CEMENT BY MEANS OF THE WAGNER TURBIDIMETER

By Robert B. Rudy

ABSTRACT

A turbidimetric method is described for the rapid routine determination of sulphuric anhydride in portland cement by means of the Wagner turbidimeter. The results of several determinations on different brands of cement are tabulated and compared with the results obtained by the standard method.

CONTENTS

	Page
I. Introduction	555
II. General considerations	556
III. Experimental details	557
1. Description of apparatus	557
2. Calibration of turbidimeter	558
IV. Recommended procedure	560
V. Data and discussion of results	561

I. INTRODUCTION

For the past 40 years various attempts have been made to develop a satisfactory turbidimetric method for the determination of sulphuric anhydride in portland cement. The Federal specification for portland cement (SS–C–191) and the American Society for Testing Materials standards call for the usual barium sulphate precipitation—a procedure which is entirely satisfactory for umpire determinations but too time-consuming for routine tests. A sufficiently accurate and dependable turbidimetric method would afford considerable saving in time and effort in cement plants and other laboratories making large numbers of control tests.

As early as 1896 Hinds [1] developed a candle turbidimeter for this purpose. Five years later Jackson [2] published a modification of Hinds' method, in which details of technique were more carefully worked out. The Jackson-Hinds method is given without change in Meade's book [3] on portland cement, published in 1926.

Since these first efforts, various investigators have offered improvements in both method and apparatus. Muer [4] improved the precision of his results by using solid barium chloride as the precipitant.

[1] J. I. D. Hinds, J. Am. Chem. Soc. **18**, 661 (1896).
[2] D. D. Jackson, J. Am. Chem. Soc. **23**, 799 (1901).
[3] Richard K. Meade, Portland Cement, p. 466 (1926).
[4] H. F. Muer, J. Ind. Eng. Chem. **3**, 553 (1911).

McBride and Weaver,[5] in their work on the determination of sulphur in illuminating gas by means of a turbidimeter, studied the effect of variations in acid concentration and temperature of the solution. In 1931 Parr and Staley [6] developed a turbidimeter which was notable for several mechanical improvements.

All the instruments and methods referred to depend for their accuracy upon the operator's ability to judge the point of disappearance of a candle-flame image or lamp filament, when obscured by a turbid solution. With the development of the photoelectric cell and its application to turbidimetric measurements, it has become possible to eliminate the personal factor in these observations and to increase the accuracy and dependability of the results. In 1933 Wagner [7] constructed a turbidimeter using a photoelectric cell (Weston photronic type) for determining the fineness of portland cement. With this improved instrument a satisfactory technique was evolved for the determination of sulphuric anhydride in cement.

II. GENERAL CONSIDERATIONS

In addition to a sufficiently sensitive apparatus for measuring turbidity, the success of a nephelometric method for the determination of sulphuric anhydride depends upon the reproduction of approximately the same barium sulphate particle size in suspensions obtained from a given concentration of sulphate ions. The most important variables affecting the particle size of a barium sulphate precipitate obtained from a solution of portland cement are as follows:

1. Acid concentration of the solution.
2. Concentration of other substances in the solution.
3. Temperature of the solution.
4. The crystal size and amount of barium chloride.
5. The manner in which the solution is agitated after the addition of the barium chloride.

Several authors have pointed out that variations in acid concentration have a marked effect on the results obtained, but this factor may be adequately controlled without loss of time by the use of some simple measuring device such as a pipette with the delivery tube cut off near the bulb, to facilitate handling of the acid when a sample is being dissolved. There is reason to believe that variations in the amounts of other substances in the solution affect the particle size of the barium sulphate, but it was found that variations in turbidity, due to differences in composition of the cements studied, were negligible. It is not difficult to maintain the solution within a degree or two of the specified temperature and more accurate control is not necessary. In the method described, 25° C is specified, but the calibration and subsequent determinations could be made at any convenient and arbitrarily chosen temperature between 20 and 30° C.

Probably the most important factor in the reproduction of particle size is the form of the precipitating reagent. Even with less sensitive types of turbidimeters the use of barium chloride solutions was found to be unsatisfactory. Muer recommends the use of barium chloride tablets, which were fairly effective with a visual

[5] R. S. McBride and E. R. Weaver, BS Tech. Pap. 3, 1 (1913), T20.
[6] S. W. Parr and W. D. Staley, Ind. Eng. Chem. Anal. ed. 3, no. 1, 66 (1931).
[7] L. A. Wagner, Proc. Am. Soc. Testing Materials, 33, II, 553 (1933).

type of instrument, but it was found in this laboratory that they were not suitable for use with the more sensitive type of turbidimeter utilizing a photoelectric cell. Experiments show that approximately 0.5 g of 40- to 80-mesh barium chloride crystals gives satisfactory results. Smaller crystals dissolve too rapidly and cause erratic results like those which accompany the use of barium chloride solutions. Larger crystals can be used but are troublesome to obtain. Furthermore, if a wide range of sizes is used, different bottles of crystals may vary too much in size distribution. Muer has pointed out the variations in turbidity which result from the use of different sizes of crystals and his findings have been confirmed in this laboratory.

The manner in which the solution is stirred after the addition of the barium chloride has a decided effect on the particle size of the precipitate. Violent agitation causes the barium chloride to dissolve too rapidly, and if the solution is stirred too gently, precipitation of the barium sulphate takes place so slowly that the turbidity changes (increases) while the determination is in progress. The best rate of stirring is one which causes nearly all the barium chloride to dissolve during the prescribed 30-second period of stirring. When the barium sulphate precipitation is conducted according to the recommended method, no change (decrease) in turbidity due to crystal growth or settling of the precipitate is indicated by the microammeter in less than 2 minutes after precipitation is complete.

III. EXPERIMENTAL DETAILS

1. DESCRIPTION OF APPARATUS

A detailed description of the Wagner turbidimeter may be found in the proceedings of the American Society for Testing Materials, volume 33, part II, pages 566–570 (1933), but for convenience a brief description is included here. Referring to figure 1, light source L is a 6-candlepower electric lamp operated by a 6-volt storage battery. A parabolic reflector rigidly attached to the lamp mounting throws a beam of approximately parallel light rays through water cell W [8] and into glass tank T containing a suspension of barium sulphate particles. The light passing through the tank strikes photoelectric cell C (Weston photronic type) and the current generated in the cell is measured with a microammeter. The reading obtained affords a measure of the turbidity of the suspension. R_1 and R_2 are rheostats for regulating the intensity of the light. Filter F (Eastman filter no. 35D has been found suitable), mounted in front of the opening in shield S, reduces the intensity of the light when the tank containing the barium sulphate suspension is not in place, and also serves as a reference standard for light intensity.

The stirring requirement is readily met by agitating the solution with a glass rod which is rotated at about 225 rpm by means of any suitable mechanical device. The rod should be bent about 2 inches from the end so that the tip describes a circle about 1 inch in radius. Its position should be adjusted so that the end of the rod is ¼ to ½ inch

[8] The function of the water cell is to absorb most of the radiant heat of the light. This cell is a desirable feature of the apparatus when used for the determination of specific surface but it is not essential for determinations of sulphuric anhydride. Movable base B is likewise not needed for these determinations, and is allowed to remain in its lowermost position.

above the bottom of the beaker. A 250-ml beaker is recommended, and it is also to be noted that the same size of beaker must always be used in order that the stirring action be uniform. It is desirable to maintain the speed of the stirring device constant within 25 rpm and at all times within the limits of 200 to 250 rpm. The speed of the stirrer can be readily ascertained by allowing the stirring rod to strike a finger and counting the revolutions over a short interval, such as 15 or 20 seconds.

When the instrument is in use, it is necessary that the lamp in the turbidimeter be maintained at some "standard" brightness. This is accomplished by adjusting the filament temperature by means of the rheostats so that the reading on the microammeter, observed with the colored-glass filter in place but with the solution tank removed, reaches a predetermined value. This value is obtained in the following manner.

Using a sample of cement of known sulphuric anhydride content (determined by the standard gravimetric method), weigh an amount which will furnish exactly 0.100 g of the anhydride. For example, if a sample containing 1.80 percent of sulphuric anhydride is used, 0.5555 g will be required. Dissolve this sample, and precipitate the barium sulphate as directed in the recommended procedure. Transfer to the turbidimeter tank a portion of the solution sufficient to bring its surface well above the light beam. Carefully place the tank against the stops in the instrument. Remove the colored-glass filter and close the cabinet. Adjust the brightness of the lamp so that a reading of approximately 24 microamperes is obtained about 1 minute after the solution is removed from the stirrer and placed in the instrument. Replace the colored-glass filter,[9] remove the tank containing the turbid solution, and observe the reading on the microammeter. This value will then constitute the "standard setting" of the instrument for the particular filter used. This setting is, of course, arbitrary, and the nearest whole-scale division on the meter may be chosen as the standard setting. Subsequently, when the turbidimeter is used, the brightness of the lamp must first be adjusted so that exactly the same predetermined reading is obtained through the colored-glass filter, after the lamp has been allowed to burn for about 5 minutes in order to give the photoelectric cell an opportunity to reach a state of equilibrium.

If a reliable storage battery is used, the reading will remain quite constant for a period sufficient to make several tests. However, it is advisable to check this reading from time to time during a series of determinations and adjust the rheostats in case there has been any change in the brightness of the lamp.

2. CALIBRATION OF TURBIDIMETER

To obtain the data for the calibration curve of the turbidimeter, a single cement is used, of which the sulphuric anhydride content has been determined by the method given in Federal Specification SS–C–191. Various weights of the cement are taken in order to obtain the desired amounts of sulphuric anhydride. The weights of sulphuric anhydride are then calculated as percentages based on a

[9] To avoid possible injury to the microammeter, be sure that either the filter or the tank containing a barium sulphate suspension is in the path of the light beam at all times.

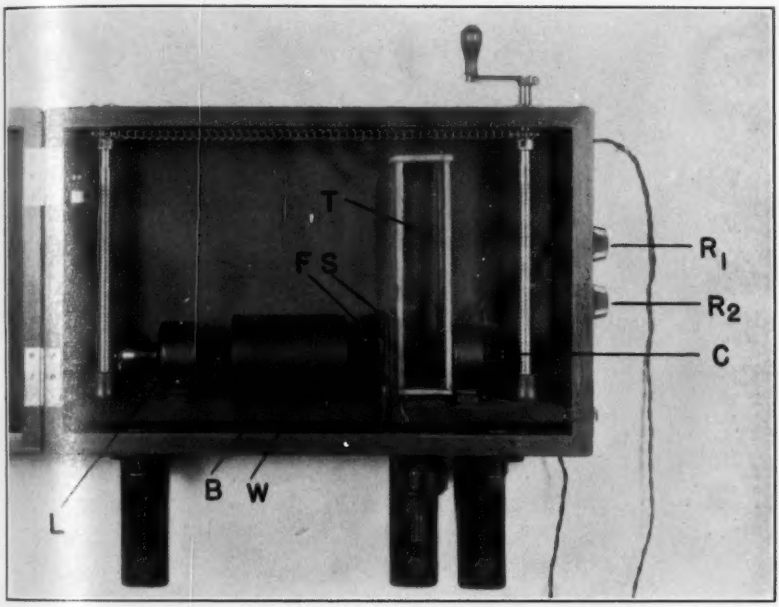

FIGURE 1.—*The Wagner turbidimeter.*

0.500–g sample (instead of the weight of sample actually taken) and these percentages are plotted against the corresponding microammeter readings. Subsequently, when determinations are made on 0.500–g samples, the percentages of sulphuric anhydride may be read directly from the curve. In this method of calibration, there is

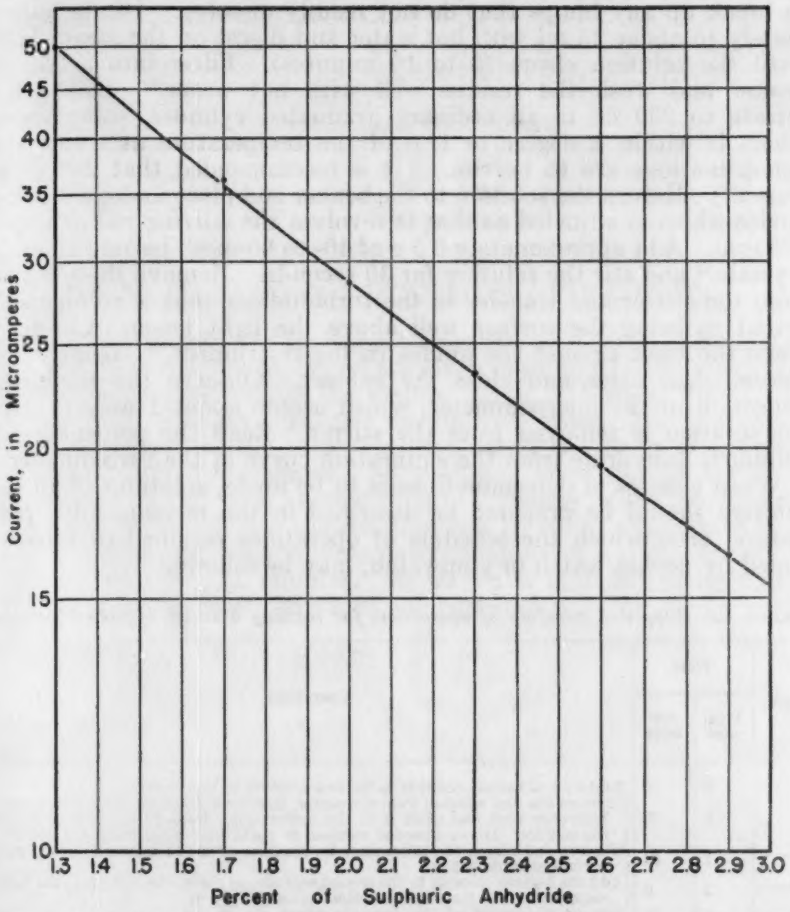

FIGURE 2.—*Typical curve showing the relation between microammeter reading and the percentage of sulphuric anhydride in 0.5-g samples.*

of course some variation in the amounts of materials in solution (other than sulphates). These variations probably have some effect on the particle size of the barium sulphate, but the error thereby introduced is small as compared with the effects of other variables. The typical curve shown in figure 2 was prepared in the manner described. Each of the points is the average of three determinations It will be noted that the curve, plotted on semilog paper, very nearly approaches a straight line. Changes in the optical system, such as replacement of the photoelectric cell or the solution tank, will necessitate recalibration of the instrument.

IV. RECOMMENDED PROCEDURE

To 0.500 g of cement in a 150-ml beaker add 10 ml of cold water (room temperature) and swirl the mixture until the sample is thoroughly dispersed. Continue swirling and add 5 ml of hydrochloric acid (sp gr 1.18). When necessary, a glass rod may be used to break up any lumps that do not readily dissolve. Dilute immediately to about 35 ml with hot water and digest on the steam bath until the solution clears (5 to 10 minutes). Filter into a 250-ml beaker and wash the residue well with hot water.[10] Dilute the filtrate to 200 ml in an ordinary graduated cylinder, using water which is within a degree or two of the temperature at which the determinations are to be run. (It is recommended that 25° C be chosen.) Return the solution to the beaker and place under a stirring device which is adjusted so that it revolves the stirring rod at about 225 rpm. Add approximately 0.5 g of 40- to 80-mesh barium chloride crystals,[11] and stir the solution for 30 seconds. Remove the solution from the stirrer and transfer to the turbidimeter tank a volume sufficient to bring the surface well above the light beam. Carefully place the tank against the guides in the instrument,[12] remove the colored-glass filter and close the cabinet. Observe the minimum deflection of the microammeter, which occurs about 1 minute after the solution is removed from the stirrer. Read the percentage of sulphuric anhydride from the calibration curve of the turbidimeter.

When a series of determinations is to be made, solutions of all the samples should be prepared as described in the recommended procedure, after which the schedule of operations outlined in table 1, timed by pocket watch or stopwatch, may be followed.

TABLE 1.—*Suggested schedule of operations for making a series of determinations*

Series	Time		Operations
	Minutes	Seconds	
A	0	0	Add 0.5 g of barium chloride to the first solution on the stirrer.
B	0	30	Remove the first solution from the stirrer, transfer a sufficient portion to the turbidimeter tank and place it in the instrument. Remove the filter and close the cabinet. Dilute a second solution to 200 ml and place under the stirrer.
C	1	30	Observe and record the microammeter reading. Fill the measuring scoop with barium chloride (0.5 g).
A1	2	0	Add the barium chloride to the second solution on the stirrer. Replace the filter, remove the tank from the turbidimeter and empty it.
B1	2	30	Remove the second solution from the stirrer, etc., etc.

[10] Some cements contain so little insoluble material that this filtration may be omitted if only approximate values are desired.

[11] Barium chloride crystals may be measured with sufficient accuracy by means of a small scoop, which can be readily made from a piece of ¼ inch inside diameter brass tubing about 7/16 inch long, attached to a suitable handle. (Volume about 0.022 cu in or 0.35 ml).

[12] Care must be exercised to see that the tank containing the turbid solution is placed in exactly the same position each time.

TABLE 2.—*Comparison of gravimetric and turbidimetric results*

GRAVIMETRIC RESULTS

Analyst	Sample					
	1	2	3	4	5	6
	%	%	%	%	%	%
A	2.24	1.77	2.44	1.53	2.08	1.35
E	2.26	1.78	2.44	1.50	2.08	1.33

TURBIDIMETRIC RESULTS

A	2.27	1.79	2.45	1.56	2.09	1.35
B	2.24	1.80	2.43	1.56	2.08	1.36
C	2.24	1.82	2.45	1.54	2.05	1.34
D	2.26	1.79	2.48	1.53	2.09	1.33

V. DATA AND DISCUSSION OF RESULTS

The results obtained by several operators on a series of six samples tested in the manner described are given in table 2. The gravimetric figures were obtained by the method given in Federal Specification SS–C–191. The turbidimetric results were obtained in the numerical order given in the table, rather than in the order of increasing sulphuric anhydride content, so that any error due to lag of the photoelectric cell with change in light intensity might be apparent.

It will be noted that the readings can be taken at the rate of one every 2 minutes. A complete determination on a single sample can be made in about 15 minutes. As shown in table 2, the turbidimetric method is accurate to about one part in fifty.

WASHINGTON, April 18, 1936.

U. S. DEPARTMENT OF COMMERCE NATIONAL BUREAU OF STANDARDS

RESEARCH PAPER RP894

Part of Journal of Research of the National Bureau of Standards, Volume 16, June 1936

AN ALTERNATING-CURRENT MAGNETIC COMPARATOR, AND THE TESTING OF TOOL-RESISTING PRISON BARS

By Raymond L. Sanford

ABSTRACT

This paper describes an instrument developed primarily for the purpose of testing tool-resisting prison bars, but which can be used for other practical applications of magnetic analysis. It is essentially an alternating-current bridge whose indications depend upon differences in the shapes of the magnetic hysteresis loops of the test specimen and a reference specimen of known quality. The instrument is simple to operate, portable, comparatively rugged, and operates from the ordinary alternating-current lighting circuit.

CONTENTS

		Page
I.	Introduction	563
II.	Preliminary experiments	564
III.	Description of the instrument	566
IV.	Auxiliary apparatus	569
V.	Experimental results	569
VI.	Conclusion	574

I. INTRODUCTION

The purpose of this paper is to describe the alternating-current magnetic comparator developed during the course of an investigation on the nondestructive testing of tool-resisting prison bars and to discuss some of the results obtained with it. The investigation was undertaken at the request and with the support and cooperation of the Bureau of Prisons of the United States Department of Justice. The term "tool-resisting", for the present purpose, relates to material having such properties that it cannot be cut through with any tool or implement likely to come into the possession of a prison inmate. Obviously, it is very desirable to be able to inspect such bars in order to be sure that they have the requisite tool-resisting properties. It is also desirable that the testing method shall be reliable, convenient to apply, and nondestructive. The usual types of tool-resisting bars are of composite material consisting of two components, one hard and the other soft. The hard component is entirely surrounded by the soft material and, consequently, the ordinary tests for hardness cannot be applied.

Magnetic methods appeared to be the most feasible way of accomplishing the desired object and were given first consideration. A certain degree of success has been attained, and it seems likely that the remaining difficulties can be overcome.

II. PRELIMINARY EXPERIMENTS

There are several types of tool-resisting bars in use which differ with respect to the kind of steel employed and in the arrangement of the hard inserts. Two different arrangements of the inserts are illustrated in figure 1. This shows cross sections which have been etched so as to reveal the location of the inserts. The light-colored portions are the soft matrix material and the dark portions are the hard inserts. It is easy to see that the magnetic testing of such specimens presents some difficulties not ordinarily encountered in other applications of magnetic analysis. The principal difficulty is due to the small proportion of the material represented by the hard inserts whose properties are of primary importance. The main problem, therefore, was to discover some magnetic characteristic of the bars depending primarily on the condition of the hard inserts and whose variations are not masked by variations in the characteristics of the soft matrix material, which constitutes about three-quarters of the whole bar.

Before undertaking a systematic study of the magnetic characteristics of the bars, experiments were made with the apparatus shown in figure 2, which seemed to offer some promise. A short section of the bar to be tested was magnetized by means of a small U-shaped electromagnet. A magnetic balance was placed on the opposite side of the bar in a definite position with respect to the poles of the electromagnet. The balance consisted essentially of a short bar of magnetically soft material mounted on pivots in jewel bearings and mechanically balanced. By means of a spiral spring and a graduated dial, a measure of the force with which one end of the balance bar was attracted to the specimen could be obtained. A stop prevented the pivoted bar from making actual contact with the specimen. Readings were taken with the balance applied opposite each pole of the electromagnet and the results were averaged. In general, bars with hard inserts gave higher readings than those with soft inserts.

The apparatus was taken to the United States Industrial Reformatory at Chillicothe, Ohio, where tests were made on 152 bars. Two bars whose readings were 38.5 and 29, respectively, were removed from one window. The bar which gave the higher reading could not be cut through with a hand hacksaw, but the other was cut in two with little difficulty. The results on the other bars, however, were not very satisfactory. There was no definite separation into groups having high and low readings, respectively, and therefore the results could not be interpreted with any degree of certainty. Subsequent experiments in the laboratory led to the conclusion that variations in experimental conditions, not subject to control, influenced the results to such an extent that they could not be relied upon to indicate the quality of the bars. For this reason, no attempt at further development of the apparatus was made and attention was turned toward the discovery of some other method not subject to the same limitations.

Further experimental work was greatly facilitated by an experimental grille furnished by the Bureau of Prisons. This grille consisted of interchangeable bars of both kinds illustrated in figure 1. Some of the bars were hardened and some were soft. By the use of

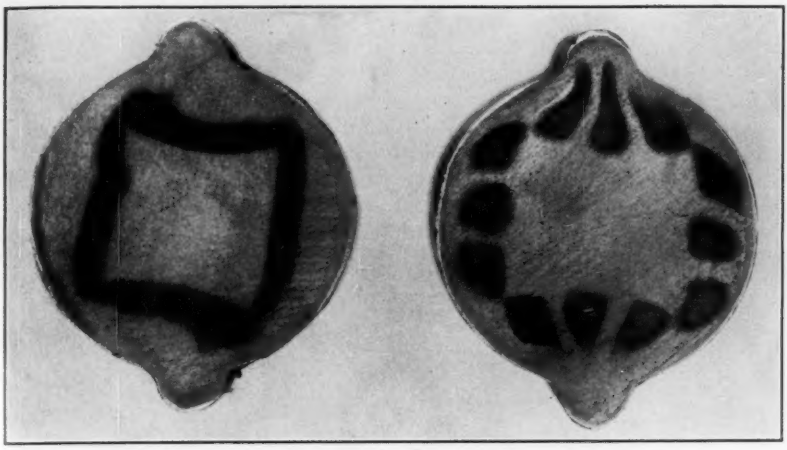

FIGURE 1.—*Typical sections of tool-resisting prison bars.*
The dark parts are the hardened inserts and the light part is the soft matrix material

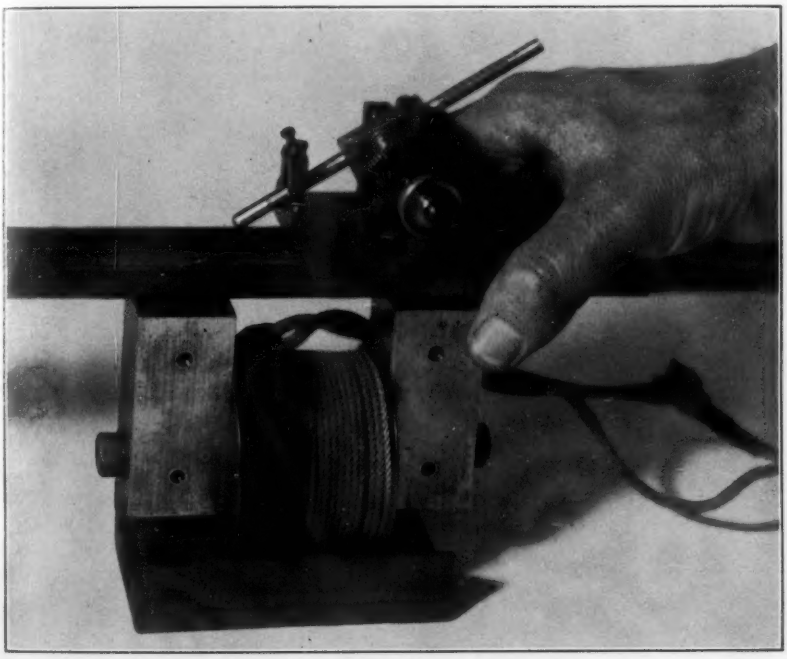

FIGURE 2.—*Magnetic balance applied to a tool-resisting prison bar.*

UNIV. OF MICH.

this grille, it was possible to set up in the laboratory various conditions likely to be encountered in the field.

Before attempting to devise new testing apparatus, the ordinary magnetic properties of several bars, both hard and soft, were determined by the usual methods. Figure 3 shows the normal induction curves for two bars. The lower curve was obtained for a bar so hard that it could not be cut with a hacksaw. The other bar had soft inserts and could easily be cut in two. Although these bars show a definite difference in permeability, small differences in the permeability of the soft matrix material, which constitutes three-quarters of the whole, could easily mask the effect of relatively large variations in the inserts.

Hysteresis loops for the same two bars are shown in figure 4. Although there is little difference in the values of residual induction

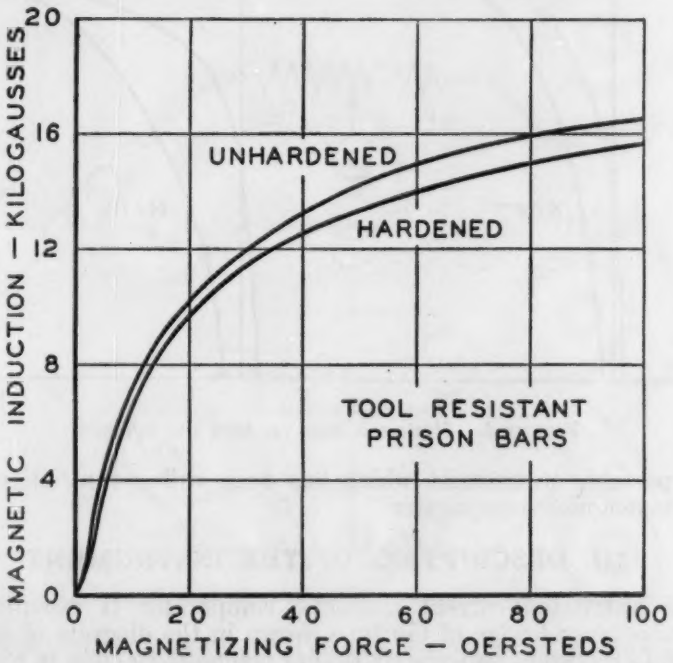

FIGURE 3.—*Normal induction curves for prison bars having hard and soft inserts.*

or coercive force, there is a marked difference in the shape of the two loops. The broadening of the upper part of the loop is characteristic of magnetically inhomogeneous materials and is due to the difference in the magnetic characteristics of the two kinds of steel of which the bars are composed. These results indicated that the shape of the hysteresis loop was the criterion most likely to be useful for distinguishing between hard and soft inserts.

As the determination of hysteresis loops by the usual direct-current methods is a rather tedious procedure, it seemed best to investigate the possibility of using an alternating-current method. Although

most of the alternating-current tests which have been applied to other types of test specimen depend primarily on variations in permeability, several of these were tried out, but none of them proved to be satisfactory. A circuit was then tried out by which the distortion of the wave form of the magnetizing current due to hysteresis was shown by means of an oscillograph. By this method it was possible to distinguish between very hard bars and very soft ones, but it was not possible to detect smaller differences satisfactorily. However, a circuit was finally hit upon by means of which differences in distortion are indicated in numerical terms, and this circuit was incorporated

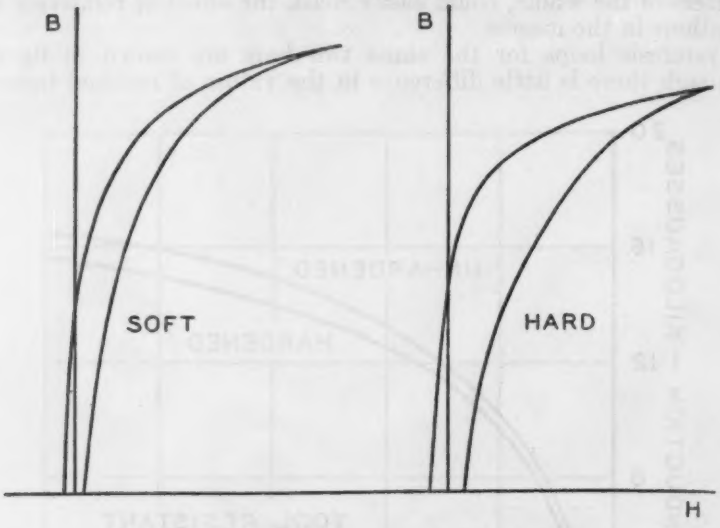

FIGURE 4.—*Hysteresis loops for hard and soft bars.*

in a portable instrument which has been called the "alternating-current magnetic comparator."

III. DESCRIPTION OF THE INSTRUMENT

The alternating-current magnetic comparator is essentially an a–c inductance bridge of the type shown in the diagram of figure 5. L_1 and L_2 represent two exactly similar magnetizing coils, in which are inserted a standard bar of known quality and the bar under test, respectively. The capacitors C_3 and C_4 are equal in value, and, in the present instance, each has a capacitance of approximately 20 microfarads. The detector circuit is connected between movable contacts on the slide wires R_1R_2 and R_3R_4. In the actual instrument, these slide wires are shunted by auxiliary resistors of sufficient current-carrying capacity not to overheat when the maximum current of 5 amperes is flowing. This also serves to make the setting of the contacts less critical. Current is controlled by means of a General Radio Variac connected to the ordinary a–c lighting circuit. The Variac is an autotransformer of special design and gives a very smooth control of the current, which is measured by a–c ammeter A. With

no iron in coils L_1 and L_2, the bridge can be balanced so that no current flows in the detector circuit, and the following relation holds:

$$L_1 - L_2 = C(R_2R_4 - R_1R_3),$$

where

L_1 and L_2=inductance, in henrys,

and

$C=C_3=C_4$=capacitance, in farads,

and

R_1, R_2, R_3, and R_4=resistances, in ohms

R_1 and R_2 include the resistances of L_1 and L_2, respectively.

If there is iron in the coils L_1 and L_2 the situation is more complicated. When a coil surrounding a core of iron is energized by a

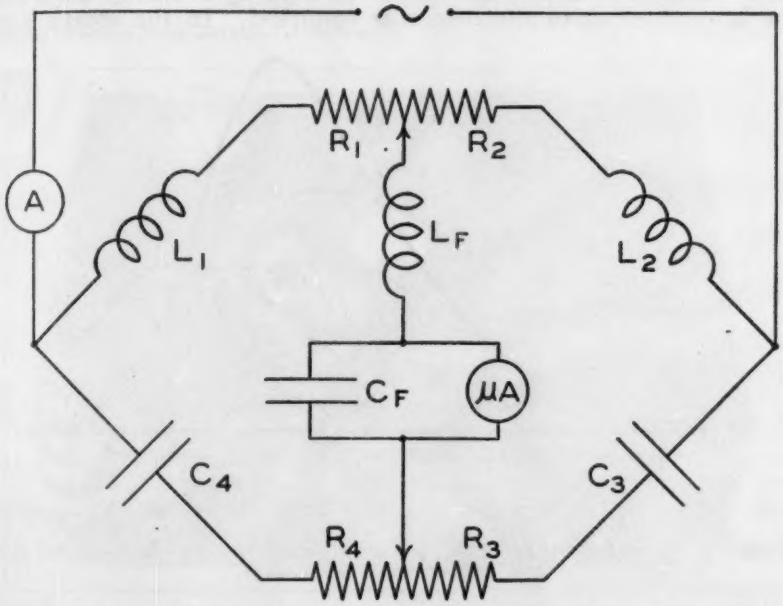

FIGURE 5.—*Diagram of connections of the alternating-current magnetic comparator.*

sinusoidal electromotive force, the flux also varies sinusoidally. The current wave, however, is distorted from the sine wave form on account of the magnetic hysteresis in the iron. The distorted current wave is made up of a combination of sine waves; a fundamental, having the frequency of the impressed voltage, and harmonics having frequencies which are odd multiples of the fundamental frequency. These harmonics differ in amplitude and phase. The amplitude is generally less the higher the harmonic, and harmonics above the seventh can generally be neglected. In figure 6, the magnetizing current corresponding to a sinusoidal variation of flux in the hard bar of figure 4 is shown, together with the fundamental, third, and fifth harmonics. If the magnetizing current is forced to have a sine wave form, the distortion is transferred to the flux wave.

The effect of the distortion due to hysteresis is to introduce in the arms L_1 and L_2 of the bridge electromotive forces having frequencies which are odd multiples of the fundamental frequency and which, in general, differ from each other in magnitude and phase. It is possible to obtain a complete balance only when the two specimens are exactly alike magnetically. When the specimens are not alike, the slide wire contacts are set to give the minimum value of current in the detector circuit and this is taken as the reading. By using a filter circuit in connection with the detector, comparison can be made in terms of differences in a given harmonic. These differences depend not only upon the respective magnitudes of the harmonics but also upon their phase relations. There is no provision in the present instrument for differentiating between differences in magnitude and differences in phase relation so the comparison is on a purely arbitrary basis and the interpretation of the results is empirical. In the comparator,

FIGURE 6.—*Wave form of magnetizing current (heavy line) and fundamental, third and fifth harmonic components.*

provision is made for comparison in terms of the third, fifth, or seventh harmonic by means of interchangeable capacitors in the filter circuit. The detector is a rectifier-type microammeter, which gives full-scale deflection for 100 microamperes. It is connected across the filter capacitor C_F, as shown. The indications of this instrument do not give the sign of the difference. This is determined by short-circuiting an auxiliary winding of a few turns on L_1. This reduces the effect of L_1, and if the reading is increased thereby, the effect of L_1 is less than that of L_2. If the reading is decreased, L_1 is the greater.

Figure 7 shows the complete instrument. In the upper left-hand corner is the ammeter and below it the dial of the autotransformer by which the current is controlled. The instrument in the middle is the microammeter. Below this instrument are the dials controlling the contacts on the slide wires. The sensitivity switch is just beneath. In the position O, the microammeter is disconnected, position H gives full sensitivity, and position L gives approximately half sensitivity. The four-point switch is the harmonic selector. By means of the other selector switches and the binding posts at the right, either an

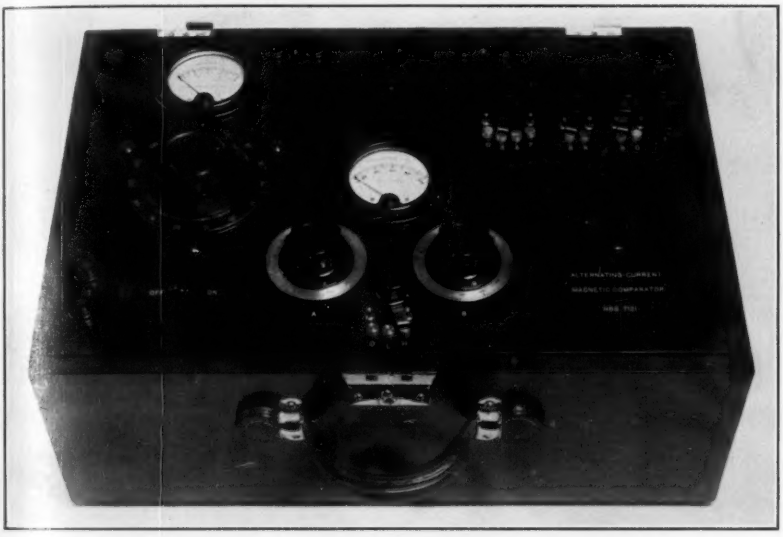

FIGURE 7.—*Alternating-current magnetic comparator.*

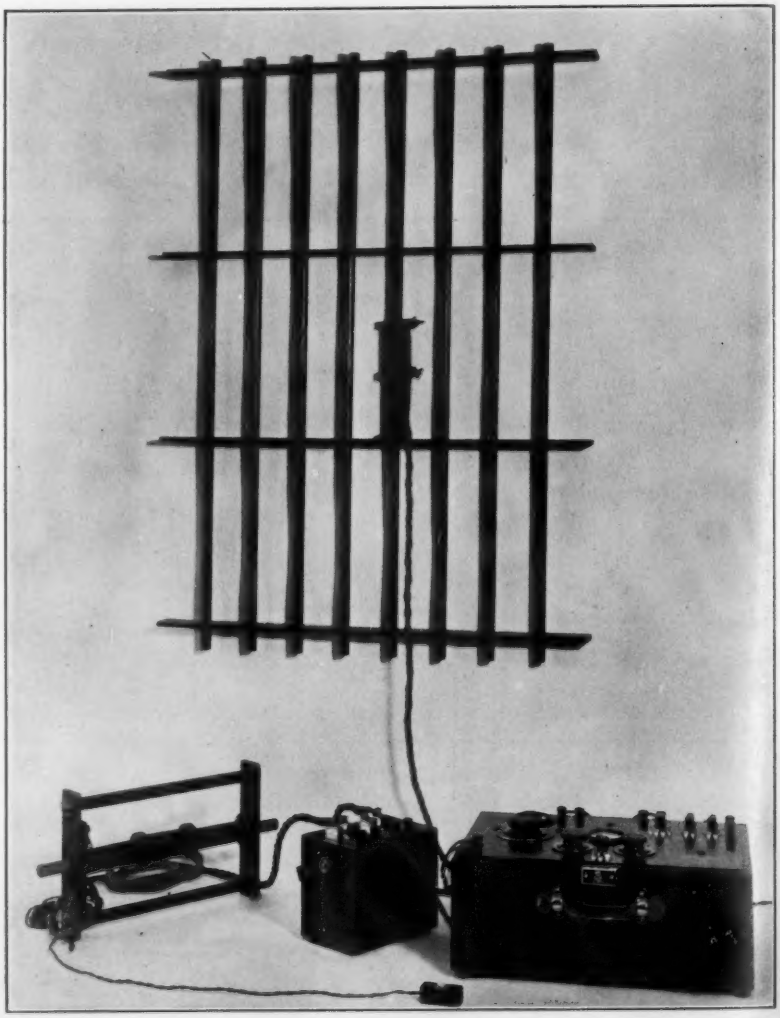

FIGURE 8.—*Comparator with accessory apparatus connected for testing a bar in the experimental grille.*

oscillograph or another instrument can be substituted for the microammeter as the detector. The coils L_1 and L_2 are connected to the binding posts at the top and the power supply is connected to the posts at the lower left-hand corner.

IV. AUXILIARY APPARATUS

The preliminary experiments with the comparator were carried out using magnetizing coils of 200 turns. When bars are to be tested in place, however, it is not convenient to wind on so many turns. In order to obviate this difficulty, two similar transformers were constructed having a turn-ratio of 10 to 1. The high-voltage sides of these transformers are connected to the bridge and the low-voltage sides to 20-turn coils capable of carrying 40 to 50 amperes without overheating. These transformers are so nearly alike that there is no difficulty in obtaining a balance at full current when there is no iron in the test coils. Heavy twisted cable is used in making the connections on the low-voltage side. The test coil for the test specimen is of very flexible stranded wire and is wound on a split form directly on the test bar.[1] This procedure was adopted originally to avoid uncertainties in resistance which might occur if a split coil were to be used. Experience in the field has shown, however, that a split coil would be much more satisfactory if reliable contacts can be obtained.

It is important that the magnetic circuits associated with the two bars shall be as nearly alike as possible. For this reason, a yoke consisting of bars and cross pieces like those used in the actual installations was built up in which the bar used as a standard is inserted. A fixed coil surrounding the standard bar is mounted on this yoke. The auxiliary coil for determining the sign of the difference is wound on the same form. The experimental grille, comparator, and auxiliary apparatus are shown in figure 8.

V. EXPERIMENTAL RESULTS

Before taking the apparatus into the field, experiments were made to determine the best operating conditions and the range of readings to be expected for good and bad bars. Readings were made corresponding to many different combinations of bars in the experimental grille and using several different bars as standards. One of the first points considered was the best value of current to use. Readings on four bars at different values of current are plotted in figure 9. In the light of these results, 3 amperes was decided upon as a suitable value. This corresponds to about 30 amperes in the coils, or 600 ampere turns.

The question of uniformity of the bars along their length was also of interest. Wide differences were found among the bars in this respect. Typical results on four different bars are shown in figure 10. It can be seen that two of these bars are fairly uniform, but that the others show much greater variation along their length.

Experiments were made to determine the effects of using different bars as reference standards and one bar having round inserts was chosen as giving the most satisfactory results, not only for the bars

[1] Attempts were made to apply the magnetizing force by means of a yoke carrying the magnetizing winding, but it was found that there was too much variation in contact reluctance and that the properties of the oke predominated. It was necessary, therefore, to wind the coil directly on the bars.

having round inserts but also for those having square inserts. It is probable that the two types of bar are similar in composition and relative proportion of matrix and insert material. If bars of different composition are to be tested, a standard of the same kind of material and of known quality should be used.

After the preliminary tests were completed, the apparatus was tried out at the United States Industrial Reformatory at Chillicothe, Ohio, and at the United States Northeastern Penitentiary at Lewisburg, Pa.

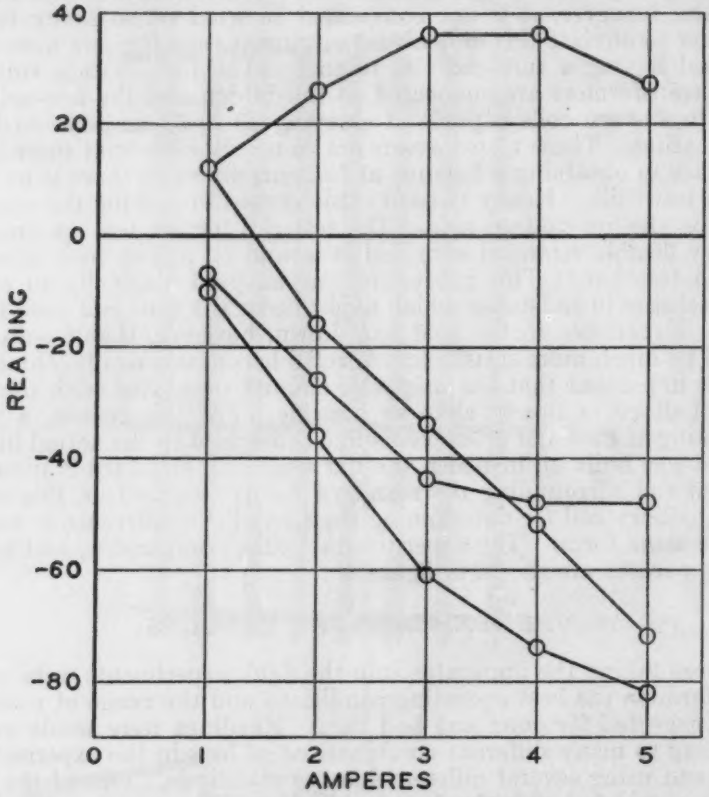

FIGURE 9.—*Relation between current and reading of the comparator for four different bars.*

At Chillicothe, drill tests had been made on a number of bars and it was thought that this would furnish an excellent opportunity to determine the reliability of the comparator. In view of tests on the experimental grille, a reading of −60 was tentatively chosen as the dividing line between good and bad bars. On this basis, bars giving a plus reading or one numerically less than 60, in the minus direction, would be considered good, and bars giving readings numerically greater than 60 in the minus direction would be considered too soft. A few of the results on the drilled bars are indicated in figure 11. If the criterion had been correctly chosen, points representing bars in which holes were drilled, indicated by circles, should all be below the −60 line and points representing bars in which no holes could be

drilled, indicated by crosses, should be above the line. Points indicated by dots show results obtained at places where no drill test had been made.

At first glance the results appear to be rather disappointing. The apparent lack of correlation was explained, however, when additional drill tests were made. In general, when the comparator reading was below the −60 line, it was possible to find some place within the length covered by the test coil where a hole could be drilled com-

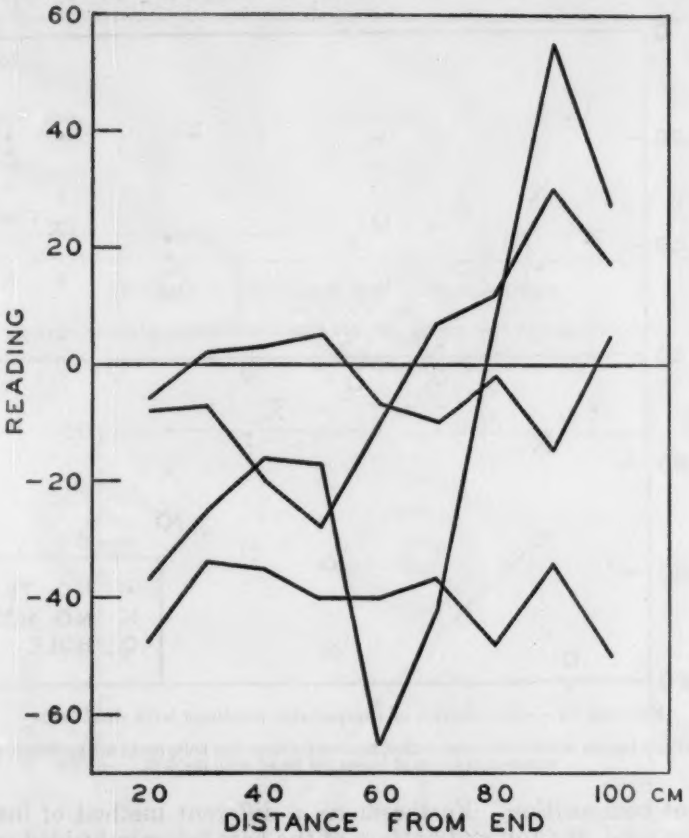

FIGURE 10.—*Degree of uniformity of four bars.*

pletely through the bar. The bars were extremely nonuniform along their length and neither the drill test nor the magnetic test could be expected to give a reliable result when applied at only one point on the bar. In some instances it was impossible to drill holes at points less than 1 inch away from holes which had been drilled, without difficulty.

A few tests were also made on bars which had been installed to replace others previously found to be unsatisfactory. Some of these were new bars with round inserts and others were bars with square inserts which had been removed, retreated, and replaced. In figure 12, the circles indicate the results obtained on the bars with round

inserts and the squares show the readings for bars with square inserts. The great variation in the bars with square inserts compared with the others is evident. The large negative reading for several of the replaced bars would lead to some doubt of their quality, but in view of the fact that they were carefully inspected and tested with a drill at the plant before being installed, it may be that the standard which was used was not satisfactory for these retreated bars.

At Lewisburg, conditions were found to be quite different from those at Chillicothe. The bars are of a different type and probably have a

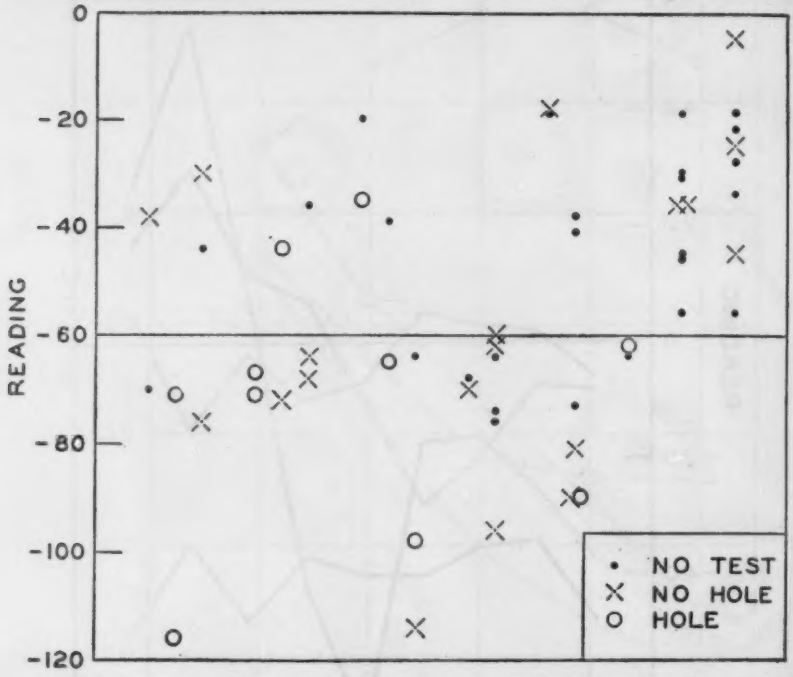

FIGURE 11.—*Correlation of comparator readings with drill tests.*

Circles indicate bars in which holes were drilled, squares indicate that holes could not be drilled, and dot represent readings at points not tested with the drill.

different composition. Furthermore, a different method of installation was used, the top and bottom of the bars being imbedded in concrete. As no similar bar known to be of satisfactory quality was available, the same standard was used as at Chillicothe. It was necessary, therefore, to compare the bars in terms of their respective readings against this standard. Two bars giving the same reading were considered to be similar. Since several of these bars had previously been found, by trial, to be satisfactorily tool-resisting, this was considered to be a safe procedure. It was also necessary to consider each group separately on account of differences in the magnetic circuits of the different kinds of grille. For each group of bars of the same diameter and having similar magnetic circuits, the readings against the standard were averaged and this average taken as normal

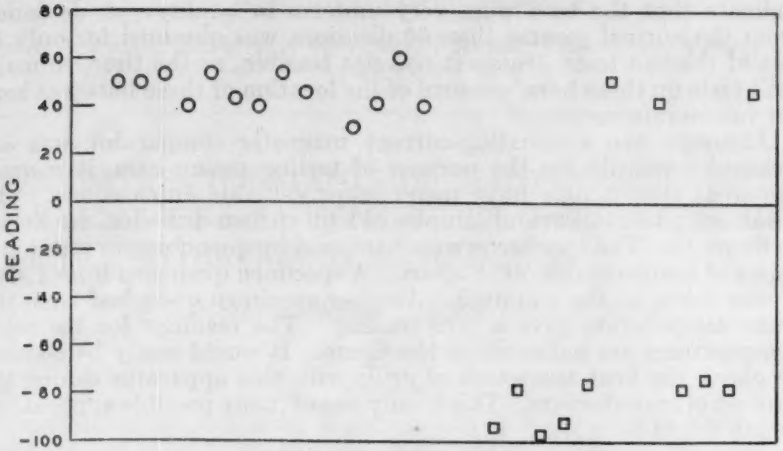

FIGURE 12.—*Results of tests on replaced bars.*

Circles represent bars with round inserts, squares represent bars with square inserts.

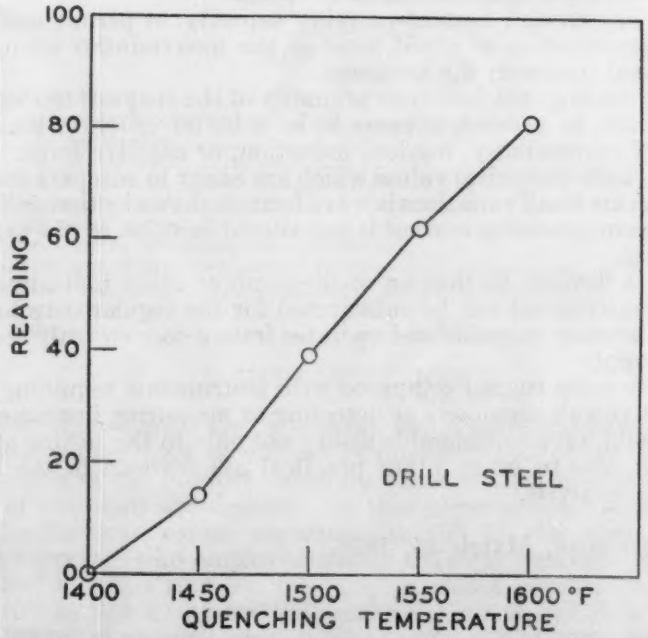

FIGURE 13.—*Relation between quenching temperature and reading on hardened drill rod.*

A specimen quenched at 1,400° F was taken as the reference standard.

for the group. The average deviation from this normal value for all bars tested was 23 scale divisions. This small deviation was taken to indicate that the bars were very uniform in quality. A deviation from the normal greater than 60 divisions was obtained for only 12 out of the 243 tests. Since it was not feasible, at the time, to make drill tests on these bars, a record of the location of these bars was kept for future reference.

Although the alternating-current magnetic comparator was developed primarily for the purpose of testing prison bars, it is quite apparent that it may have many other valuable applications. The results of a test on several samples of high-carbon drill steel are shown in figure 13. The specimens were hardened by quenching in water at a series of temperatures 50° F apart. A specimen quenched from 1,400° F was taken as the standard. Another specimen quenched from the same temperature gave a zero reading. The readings for the other temperatures are indicated in the figure. It would easily be possible to check the heat treatment of drills with this apparatus during the process of manufacture. This is only one of many possible applications which might be made.

VI. CONCLUSION

In comparison with other alternating-current methods for the application of magnetic analysis, the alternating-current magnetic comparator has several advantages.

1. It is simple and convenient to operate.
2. It has enough current-carrying capacity to permit sufficiently high magnetization to avoid most of the uncertainties arising from mechanical strains in the specimen.
3. Its readings are functions primarily of the shape of the hysteresis loop, which, in general, appears to be a better criterion than single values of permeability, residual induction, or coercive force.
4. It yields numerical values which are easier to compare and interpret than are small variations in wave form as shown by the oscillograph.
5. The magnetizing current is not altered in value by the process of balancing.
6. It is flexible, in that an oscillograph or other indicating or recording instrument can be substituted for the regular detector.
7. It is easily portable and operates from a conveniently accessible power supply.
8. It is quite rugged compared with instruments requiring the use of sensitive galvanometers as detecting or measuring instruments.

It should have considerable utility not only in the testing of prison bars but also in many other practical applications in the field of magnetic analysis.

WASHINGTON, March 13, 1936.

U. S. Department of Commerce National Bureau of Standards

RESEARCH PAPER RP895

Part of Journal of Research of the National Bureau of Standards, Volume 16, June 1936

DISSOCIATION CONSTANTS OF MALONIC ACID IN ITS SODIUM-SALT SOLUTIONS AT 25° C FROM ELECTROMETRIC TITRATION MEASUREMENTS

By J. O. Burton,[1] Walter J. Hamer, and S. F. Acree

ABSTRACT

Electrometric titration of 0.1 *M* malonic acid by 0.1007 *N* sodium hydroxide was completed at 25° C for the determination of the pH titration curve and the calculations of the primary and secondary dissociation constants. The treatment of the data embodied the application of the Henderson equation for liquid-junction potential, the Debye-Hückel theory of interionic attraction, and the Guggenheim-Hückel expression for the variation of the ionic activity coefficients with concentration. The dissociation constants found for malonic acid at 25° C are $K_1=2.06\times10^{-3}$ and $K_2=2.94\times10^{-6}$.

CONTENTS

		Page
I.	Introduction	575
II.	Experimental measurements	576
	1. Apparatus	576
	2. Materials	577
	3. Procedure	577
III.	pH determinations	578
IV.	pH titration curve	583
V.	Calculation of the dissociation constants	585
VI.	Calculation of the intermediate range	587
VII.	Discussion	588
VIII.	Summary	591
IX.	References	592

I. INTRODUCTION

Dibasic organic acids are, in general, found in the oxidized portions of natural sugars. As an aid in the interpretation of the oxidation and analysis of the product, accurate values of the dissociation constants of the acids are desired. In this paper malonic acid is considered. Previous values reported (at 25° C) for this acid by investigators [1],[2] who employed widely different methods, vary from 1.40×10^{-3} to 2.11×10^{-3} for the first ionization constant and from 1.36×10^{-6} to 10.0×10^{-6} for the second. Part of this divergence is due to the use of classical dilution laws and neglect of interionic attrac-

[1] This paper includes data presented in a dissertation submitted by John O. Burton to the Faculty of the Graduate School of the University of Maryland, represented by Prof. M. M. Haring of the Department of Chemistry, in partial fulfillment of the requirements for the degree of Master of Science.

[2] The numbers in brackets here and throughout the text refer to the numbered references at the end of this paper.

tion theories developed by Milner [2] and by Debye and Hückel, [3] and, in part, to assumptions that the sodium salts of malonic acid have colligative properties similar to those of the sodium salts of other monobasic and dibasic acids. In this paper the electrometric titration of malonic acid by sodium hydroxide is presented, and the data are treated with the use of the interionic attraction theory and

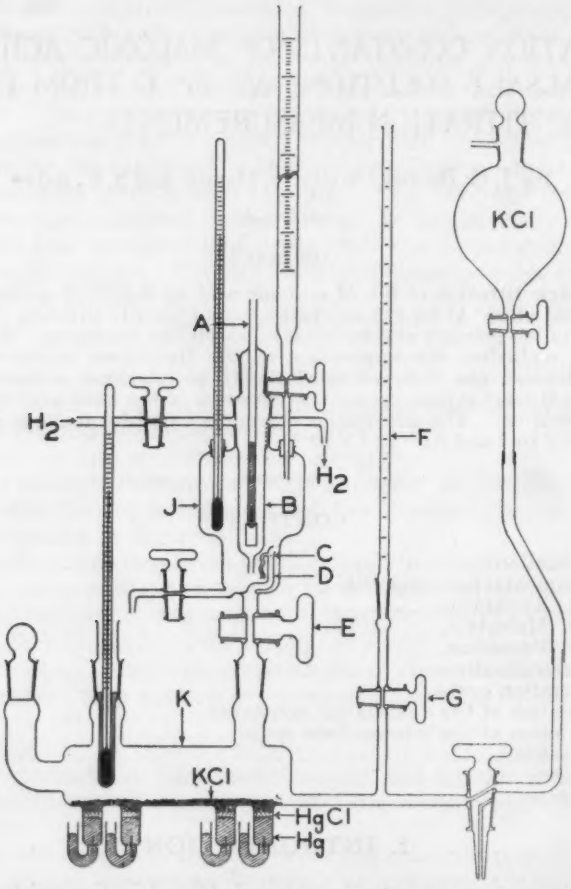

FIGURE 1.—*Hydrogen and calomel electrodes for making* pH *titrations.*

independently of assumptions as regards structural and colligative identity with other salts.

II. EXPERIMENTAL MEASUREMENTS

1. APPARATUS

The pH measurements were made with a hydrogen electrode in an electrode vessel, as shown in figure 1. The reference electrode consisted of a battery of four saturated calomel electrodes, K. These were brought to constant potential with each other by short-circuiting as recommended by Loomis and Acree [4]. The electromotive-force

measurements were made with a Leeds and Northrup type K potentiometer and 2500–e galvanometer, with lamp and scale. The titrations were made in an air thermostat, controlled at 25° C to within ±0.2° C.

2. MATERIALS

Tank hydrogen, purified from oxygen by passing through a tube containing palladinized asbestos heated to 220° C, was employed. The gas was subsequently passed through water before admission to the titration vessel, in order to insure against concentration changes due to evaporation in the solution to be titrated.

The hydrogen electrode was gold foil (about 0.5 by 1 cm) plated with palladium black from a 3 percent palladous chloride solution containing a small amount of lead acetate. Mercury cleaned in nitric acid and redistilled and electrolytic calomel manufactured by Eppley were employed for the calomel electrodes.

Potassium chloride was recrystallized twice from conductivity water. The saturated solution was prepared by adding an excess of purified potassium chloride to conductivity water.

Malonic acid obtained from the Eastman Kodak Co., was used without further purification. A dried sample of the acid neutralized the theoretical amount of standard alkali to within 0.1 percent, which corresponds to an error of approximately ±0.1 mv, or an error of ±0.3 percent in pH, provided that the impurity is untitratable, which is probably the case.

The solution to be titrated was prepared by dissolving a calculated weight of dry acid in conductivity water and diluting to the desired volume in a calibrated Pyrex-glass flask. The sodium hydroxide employed for the titration was freed from carbonate by preparing the saturated solution, siphoning off the supernatant liquid above the insoluble sodium carbonate into a bottle protected from the atmosphere by soda-lime tubes, and diluting to 0.10 *N*. The solution was then standardized against potassium acid phthalate, National Bureau of Standards Sample 84.

3. PROCEDURE

The apparatus and solutions were placed in the air thermostat 2 hours before making the measurements. The electrodes were checked against an 0.05 *N* potassium acid phthalate buffer immediately before the titration. The electromotive force obtained was 0.4796 at 25° C, which corresponds to a pH of 3.96, and is in good agreement with 3.97 obtained by Clark [5] for this buffer.

Twenty-five milliliters of the acid was then pipetted into the titration vessel. Stopcock E was then opened and solution contact was made by gently raising the level of the saturated potassium chloride to C by admitting the potassium chloride solution from the reservoir, at which point, C, a diffusion junction was formed. This type of junction is considered to be the better type for a junction between solutions of different electrolytes, whether they are of like or unlike valence type [6]. Stopcock E was then closed, and hydrogen was passed over the electrode and through the solution. After the hydrogen had bubbled for 3 minutes, tube B was rotated through an angle of 180 degrees to force solution into B and make contact with the electrode, the hydrogen was turned off, stopcock E opened, and a liquid junction was made as described before. The electromotive

force was then recorded. This procedure was repeated until successive readings of electromotive force agreed to within ± 0.2 mv. After the electromotive force was found to be constant within this limit, standard sodium hydroxide solution was added by means of the burette, and the new electromotive force was obtained by repetition of the procedure outlined above. It was found that for the first measurement it was necessary to pass hydrogen through the solution several times for 3 minutes each, before a constant potential could be obtained. Subsequent measurements were found to be constant after passing the hydrogen through the solution for 3 minutes, except near the end of the pH titration curve, where the pH was changing rapidly. However, for each point on the curve the hydrogen was bubbled for at least two 3-minute periods. The temperatures in the titration vessel and calomel electrode were checked frequently throughout the titration and always were found to agree within ± 0.1° C with each other and the temperature reported for the titration. The electromotive forces were corrected to one atmosphere hydrogen pressure, as recommended by Acree and coworkers [7].

III. pH DETERMINATIONS

In the electrometric titration of malonic acid with sodium hydroxide, the three galvanic cells

$$\mathrm{Pt|H_2(g)|H_2An}(c_1),\ \mathrm{NaHAn}(c_2)\mathrm{|KCl(sat.)|Hg_2Cl_2(s)|Hg(1)+} \quad (1)$$

$$\mathrm{Pt|H_2(g)|H_2An}(c_1),\ \mathrm{NaHAn}(c_2),\ \mathrm{Na_2An}(c_3)\mathrm{|KCl(sat.)|Hg_2Cl_2(s)|Hg(1)+} \quad (2)$$

and

$$\mathrm{Pt|H_2(g)|NaHAn}(c_2),\ \mathrm{Na_2An}(c_3)\mathrm{|KCl(sat.)|Hg_2Cl_2(s)|Hg(1)+} \quad (3)$$

are, in reality, measured. Cell 1 corresponds to the first part of the titration during which neutralization of the first acid group (HAn^-) occurs; cell 2 to the intermediate range, where both groups (HAn^- and $An^=$) are simultaneously neutralized; and cell 3 to the final range, in which only the second group ($An^=$) is titrated. The parallel lines indicate separate phases, and the commas are employed to indicate different components within one phase, as is the convention adopted by the International Critical Tables [8]. "An", abbreviation for anion, is employed to represent the malonate ion, and "HAn" to represent the acid malonate ion. The measured electromotive forces of these three cells are all given by the semi-thermodynamic equation

$$E = E_0 + E_j - \frac{RT}{F} \ln c_H f_H, \quad (4)$$

where E is the measured electromotive force; E_0 the normal electrode potential of the reference electrode Hg(1) Hg_2Cl_2(s) KCl(sat.); E_j the liquid-junction potential at the boundary, acid, salts|KCl(sat.); c_H the hydrogen-ion concentration, in moles per liter; and f_H the practical activity coefficient of the hydrogen ion, respectively.

The liquid-junction potential E_j is equal to the sum of the diffusion potential E_D and the activity potential E_t, which corrects for the

deviations of E_D from the classical dilution laws due to interionic attraction. Upon substitution and rearrangement, the equation

$$(E-E_0-E_D)/0.05915-E_t/0.05915+\log f_H=-\log c_H=\text{pH} \quad (5)$$

results, where the numerical value of $RT/2.3026F$ at 25° C is 0.05915. Since E, the measured value, and E_0, which has been shown by Scatchard [9] to be equal to 0.2454 volt, are the only values obtained directly by experiment, it is necessary to evaluate E_D, $E_t/0.05915$, and $\log f_H$ in order to obtain values for the hydrogen-ion concentration or pH. The former two are given by the integrals [10]

$$E_D=-\sum_1^p 0.05915\int_1^2 t_i d\ln c_i, \quad (6)$$

$$E_t=-\sum_1^p 0.05915\int_1^2 t_i d\ln f_i, \quad (7)$$

and their sum E_j by

$$E_j=-\sum_1^p 0.05915\int_1^2 t_i d\ln a_i, \quad (8)$$

where the limits 1 and 2 refer to solution (sat. KCl) and solution (acid-salt), respectively, and t_i represents the ionic transference number and a_i the ionic activity of the ions involved in the transfer of electrolyte at the boundary. The integral refers to an individual ion, but the sum is for all the ions involved, p.

Henderson [11] arrived at a solution of equation 6 by assuming an initial mixing of the solutions at a sharp boundary. His solution gives, respectively, for cells 1, 2, and 3 the following equations:

$$E_D=-(RT/F)\frac{c_s(U_s-V_s)-c_HU_H-c_2(U_2-V_2)}{c_s(U_s+V_s)-c_HU_H-c_2(U_2+V_2)}\ln\frac{c_s(U_s+V_s)}{c_HU_H+c_2(U_2+V_2)} \quad (9)$$

$$E_D=-(RT/F)\frac{c_s(U_s-V_s)-c_HU_H-c_2(U_2-V_2)-c_3(U_3-V_3)}{c_s(U_s+V_s)-c_HU_H-c_2(U_2-V_2)-c_3(U_3-V_3)}\ln\frac{c_s(U_s+V_s)}{c_HU_H+c_2(U_2+V_2)+c_3(U_3+V_3)} \quad (10)$$

$$E_D=-(RT/F)\frac{c_s(U_s-V_s)-c_HU_H-c_3(U_3-V_3)}{c_s(U_s+V_s)-c_HU_H-c_3(U_3+V_3)}\ln\frac{c_s(U_s+V_s)}{c_HU_H+c_3(U_3+V_3)}, \quad (11)$$

where c_s is the concentration of saturated potassium chloride (4.13 N); U refers to cationic mobility; and V to anionic mobility of the salts denoted by the same subscripts as were employed in the formulation of cells 1, 2, and 3. Numerical values of the mobilities are U_s [12] = 73.50; V_s [12] =76.32; U_H [12] =349.72; $U_2=U_3$ [12] =50.10; V_2 [13] =35.5; V_3 [14] =63.0 (corrected by 0.014 percent for error in cell constant of Kohlrausch's [15] conductance measurements),

and values of c_2 and c_3 are obtained from the stoichiometrical concentrations of NaHAn and Na_2An, which are given in columns 6 and 7 of table 1, and from the hydrogen-ion concentration found prior to liquid-junction corrections.

Values of E_D calculated by equations 9 and 11 are given in column 3 of table 2. These calculations are for the treatment of malonic acid and its acid salt as monobasic acids. For the intermediate range where the acid is treated as a dibasic acid equation 10 is employed. Values calculated by its use are given in column 2 of table 3. The corrections produced by the use of E_D give new values of the hydrogen-ion concentration, c_H. These new values of c_H are then substituted in the above equations and the process repeated until values of c_H and E_D are consistent with each other. In this work only one calculation was found necessary for consistency, owing to the low magnitude of c_H, the hydrogen-ion concentration.

TABLE 1.—*Stoichiometrical concentrations prevailing in the titration of 25 milliliters of 0.10 M malonic acid by 0.1007 N sodium hydroxide*

0.1007 *N* NaOH	Moles NaOH per mole acid	*J*=equiv. conc. of Na salts	M_{H_2An}	$M_{H_2An}=U$	M_{NaHAn}	M_{Na_2An}
ml						
0.00	0.000000	0.000000	0.100000	0.100000	0.000000	----------
1.00	.040285	.003873	.096154	.092281	.003873	----------
2.06	.08299	.007666	.092387	.084721	.007666	----------
3.21	.12931	.011459	.088621	.077162	.011459	----------
4.26	.17161	.014661	.085437	.070776	.014661	----------
5.11	.20586	.017090	.083029	.065939	.017090	----------
6.10	.24574	.019751	.080386	.060637	.019751	----------
7.12	.28683	.022322	.077833	.055511	.022322	----------
9.10	.3666	.026873	.073314	.046441	.026873	----------
11.08	.4464	.030925	.069290	.038365	.030925	----------
13.10	.5277	.034624	.065627	.031003	.034624	----------
15.10	.6083	.037919	.062344	.024423	.037919	----------
17.10	.6889	.040902	.059382	.018480	.040902	----------
19.10	.7694	.043614	.056690	.013076	.043614	----------
20.10	.8097	.044880	.055432	.010552	.044880	----------
21.10	.8500	.046090	.054230	.008140	.046090	----------
22.10	.8903	.047248	.053079	.005831	.047248	----------
23.14	.9322	.048405	.051930	.003525	.048405	----------
23.66	.9531	.048964	.051377	.002413	.048964	----------
24.25	.9769	.049583	.050761	.001178	.049583	----------
24.86	1.00148	.050209	.050209	.000000	.050209	0.000000
25.36	1.02162	.050710	.049642	----------	.048574	.001068
25.86	1.04177	.051202	.049155	----------	.047108	.002047
26.35	1.06151	.051674	.048685	----------	.045696	.002989
27.40	1.10380	.052656	.047710	----------	.042764	.004946
28.35	1.14208	.053512	.046861	----------	.040210	.006651
29.35	1.18236	.054380	.045998	----------	.037616	.008382
30.39	1.22426	.055250	.045135	----------	.035020	.010115
31.85	1.28307	.056417	.043975	----------	.031533	.012442
33.85	1.36364	.057922	.042481	----------	.027040	.015441
35.85	1.44421	.059328	.041085	----------	.022842	.018243
37.85	1.52478	.060644	.039777	----------	.018910	.020867
39.85	1.60535	.061880	.038551	----------	.015222	.023329
41.85	1.68662	.063040	.037398	----------	.011756	.025642
42.85	1.72631	.063600	.036846	----------	.010092	.026754
43.83	1.76578	.064128	.036321	----------	.008514	.027807
44.83	1.80607	.064652	.035802	----------	.006952	.028850
45.83	1.84635	.065161	.035296	----------	.005431	.029865
46.83	1.88664	.065655	.034804	----------	.003953	.030851
47.58	1.91685	.066017	.034445	----------	.002873	.031571
48.08	1.93699	.066255	.034209	----------	.002163	.032046
48.58	1.95714	.066489	.033977	----------	.001465	.032512
48.84	1.96761	.066609	.033857	----------	.001105	.032752
49.10	1.97809	.066729	.033738	----------	.000747	.032991
49.35	1.98816	.066843	.033625	----------	.000407	.033218
49.61	1.99863	.066961	.033508	----------	.000055	.033453
49.84	2.00790	.067065	.033404	----------	----------	.033661

Since no functional or analytical expression is known which defines a relation between t_1 and f_1, it is necessary to resort to graphical integration to evaluate E_t. This may be done by the method suggested by Harned [16]. In this, transference numbers of each ion involved at the junction are calculated for various mixtures between saturated potassium chloride and the titrated solution, assuming uniform mixing of the solutions at the boundary. Then these values of t_1 are each plotted against $\log f_1$ of the acid-salt mixtures, employing the law of the linear variation of activity coefficients at constant total molality [17], and the area under the integral is evaluated by counting the squares. For instance, after 1.00 cm^3 of alkali has been added, this integral equals -0.00203. Details and further discussion are omitted for reasons to be given in the following paragraph.

The magnitude of f_H remains to be determined. For dilute solutions these values may be calculated from data on pure hydrochloric acid and pure potassium chloride. First the values of the activity coefficients for potassium chloride obtained by Robinson and Sinclair [18] are employed. Since the mobilities of the ions of this salt are nearly the same [12] their activity coefficients are taken as equal. Then the mean activity coefficients of hydrochloric acid obtained by Harned and Ehlers [19] or by Randall and Young [20] are squared and divided by the activity coefficient of the chloride ion, which gives the activity coefficient of the hydrogen ion at the same concentration for which the values of potassium chloride and hydrochloric acid were used. This procedure embodies the assumption that the activity coefficient of an ion is uninfluenced by the ion with which it is associated, and in dilute solutions this is very nearly the case. For instance, the mean activity coefficient at 0.01 N for hydrochloric acid [19, 20] is 0.904 and for potassium chloride [18] it is 0.903. This procedure for the calculations of the activity coefficient of the hydrogen ion is that proposed by MacInnes [21] and employed by others [22], except that, in this case, the calculations were made in terms of normality and not in terms of molality as was done by MacInnes. The activity coefficients obtained by Robinson and Sinclair and by Harned and Ehlers for potassium chloride and hydrochloric acid were consequently corrected to the normality basis by multiplying their values by the ratio of molality to normality. Values of f_H thus calculated are given in column 9 of table 2. A comparison of the magnitude of E_t and $\log f_H$ may now be made. From table 2 the value of f_H after the addition of 1.00 ml alkali is found to be 0.893. The logarithm of this value multiplied by 0.05915, since $E_t = 0.05915 \log f_H$, gives 0.00291. E_t at the same point was found above to be 0.00203, hence E_t is *approximately* equal to $0.05915 \log f_H$ in value.* At this point of the titration the hydrogen-ion concentration has its highest value (first point excepted).

Therefore, this difference in E_t and $0.05915 \log f_H$ becomes even less as the titration proceeds. Since the difference observed is beyond

* The relative nature of this treatment has been clearly defined by Harned, J. Phys. Chem. **30**, 499 (1926).

the experimental error these two quantities may be taken as exactly equal, and equation 5 is then written in the form

$$(E-E_0-E_D)/0.05915=\text{pH}=-\log c_H. \quad (12)$$

Values of pH calculated by this equation are given in table 2, column 4.

TABLE 2.—*Data for titration of 0.10 M malonic acid at 25° C as a monobasic acid*

FIRST EQUIVALENT OF SODIUM HYDROXIDE

0.1007 *N* NaOH	*E*	$E_D \times 10^4$	pH	$c_H \times 10^8$	*n*	$K'_1 \times 10^3$	μ	f_H	$K^a_1 \times 10^3$
ml	*Volts*	*Volts*							
0.00	0.3569	34	1.83	1.4860	2	2.56	0.022290	0.887	1.95
1.00	.3603	32	1.89	1.2942	2	2.74	.023286	.893	2.10
2.06	.3648	31	1.97	1.0815	2	2.70	.023829	.901	2.08
3.21	.3695	30	2.05	8.974	3	2.69	.024920	.909	2.09
4.26	.3736	30	2.12	7.638	3	2.70	.026118	.915	2.10
5.11	.3771	30	2.18	6.668	3	2.67	.027092	.920	2.08
6.10	.3808	29	2.24	5.754	3	2.67	.028382	.925	2.09
7.12	.3848	29	2.31	4.920	3	2.65	.029702	.929	2.06
9.10	.3922	28	2.43	3.681	3	2.63	.032395	.938	2.06
11.08	.3997	28	2.56	2.748	3	2.60	.035047	.945	2.04
13.10	.4074	27	2.69	2.028	3	2.57	.037666	.952	2.03
15.10	.4153	27	2.83	1.489	3	2.56	.040153	.959	2.02
17.10	.4239	27	2.97	1.067	3	2.57	.042503	.965	2.03
19.10	.4343	26	3.15	7.080	4	2.54	.044676	.970	2.01
20.10	.4401	26	3.25	5.662	4	2.58	.045729	.973	2.05
21.10	.4468	26	3.36	4.355	4	2.63	.046744	.976	2.09
22.10	.4541	26	3.48	3.281	4	2.84	.047740	.979	2.26
23.14	.4633	26	3.64	2.291	4	3.38	.048749	.982	2.69
23.66	.4688	26	3.73	1.849	4	4.12	.049241	.983	3.28
24.25	.4747	26	3.83	1.469	4	7.09	.049241	.986	5.66

SECOND EQUIVALENT OF SODIUM HYDROXIDE [1]

						$K'_2 \times 10^6$			$K^a_2 \times 10^6$
24.86	0.4814	23	3.95	1.1195	4	0.25	0.050489	0.987	0.13
25.36	.4865	23	4.04	9.1833	5	2.20	.052007	.989	1.14
25.86	.4916	23	4.12	7.5335	5	3.40	.053437	.991	1.75
26.35	.4961	23	4.20	6.3241	5	4.23	.054821	.992	2.16
27.40	.5049	23	4.35	4.4874	5	5.27	.057714	.993	2.66
28.35	.5118	23	4.47	3.4276	5	5.70	.060249	.994	2.85
29.35	.5183	24	4.57	2.6730	5	6.01	.062829	.996	2.97
30.39	.5242	24	4.67	2.1232	5	6.15	.065418	.996	2.98
31.85	.5319	24	4.80	1.5740	5	6.22	.068898	.997	3.00
33.85	.5411	25	4.96	1.1041	5	6.31	.073396	.998	2.99
35.85	.5497	25	5.10	7.9068	6	6.32	.077591	.999	2.95
37.85	.5581	25	5.24	5.7016	6	6.30	.081525	.999	2.89
39.85	.5667	26	5.39	4.0926	6	6.28	.085219	1.0	2.85
41.85	.5763	26	5.50	2.8184	6	6.15	.088689	1.0	2.76
42.85	.5815	26	5.64	2.3015	6	6.10	.090360	1.0	2.72
43.83	.5871	26	5.73	1.8493	6	6.04	.091940	1.0	2.68
44.83	.5938	27	5.84	1.4322	6	5.95	.093506	1.0	2.62
45.83	.6020	27	5.98	1.0400	6	5.72	.095079	1.0	2.51
46.83	.6127	27	6.16	6.8550	7	5.35	.096508	1.0	2.34
47.58	.6243	27	6.36	4.3652	7	4.80	.097587	1.0	2.09

[1] Since K^a_2 drops rapidly near the end of the titration, owing to rapid change in pH, which magnifies the experimental error, these values have not been incorporated into the table. From 47.58 ml of added alkali to end of the titration, the electromotive forces are, respectively, for the milliliter of added alkali listed in table 1: 0.6352, 0.6556, 0.6734, 0.7143, 0.7715, 0.8069, and 0.8310 volt, and E_D is 0.0027 volt for all. The corresponding pH values are, respectively, 6.54, 6.89, 7.19, 7.88, 8.85, 9.45, and 9.86.

TABLE 3.—*Data for titration of 0.10 M malonic acid at 25° C as a dibasic acid*

0.1007 *N* NaOH	$E_D \times 10^4$	$c_H \times 10^5$	n	$c_{Na_2An} \times 10^6$	$c_{NaHAn} \times 10^5$	$c_{H_2An} \times 10^6$	μ	$K_1^c \times 10^3$	$K_2^c \times 10^6$
ml									
17.10	27	1.067	3	----------	0.04597	17411	0.042503	[a]2.03	----------
19.10	26	7.080	4	----------	.04432	12372	.044676	[a]2.01	----------
20.10	26	5.662	4	----------	.04545	9984	.045729	[a]2.05	----------
21.10	26	4.355	4	644	.04598	761	.04813	2.08	3.17
22.10	25	3.266	4	867	.04643	579	.04919	2.08	3.17
23.14	25	2.280	4	1248	.04665	404	.05051	2.09	3.16
23.66	25	1.841	4	1543	.04657	327	.05129	2.08	3.14
24.25	25	1.466	4	1924	.04624	260	.05209	2.09	3.14
24.86	25	1.127	4	2474	.04572	195	.05319	2.09	3.12
25.36	25	9.247	5	2974	.04508	158	.05410	2.10	3.12
25.86	25	7.586	5	3563	.04431	128	.05504	2.09	3.11
26.35	25	6.368	5	4164	.04347	106	.05603	2.09	3.10
27.40	25	4.519	5	5589	.04140	72	.05819	2.08	3.07
28.35	25	3.452	5	6959	.03938	52	.06028	2.08	3.04
29.35	25	2.686	5	8347	.03727	38	.06232	2.07	3.02
30.39	25	2.133	5	9836	.03504	29	.06452	2.07	2.99
31.85	24	1.574	5	12943	.03104	----------	.068898	----------	[a]3.00
33.85	25	1.1041	5	15462	.02701	----------	.073396	----------	[a]2.99
35.85	25	7.9068	6	18260	.02253	----------	.077591	----------	[a]2.95

[a] Values obtained by the monobasic treatment.

IV. pH TITRATION CURVE

In figure 2 the titration curve of 0.10 *M* malonic acid with 0.1007 *N* sodium hydroxide is shown graphically by curve C. Since the stoichiometrical concentrations of malonic acid, sodium acid malonate, and disodium malonate may each be calculated from the stoichiometrical equations for each volume formed by the addition of alkali, and the total concentration of the acid is known, the mole fraction of each may be obtained. Curve A shows the change of the mole fraction of sodium acid malonate with pH; curve D the change of the mole fraction of disodium malonate with pH. Curve B is 1 minus the mole fraction of un-ionized acid, thus showing the amount of acid ionized and titrated at each pH value. For curve A and B, therefore, the abscissas, given as moles NaOH per mole acid, can also be read between 0 and 1.0 as mole fractions of sodium acid malonate present and of acid titrated or ionized. If the abscissas are read as 1 less than the value given between 1.0 and 2.0, they will then indicate the mole fractions of disodium malonate. In this figure the pH values plotted are those obtained without liquid-junction corrections, so that a comparison with those obtained with such corrections may be briefly made. The liquid-junction corrections merely displace all these curves by approximately −0.06 pH unit. This emphasizes the fact that for the determination of absolute values, corrections for liquid junction are essential, but no large effect is introduced for percentage determinations. Consequently, in routine work if only percentage change is desired, the liquid-junction corrections may be omitted.

Values of the moles of NaOH per mole malonic acid and the stoichiometrical concentrations of added alkali (total equivalent concentration of Na salts=J), total acid, and unneutralized acid are given in table 1, columns 2, 3, 4, and 5, respectively. Stoichiometrical concentrations of the sodium acid malonate and disodium malonate ions are given in the same table in columns 6 and 7, respectively. The ionic concentration of the hydrogen ion is given in column 5 of table 2 and column 3 of table 3. If M represents stoichiometrical concentra-

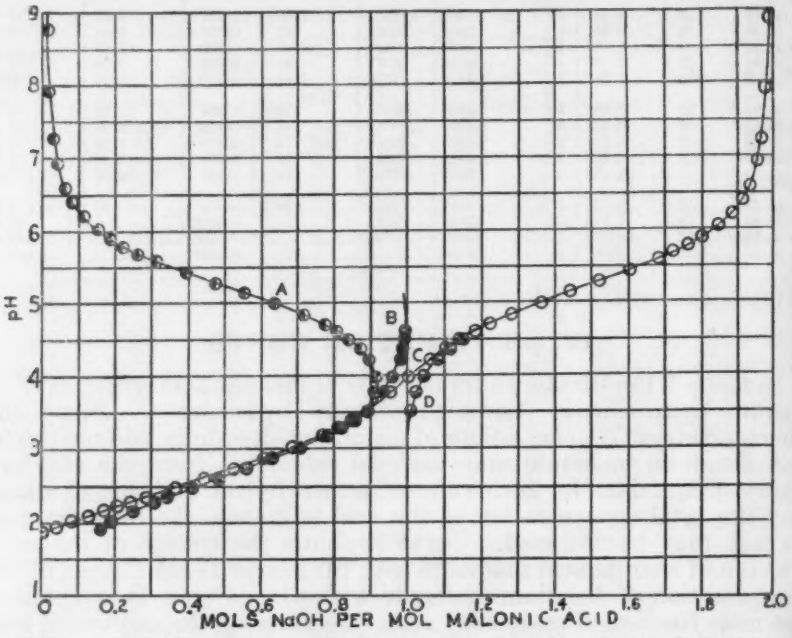

FIGURE 2.—*Change of composition of malonic acid solution with* pH.

A. Mole fractions monosodium salt=◐ and ○ below 0.9 mole NaOH.
B. Mole fraction total ionized and titrated acid=●
C. pH titration curve=○
D. Mole fraction disodium salt=◒

tions and c ionic concentrations, the following equations define their relation throughout the titration:

$$c_{NaHAn}=J+c_H, \tag{13}$$
$$M_{NaHAn}=J=M_{NaOH}, \tag{14}$$
$$c_{H_2An}=M_{H_2An}-c_{NaHAn}=M_{H_2An}-J-c_H, \tag{15}$$
$$c_{H_2An}=M_{H_2An}\ (\text{unneutralized})-c_H=M_U-c_H, \tag{16}$$
$$M_U=M_{H_2An}-J, \tag{17}$$

for the titration to the first equivalent point. From the first equivalence point to end of the titration, the relations are

$$c_{Na_2An}=J-M_{H_2An}+c_H, \tag{18}$$
$$M_{Na_2An}=J-M_{H_2An}, \tag{19}$$
$$c_{NaHAn}=2M_{H_2An}-J-c_H, \tag{20}$$
$$=M_{H_2An}-M_{Na_2An}-c_H, \tag{21}$$
$$M_{NaHAn}=M_{H_2An}-M_{Na_2An}. \tag{22}$$

These relations hold only for the treatment of the acid groups each as a monobasic acid. In a later section it will be shown that overlapping occurs in the intermediate range of 0.85 to 1.15 mole added alkali.

In the above, stoichiometrical and ionic concentrations have been employed. They are self-explanatory. Stoichiometrical concentration means the concentration calculated from molecular weights and chemical reactions, while ionic concentration means the concentration of ions alone which are prevalent in the solution. Thus, if an electrolyte (like NaCl) is completely dissociated, the stoichiometrical and ionic concentrations are equal. However, for a weak acid like malonic, these concentrations differ. Thus, the stoichiometrical concentration of 0.10 *M* acid is 0.10 *M*, but its ionic concentration is equal to the hydrogen-ion concentration, since only H^+ and HAn^- ions are present and are of equal value. Similarly, along the titration curve, the ionic concentrations and stoichiometrical concentrations differ. For example, the ionic concentration of HAn^- ion is equal to the stoichiometrical value of NaHAn formed by neutralization, plus H^+, due to ionization of the acid into H^+ and HAn^- ions. Thus, the stoichiometrical and ionic values differ merely by a H^+ ion concentration (apparent in above equations). This treatment and distinction make it simpler to visualize the changing concentrations which occur during a titration in which there is a volume change. It is the ionic values that are employed in the calculations of the dissociation constants.

V. CALCULATION OF THE DISSOCIATION CONSTANTS

Malonic acid ionizes in two steps, thus:

$$H_2An \rightleftharpoons H^+ + HAn^-,$$

$$HAn^- \rightleftharpoons H^+ + An^=,$$

and the law of mass action postulated by Guldberg and Waage [23] gives for these ionizations the respective constants

$$K_1 = \frac{a_H a_{HAn}}{a_{H_2An}} = \frac{c_H c_{HAn} f_H f_{HAn}}{c_{H_2An} f_{H_2An}} = K_1^c \frac{f_H f_{HAn}}{f_{H_2An}} \tag{23}$$

and

$$K_2 = \frac{a_H a_{An}}{a_{HAn}} = \frac{c_H c_{An} f_H f_{An}}{c_{HAn} f_{HAn}} = K_2^c \frac{f_H f_{An}}{f_{HAn}}, \tag{24}$$

where a, f, and c are the activity, the practical activity coefficient, and the concentration, in moles per liter, of the species denoted by subscripts, respectively. Guldberg and Waage's first postulation, as well as those followed by their contemporaries, was based entirely upon the c term and represented by K_1^c and K_2^c. Experiments, as well as theory, have shown, however, that the law of mass action defines the relation between products and reactants of a reaction in terms of activity rather than in concentration terms. The activity is equal to the product of the concentration and the activity coefficient as given in above equations. For dilute solutions (approximately 0.01 *N*) the activity coefficient is given as a function of the concentration by the theory of Debye and Hückel [3] in the form

$$\log f_i = -\frac{2.954 \times 10^6}{2.3026 D^{3/2} T^{3/2}} z_1 z_2 \sqrt{\Sigma c_i z_i^2} = -A z_i^2 \sqrt{\mu}, \tag{25}$$

where D=solvent dielectric constant; T=absolute temperature; z=ionic charge; and 2.954×10^6 is equal to the numerical product of Boltzman's constant and the electronic charge. For solvent water, Wyman [24] obtained 78.54 for D. Since all these values are constant at a constant temperature and for a particular solvent, they may be grouped as one constant, A, whose numerical value is 0.506 at 25° C. For better average values, Guggenheim [25] employs an equation with higher powers and his equation gives

$$\log f_i = -Az_i^2\frac{\sqrt{\mu}}{1+\sqrt{\mu}}, \tag{26}$$

in which electrolytes are treated essentially as though they have equal ionic parameters or ionic radii with an average value of 3.0 angstroms. For more concentrated solutions

$$\log f_i = -Az_i^2\frac{\sqrt{\mu}}{1+\sqrt{\mu}}+\beta\mu \tag{27}$$

This β term is a constant due to salt effects and is called the "salt coefficient." It arises from repulsive forces between ions in moderately concentrated solutions [26]. It is to be distinguished from the "ion-mole" coefficient, a solution parameter given by Acree and his collaborators [27], which comes into effect in more concentrated solutions where reaction between ions and neutral molecules may take place. If the "ion-mole" reaction, arising as it does from a triple-body collision, does take place in the dilute solutions under consideration here, it will be small and may be considered as a small part of the β term. Upon substitution of equation 27 for the activity coefficients in equations 23 and 24, the equations

$$\log K_1 = \log K_1^c + \log f_H - A\frac{\sqrt{\mu}}{1+\sqrt{\mu}}+\beta\mu, \text{ and} \tag{28}$$

$$\log K_2 = \log K_2^c + \log f_H - 4A\frac{\sqrt{\mu}}{1+\sqrt{\mu}}+A\frac{\sqrt{\mu}}{1+\sqrt{\mu}}+\beta'\mu-\beta\mu \tag{29}$$

are obtained where the value of $f_{H_2A_2}$ is taken as unity, and β' term in equation 29 is a salt coefficient for dibasic salts and will be included subsequently in β. As may be seen, f_H is retained and evaluated from data on pure potassium chloride and pure hydrochloric acid by the MacInnes [21] assumption previously justified and described.*

Since β or the "salt coefficient" is unknown and may only be estimated [28], the term including β will be dropped. Then equations

$$\log K_1^* = \log K_1^c + \log f_H - A\frac{\sqrt{\mu}}{1+\sqrt{\mu}} \approx \log K_1, \text{ and} \tag{30}$$

$$\log K_2^* = \log K_2^c + \log f_H - 4A\frac{\sqrt{\mu}}{1+\sqrt{\mu}}+A\frac{\sqrt{\mu}}{1+\sqrt{\mu}} \approx \log K_2 \tag{31}$$

result, where K_1^* and K_2^* are the thermodynamic dissociation constants and equal the thermodynamic ionization constants in pure

* The expression for log f_i given by Debye-Hückel-Guggenheim is not employed for the evaluation of the activity coefficient of the hydrogen ion, owing to relative nature of the calculations for E_H.

water, K_1 and K_2, only if β or the "salt coefficient" is equal to zero. That this is nearly the case is evident from the constancy of K_1^* and K_2^* given in tables 2 and 3 as the ionic strength changes. Wangler [29] in some unpublished work on malic acid has found the "salt coefficients" to be of small magnitude.

Values of K_1^c and K_2^c are calculated from the values of the hydrogen-ion concentration given in tables 2 and 3 and of the ionic concentrations of sodium acid malonate and disodium malonate and concentration of unneutralized malonic acid. The latter three ionic concentrations are calculated from the stoichiometrical concentrations of table 1, the hydrogen-ion concentration and the equations 13, 18, 19, and 15 or 16, respectively. Thus in the calculations, ionic concentrations are employed and the sodium salts are taken to be completely dissociated [30]. Values calculated in this manner are given in column 7 of table 2.

The ionic strengths corresponding to the various ionic concentrations are equal to one-half the sum of each ion molality present in the solution multiplied by the square of its valence [31]. Thus, for the first part of the titration (curve A), the ionic strength, μ, is equal to $(2J+3\ c_H)/2$ and for the second part (curve D) to $(4J-M_{H_2An}+5c_H)/2$. Values of the ionic strengths are given in column 8 of table 2. K_1^* and K_2^*, the thermodynamic dissociation constants, are then calculated from the values of K_1^c and K_2^c and the ionic strengths by equations 30 and 31, in which A is equal to 0.506. Values thus obtained are given in the last column of table 2.

VI. CALCULATION OF THE INTERMEDIATE RANGE

In the preceding section the calculations for the first equivalent of NaOH (curve A) and for the second equivalent of NaOH (curve D) were made upon the postulation that each part of the titration could be calculated as though each acid group behaved like a monobasic acid, that is, that the neutralization of the first and second acid groups proceeded separately. That this is not true is evident from the variability in the values of K_1^c, K_2^c, K_1^*, and K_2^* in the middle portion of the titration (neighborhood of 24.86 ml of added alkali). This is also apparent from the ratio of the values of K_1^* or K_1^c obtained at the beginning of the titration, and of K_2^* or K_2^c obtained near the middle of the titration of the second group. This ratio is approximately 600, and it is well known [32] that a dibasic acid may be titrated as a monobasic acid within 1-percent error if this ratio is 5,000 and that the accuracy increases as the ratio becomes larger than 5,000. Since, in this case, K_1^*/K_2^* is only 600, an error much larger than 1 percent is introduced if the titration is made on the monobasic principle. In this case, the error is approximately 15 percent. A good value of K_1^* is obtained until 85 percent of the first acid group has been neutralized. Beyond this point the constant increases rapidly, indicating the formation of Na_2An or the titration of the second group. After the stoichiometrical equivalence point has been reached, values of K_2^* increase rapidly until 15 percent of the second group had been neutralized, and then good values of K_2^* are obtained. Within this 30-percent range neutralization of both acid groups occurs simultaneously, very similar in principle to the titration of a mixed acid [33].

In order to calculate the various ionic concentrations within this range [33], the values for each concentration are solved by elimination of unknowns in the equations

$$M_{NaOH}+c_H=c_{HAn}+2c_{An}, \tag{32}$$

which expresses solution neutrality, and

$$c_{H_2An}+c_{An}+c_{HAn}=M_{H_2An} \tag{33}$$

due to conservation of mass, together with the two equations 23 and 24. M and c have the same distinction as previously defined. Solving simultaneously, the concentration of the dimalonate ion is given by

$$c_{An}=\frac{M_{H_2An}K_1^cK_2^c}{c_H^2+c_HK_1^c+K_1^cK_2^c}. \tag{34}$$

For this calculation, the average value of K_1^c from 0.00 to 21.10 ml added alkali and the average value of K_2^c from 28.35 to 45.83 ml added alkali were employed. The former is equal to 2.63×10^{-3} and the latter to 6.10×10^{-6}. With these values and known values of ($M_{NaOH}=J$) and M_{H_2An} given in table 1, values of c_{An} are calculated. These values are given in column 5 of table 3. Values of the other ionic concentrations are obtained from these values of c_{An} and the same four equations, and are given in columns 6 and 7 of table 3. The ionic strengths are different from those calculated on the monobasic principle, and are larger in the first group titration and smaller in the second group titration, since the disodium malonate ion contributes more to the ionic strength than does sodium acid malonate, since the dibasic ion bears an ionic charge of 2. These new values of the ionic strength, calculated by $(4J-2M_{H_2An}+5c_H)/2$ are given in column 8 of table 3. Values of K_1^a and K_2^a are then calculated for this 30-percent intermediate range as before in the monobasic treatment, and are listed in the last two columns of table 3. Three values of K_1^a and K_2^a calculated monobasically are also listed on each side of this 30-percent range. It should be emphasized again that E_D for this range is calculated by equation 10.

VII. DISCUSSION

It is apparent from equations 28 and 29 that the thermodynamic ionization constants, K_1 and K_2, must vary as the concentration or ionic strength varies, and that this variation is a function of concentration, temperature, dielectric constant, repulsive forces due to presence of salt, and the ionic charge. This variation may be expressed by

$$K=\text{function } (c, T, D, \beta, z_i^2). \tag{35}$$

In the titration of a weak acid in which some un-ionized acid always remains, the dielectric constant of the solvent is also a variable, owing to change in the solvent as the amount of un-ionized acid varies. In this case, water is the solvent with a dielectric constant

[24] of 78.54. The dielectric constant of pure malonic acid is unknown, but it may be estimated from

$$\frac{D \text{ (malonic acid)}}{D \text{ (diethyl malonate)}} = \frac{D \text{ (tartaric acid)}}{D \text{ (diethyl tartrate)}}, \qquad (36)$$

where the other three are known and taken from the International Critical Tables [34]. This gives a value of 67.0 for malonic acid at 25° C. Since the maximum concentration of undissociated malonic acid is 0.08514, the value of D for it would be 78.53, assuming a linear variation of the dielectric constant between pure water and pure malonic acid. The effect due to this is therefore negligible. It may be observed in table 2 that K_1^* varies from 2.10 (omitting the first point where no alkali has been added) to 2.05 at 20.10 cm^3 added alkali. This small deviation (although a slight trend in K_1^*) indicates that β or the "salt coefficient" is nearly zero, and that K_1^* may be considered as approximately equal to K_1, the true thermodynamic ionization constant at this salt concentration range. Moreover, the ionic strength varies only slightly from 0.02 to 0.05, and only a slight variation in the dissociation constant should be expected. However, it is to be emphasized that these values are the dissociation constants of malonic acid at a particular concentration of its sodium salts, and therefore differ from the constants which the acid would have in pure water, and known as the ionization constants. Since the concentration of salts is low these values of the dissociation constants are undoubtedly very close to the ionization constants. Since the slight variation shows an increase with decreasing ionic strength, the ionization constants are probably somewhat higher than these dissociation constants. The somewhat larger variation in K_2^* may be explained in like manner, and is more marked, owing to larger concentrations of salts and to the presence of two salts of unlike valence type, Na^+HAn^- and $Na_2^+An^=$. Since in practice and in application dissociation constants at a particular salt concentration are as important as the ionization constants in the absence of salts, these constants are of value in the interpretation of the properties of malonate solutions found in the oxidized portions of natural sugars and in malonate buffers. For the intermediate range, K_1^* shows the same slight increase as the ionic strength decreases, and K_2^* the same decrease with decreasing ionic strength.

The average of the values of K_1^* from 0.00 to 21.10 ml of added alkali is 2.06×10^{-3}, which also agrees well with the values obtained in the intermediate range. The average of the values of K_2^* from 28.35 to 41.85 ml of added alkali is 2.94×10^{-6}, which also agrees well with the values calculated for the intermediate range, except for the points where only a small amount of $(An^=)$ion is present.

Previous values reported in the literature [1], and the methods by which they were obtained, are given in table 4. The values for both constants are seen to show a marked divergence. As stated before, this divergence is partly due to neglect of interionic attraction corrections, and partly to assumption that the sodium salts of malonic acid are incompletely dissociated and possess the same equivalent conductances at the same equivalent concentration as do the sodium salts of other dibasic and monobasic acids. Britton's values were obtained

TABLE 4.—*Primary and secondary dissociation constants of malonic acid obtained by various workers at 25° C*

Observer	Method	$K_1 \times 10^3$	$K_2 \times 10^6$
The authors	pH titration curve (activity treatment)	2.06	2.94
Burton	pH titration curve (classical treatment)	2.07	3.89
Britton	pH titration curve (analytical treatment)	2.11	4.45
White and Jones	Conductivity	1.63	----------
Salm	Colorimetric	1.6	----------
Berthelot	Conductivity	1.64	----------
Walden	do	1.63	----------
Ostwald	do	1.58	----------
Bethmann	do	1.71	----------
Vogel and Jeffery	Conductivity and the use of the parachor	1.397	----------
Datta and Dhar	CO_2 absorption	----------	1.36
Chandler	Partition	----------	2.03
Chandler and McCoy	Conductivity	----------	2.1
Wegscheider	do	----------	10.0
Smith	Conductivity and sucrose inversion	----------	1.0

in a manner similar to the treatment presented herein, but no corrections were made for liquid-junction potentials nor for interionic attraction. The former raise the constants and the latter corrections lower them. For K_1 these are seen to counteract each other to a large extent, since all ions in solution bear a charge of 1, for with no corrections whatsoever, Britton obtained 2.11×10^{-3}, while in this work a value of 2.06×10^{-3} is obtained. For K_2 these conditions do not persist as the charges on the ions (H^+, HAn, and $An^=$) differ, and Britton's value is high owing to the neglect of the interionic theory and liquid-junction corrections.

The low values obtained by the others are due, in the main, to the assumption of incomplete dissociation [30] of the sodium salts, a view generally accepted at the time of their determination, and also to the assumption that the degree of dissociation of these sodium salts was the same as for other similar basic sodium salts. To show that these low results are due to these assumptions and not so much to experimental differences, the following classical treatment has been incorporated here.

If α_1 is taken as the degree of dissociation of sodium acid malonate and α_2 as the degree of dissociation of disodium malonate, instead of assuming complete dissociation [30] of these salts, $\alpha_1 c_{NaHAn}$ is then substituted for c_{NaHAn} and $\alpha_2 c_{Na_2An}$ for c_{Na_2An} in the calculation of K_1^c and K_2^c. The value of α_1 is calculated from the ratio of the equivalent conductance of sodium acetate and the equivalent conductance of sodium acetate at infinite dilution, and α_2 from the same ratio for disodium tartrate, at the same equivalent concentration as present in the titrated solution. These salts were employed since their values [35] are known, and Noyes and Falk [36] and others [37] have shown that the basic salts have nearly the same equivalent conductance at equal equivalent concentrations. In table 5 a few values calculated in this manner are given as well as the new ionic strengths. These have been labeled with a subscript 0 to distinguish them from those obtained in the thermodynamic treatment. The subscript 0 has been chosen since this is the method Ostwald [38] and his contemporaries employed for the determination of ionization constants. It should be emphasized again in this connection that the ionization constants are expressed in terms of activity and not in concentration terms, and even though the α values have been employed, the result-

ant ionic concentrations must be multiplied by the activity coefficient, as was done in the calculations of K_1^a and K_2^a by equations 30 and 31 [39, 40, 41].

TABLE 5.—*Classical Ostwald ionization constants and their values on the Debye-Hückel basis at a few points*

0.1007 N NaOH	α_1	$K_1^{a'} \times 10^3$	μ_0	$K_1^{a} \times 10^3$	0.1007 N NaOH	α_1	α_2	$K_2^{a'} \times 10^6$	μ_0	$K_2^{a} \times 10^6$
ml					ml					
1.00	0.956	2.72	0.02312	2.08	28.35	0.869	0.803	5.30	0.05109	2.82
2.06	.940	2.64	.02343	2.05	29.35	.874	.787	5.41	.05276	2.86
3.21	.927	2.58	.02408	2.01	30.39	.878	.775	5.50	.05406	2.83
4.26	.917	2.55	.02490	1.99	31.85	.884	.757	5.63	.05686	2.80
5.11	.911	2.50	.02557	1.96	33.85	.890	.744	5.29	.05858	2.67
6.10	.904	2.48	.02649	1.89	35.85	.899	.730	5.21	.06026	2.61
11.08	.884	2.32	.03146	1.84	37.85	.906	.720	5.01	.06224	2.59
13.10	.878	2.27	.03344	1.80	39.85	.916	.711	4.98	.06347	2.47
15.10	.873	2.25	.03534	1.79	41.85	.925	.704	4.69	.06505	2.31
17.10	.868	2.24	.03710	1.79	42.85	.931	.700	4.59	.06558	2.25
19.10	.865	2.20	.03879	1.76	43.83	.936	.698	4.52	.06620	2.21
21.10	.861	2.27	.04034	1.83	44.83	.942	.695	4.39	.06670	2.14
22.10	.860	2.43	.04113	1.96	45.83	.949	.692	4.18	.06716	2.04

It may be seen that these values are lower than the values given in table 2 and closer to the conductivity values listed in table 4. Vogel and Jeffery's low value may be due to the postulation of equal conductivity for salts of the carboxyl and carbamyl groups, based upon their similar parachors.

These classical values are also seen to vary much more rapidly with the ionic strength and their average values for the same milliliter range, as was employed in the average for the thermodynamic constants, are 1.88×10^{-3} and 2.62×10^{-6}, respectively. These calculations illustrate the point for which they were intended, namely, that the low values reported in the literature are due in a large degree to the acceptance of incomplete dissociation and not so much to experimental differences. In addition, they were obtained with the use of α values, the determination of which depends upon the extrapolation to infinite dilution of the equivalent conductances. Since then, these methods of extrapolation have been greatly improved to include viscosity corrections [39], effect of Brownian movement on the ionic attraction between ions of unlike charge [40], and by the analytical treatment [41]. These corrections have not been made for the literature data, for in most cases the data did not warrant this treatment.

Since the classical values show much larger variation with ionic strength than do the thermodynamic values, and also depend upon the evaluation of α, which, at the best, can only be qualitative, the values given in tables 2 and 3 are considered to be the better. Also these values have been obtained by methods which are now generally accepted.

VIII. SUMMARY

The data for the electrometric titration of malonic acid 0.10 M by sodium hydroxide 0.1007 N at 25° C with the use of a hydrogen electrode and a saturated potassium chloride electrode are presented. Corrections for the liquid-junction potential between the titrated solution and the saturated potassium chloride are embodied in the

calculations. The pH titration curve is given and varies from 2 to 9 in pH for the solutions of malonic acid-sodium malonate salts.

The primary and secondary dissociation constants of malonic acid calculated on the activity basis, with corrections for interionic attraction, were found to be 2.06×10^{-3} and 2.94×10^{-6}, respectively. Brief discussions are given of the relation of these dissociation constants to the true ionization constants in pure water, and a comparison is made of these values with those calculated by classical methods used prior to the development of the Debye-Hückel theory.

IX. REFERENCES

[1] Britton, J. Chem. Soc. **127,** 1896 (1925);
White and Jones, Am. Chem. J. **44,** 159 (1910);
Salm, Z. phys. Chem. **63,** 83 (1908);
Berthelot, Ann. chim. Phys. [6] **23,** 1 (1891);
Walden, Z. phys. Chem. **8,** 433 (1891);
Ostwald, Z. phys. Chem. **3,** 241 (1889); **8,** 445 (1891);
Bethmann, Z. phys. Chem., **5,** 385 (1890);
Vogel and Jeffery, J. Soc. Chem. Ind. (Review) [12], **53,** 964 (1934);
Datta and Dhar, J. Chem. Soc. **107,** 824 (1915);
Chandler, J. Am. Chem. Soc. **30,** 694 (1908);
McCoy, J. Am. Chem. Soc. **30,** 688 (1908);
Wegscheider, Monatshefte Chem. **23,** 599 (1902); **26,** 1335 (1905); **37,** 251 (1916);
Burton, Dissertation, Univ. of Maryland, (1934);
Smith, Z. phys. Chem. **25,** 193 (1898).

[2] Milner, Phil. Mag. [6] **23,** 551 (1912); [6] **25,** 742 (1913).

[3] Debye and Hückel, Phys. Z. **24,** 185, 305, 334 (1923).

[4] Loomis and Acree, Am. Chem. J. **46,** 585 (1911).

[5] Clark, The Determination of Hydrogen Ions, p. 485, 3d ed. (The Williams and Wilkins Co., Baltimore, Md., 1928.)

[6] Hamer, J. Am. Chem. Soc. **57,** 662 (1935);
Kline, Meacham, and Acree, BS J. Research **8,** 101 (1932) RP403;
Scatchard and Buehrer, J. Am. Chem. Soc. **53,** 574 (1931);
Murray and Acree, BS J. Research **7,** 713 (1931) RP369;
Maclagan, Biochem. J. **23,** 309 (1929);
Guggenheim, J. Am. Chem. Soc. **52,** 1315 (1930).

[7] Loomis and Acree, Am. Chem. J. **46,** 609 and 610 (1911); **38,** 2391 (1916);
Myers and Acree, J. Phys. Chem. **21,** 334 (1917);
Myers, Clark, and Acree, J. Phys. Chem. **20,** 243 (1916);
Clark, The Determination of Hydrogen Ions, p. 676, 3d ed. (The Williams and Wilkins Co., Baltimore, Md., 1928.)

[8] Int. Critical Tables **7,** 321 (1930).

[9] Scatchard, J. Am. Chem. Soc. **47,** 696 (1925).

[10] Taylor, Treatise on Physical Chemistry, **1,** 2d. ed., chap. XII, by H. S. Harned, p. 820 (D. Van Nostrand Co., Inc., New York, 1931).

[11] Henderson, Z. phys. Chem. **59,** 118 (1907); **63,** 325 (1908).

[12] MacInnes, Shedlovsky, and Longsworth, J. Am. Chem. Soc. **54,** 2758 (1932).

[13] Vogel and Jeffery, J. Chem. Soc. 1101 (1934); J. Soc. Chem. Ind. (Review) [12], **53,** 964 (1934).

[14] Ostwald, Z. phys. Chem. **3,** 241 (1889); **8,** 445 (1891); Handbuch der allgemeinen Chemie, p. 46 (Leipzig, 1924).

[15] Kohlrausch, See Handbuch der allgemeinen Chemie by Ostwald and Drucker (Leipzig, 1924) on Conductance Data.

[16] Harned, J. Phys. Chem. **30,** 433 (1926).

[17] Harned, J. Am. Chem. Soc. **48,** 326 (1926);
Taylor's Treatise on Physical Chemistry, **1,** p. 803;
Guntelberg, Z. Phys. Chem. **123,** 199 (1926);
Hawkins, J. Am. Chem. Soc. **54,** 4480 (1932).

[18] Robinson and Sinclair, J. Am. Chem. Soc. **56,** 1830 (1934).

[19] Harned and Ehlers, J. Am. Chem. Soc. **55,** 2179 (1933).

[20] Randall and Young, J. Am. Chem. Soc. **50,** 989 (1928).

[21] MacInnes, J. Am. Chem. Soc. **41,** 1086 (1919).

[22] Scatchard, J. Am. Chem. Soc. **47,** 696 (1925);
Harned, J. Phys. Chem. **30,** 433 (1926);
Lewis and Randall, Thermodynamics, p. 379 (McGraw-Hill Book Co., Inc., New York, 1923).
[23] Guldberg and Waage, Études sur les affinités chimiques (1867); J. prakt. Chem. [2], **19,** 1 (1879)
[24] Wyman, Phys. Rev. **35,** 623 (1930).
[25] Guggenheim and Schindler, J. Phys. Chem. **38,** 533 (1934).
[26] Hückel, Phys. Z. **26,** 93 (1925).
[27] Acree, Nirdlinger, Rogers, Robertson, Harrison, Marshall, Gruse, et al., Am. Chem. J. **49,** 121, 364, 485 (1913), and other articles from 1907 to 1913; J. Am. Chem. Soc. **39,** 386 (1917);
Taylor's Treatise on Physical Chemistry **2,** p. 997.
[28] Owen, J. Am. Chem. Soc. **54,** 1758 (1932);
Harned and Owen, J. Am. Chem. Soc. **52,** 5079 (1930).
[29] Wangler, Dissertation, George Washington University, 1930.
[30] Falkenhagen, Electrolytes, p. 93, translated by R. P. Bell, Oxford, (The Clarendon Press, 1934).
[31] Lewis and Randall, Thermodynamics, p. 373 and 428, (McGraw-Hill Book Co., Inc., New York, 1923.)
[32] Kolthoff and Furman, Potentiometric Titrations, p. 97, (John Wiley & Sons, Inc., New York, 1926).
[33] Mellon, Avery, Slagle, and Acree, J. Infect. Diseases, **29,** 1,7, (1921);
Meacham, Hopfield and Acree, J. Bact. **5,** 169, 305, 309, 491 (1918).
Acree, Paper, p. 638–646, (June 1919).
Meacham, Science **48,** 449 (1918).
Acree, J. Bact. **2,** 1, 109, 137 (1917).
Brightman, Hopfield, Meacham, and Acree, J. Am. Chem. Soc. **40,** 1940 (1918).
Birge and Acree, J. Am. Chem. Soc., **41,** 1031 (1919).
Lubs, Cloukey, and Acree, J. Am. Chem. Soc. **38,** 2773, 2784 (1916).
[34] Int. Crit. Tables **6,** p. 86, 92, 94.
[35] Ostwald, Handbuch der allgemeinen Chemie, (Leipzig, 1924)
Walden, Elektrochemie Nichtwässriger Lösungen, (Leipzig, 1924).
[36] Noyes and Falk, J. Am. Chem. Soc. **34,** 485 (1912).
[37] Kohlrausch and Holborn's Leitvermögen der Elektrolyte.
[38] Ostwald, Z. phys. Chem. **3,** 241 (1889).
[39] Davies, Phil. Mag. **4,** 244 (1927).
[40] Onsager, Phys. Z. **27,** 388 (1926); **28,** 277 (1927).
[41] Shedlovsky, J. Am. Chem. Soc. **54,** 1405 (1932).

WASHINGTON, April 7, 1936.

U. S. DEPARTMENT OF COMMERCE NATIONAL BUREAU OF STANDARDS

RESEARCH PAPER RP896

Part of Journal of Research of the National Bureau of Standards, Volume 16, June 1936

TESTS OF EIGHT LARGE H-SHAPED COLUMNS FABRICATED FROM CARBON-MANGANESE STEEL

By Ambrose H. Stang, Herbert L. Whittemore, Leroy R. Sweetman

ABSTRACT

As part of its program to investigate the behavior of compression members of carbon-manganese steel, such as were used for the compression chords of the Bayonne arch bridge, the bridge department of the Port of New York Authority requested the cooperation of the National Bureau of Standards in an investigation of the strength and behavior under load of large H-shaped columns fabricated from plates and angles and material representative of those which went into the actual structure. Eight columns were tested.

The shortening and lateral deflection under load were measured. The strain was also measured on seven 2-inch vertical gage lines near the top and bottom of the column and at midheight. The properties of the material were determined by tensile tests of coupons.

It was found that:

1. The loading was more eccentric than in the tests of tower and chord columns described in Research Papers RP831 and RP897.
2. All the columns deflected in a direction perpendicular to the web. Apparently there was no relation between the direction in which the columns deflected and the distribution of yield strength of the material across the column.
3. For seven of the eight columns the strength exceeded the capacity of the testing machine (10,000 kips).
4. The column efficiency was obtained by dividing the column yield strength by the weighted yield strength of the column material. For the columns having cover plates 1.5 in. thick the average column efficiency was 95.0 percent and for the columns having cover plates 1.25 in. thick, 96.5 percent.

CONTENTS

	Page
I. Introduction	596
II. The specimens and the methods of testing	596
1. The columns	596
(a) Description	596
(b) Testing procedure	597
(1) Compressometers	597
(2) Lateral deflection	597
(3) Strains	597
(4) Loading	597
2. Method of determining the properties of the columns	598
(a) Young's modulus	598
(b) Proportional limit	598
(c) Column yield strength	598
(d) Weighted yield strength of the material	598
(e) Column efficiency	598
3. Coupons	599
(a) General	599
(b) Shape and size	599
(c) Yield strength	599
(d) Extensometer	599
(e) Testing machine	599
(f) Speed of the movable platen	599

Page
III. Results for the coupons 600
1. Tensile tests 600
2. Chemical composition 600
IV. Results for the columns 600
1. Yield strength of the longitudinal pieces 600
2. Shortening 602
3. Stress distribution 603
4. Lateral deflection 624
5. Strength 624
V. Conclusions 624

I. INTRODUCTION

Because few tests have been made on large fabricated columns of high-strength steel, the bridge department of the Port of New York Authority requested the cooperation of the National Bureau of Standards in an investigation of the strength and behavior under load of large H-shaped columns fabricated from plates and angles.

II. THE SPECIMENS AND THE METHOD OF TESTING

1. THE COLUMNS

(a) DESCRIPTION

The nominal dimensions and properties of the columns are given in table 1. There were eight columns fabricated by riveting from

TABLE 1.—*Nominal dimensions and properties of the columns*

Number of specimens tested	Symbol	Kind of steel	Cross-sectional area of steel	Length		Moment of inertia		Radius of gyration		Slenderness ratio	
						I_{x-x}	I_{y-y}	r_{x-x}	r_{y-y}	$x-x$	$y-y$
			in.²	ft	in.	in.⁴	in.⁴	in.	in.		
4	HM1 to HM4	Carbon-manganese.	145	9	8	12,186	2,899	9.17	4.47	12.6	25.9
4	HM5 to HM8	do	135	9	8	10,835	2,566	8.96	4.36	13.0	26.6

plates and angles of carbon-manganese steel. The steel was from different heats and the results of the tests of the coupons showed that the tensile properties varied over a rather wide range.

The dimensions of the columns are shown in figure 1. The columns were designated HM followed by the numerals 1, 2, etc., for the individual columns. The web plates and the angles were the same size for all the columns. For the four columns HM1, HM2, HM3, and HM4, the cover plates were 1.5 in. thick and for the remaining four, HM5, HM6, HM7, and HM8, the cover plates were 1.25 in. thick.

The longitudinal pieces of each column, that is, the longitudinal plates and angles, were cut as shown in the cutting diagram in figure 1. Each longitudinal piece of the column was match-marked to correspond with coupons cut from the same plate or angle, and its location in the column was recorded.

(b) TESTING PROCEDURE

All the columns were tested as flat-end columns by the use of the equipment and methods described in National Bureau of Standards

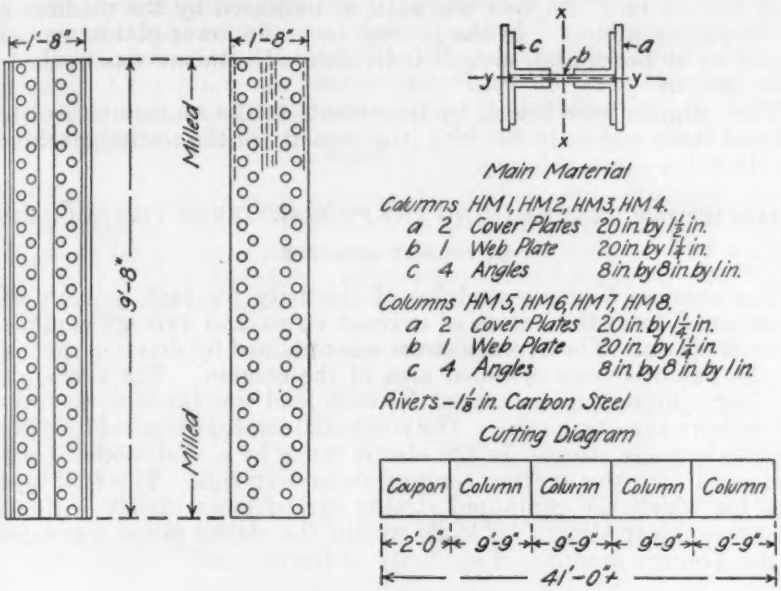

FIGURE 1.—*Dimensions of the columns.*

h Pape RP831, Tests of Steel Tower Columns for the George Washington Bridge.[1]

(1) *Compressometers.*—Compressometers similar to those used for the tower columns, except that the gage length was 5 ft, were used to measure the shortening of the columns under load. The locations of the four compressometers are shown in figure 2.

(2) *Lateral deflection.*—The lateral deflection of the columns was measured by the use of the taut-wire, mirror-scale deflectometer. The distance between the supports for the wire was 8 ft 8 in., and the middle of the wire was at midheight of the column. One division on the scale was 0.1 in., and readings were estimated to 0.1 of a division. The locations of the three deflectometers are shown in figure 2.

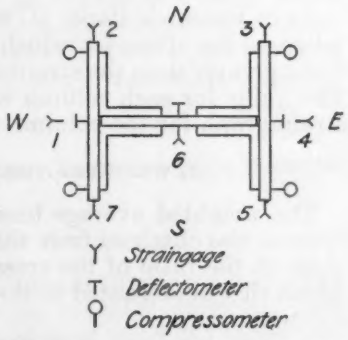

FIGURE 2.—*Locations of the straingage lines, the deflectometers, and the compressometers on the columns.*

(3) *Strains.*—At elevations of 37.5 in. from the bottom, at midheight, and at 37.5 in. from the top of each column, seven 2-in. vertical gage lines were laid off at the locations shown in figure 2.

[1] J. Research NBS 15, 317 (1935) RP831.

The strains were measured manually by the use of a Whittemore strain gage.

(4) *Loading.*—In tests on the tower columns (RP831) the lower platen of the testing machine was adjusted in its spherical seat for each column until the load was axial as indicated by the readings of the compressometers. In the present tests the lower platen was adjusted to be horizontal, and no individual adjustment was made for each column.

The columns were loaded by increments to the maximum load for column HM6 and to 10,000 kips (the capacity of the testing machine) for the other seven columns.

2. METHOD OF DETERMINING THE PROPERTIES OF THE COLUMNS

(a) YOUNG'S MODULUS

The average Young's modulus of elasticity for each column was determined from the values of average stress and average compressometer strain. The average stress was obtained by dividing the load by the nominal cross-sectional area of the column. The average of the four compressometer strains for each load was taken as the average compressometer strain. The computed strains obtained by dividing the average stresses in the elastic range by a trial modulus were compared with the average compressometer strains. The trial modulus for which the computed strains agreed most closely with the compressometer strains for loads within the elastic range was taken as the Young's modulus of elasticity of the column.

(b) PROPORTIONAL LIMIT

A proportional limit for each column was determined as the stress for which the average compressometer strain was 0.000012 greater than the strain computed by the use of the Young's modulus.

(c) COLUMN YIELD STRENGTH

As in Research Paper RP831 the yield strength of the column was taken as the stress for which the average compressometer strain was 0.002 greater than the strain computed by using the Young's modulus. The value for each column was obtained graphically from the stress-strain graph for the column.

(d) WEIGHTED YIELD STRENGTH OF THE MATERIAL

The weighted average tensile yield strength of the material in the column was obtained from the yield strengths of coupons by weighting them in the ratio of the cross-sectional area of the longitudinal piece which they represented to the total nominal cross-sectional area of the column.

(e) COLUMN EFFICIENCY

The column efficiency was obtained by dividing the column yield strength by the weighted yield strength of the material in the column.

3. COUPONS

(a) GENERAL

The coupons were machined from the piece marked "coupon" in the cutting diagram in figure 1. This diagram shows the relation of the coupons to the longitudinal pieces used in fabricating each column. From each plate three coupons were taken, one at the middle, one at the edge of the plate, and one midway between these two coupons. From each angle one coupon was taken at the middle of one of the legs of the angle.

(b) SHAPE AND SIZE

The axis of each coupon was parallel to the rolling direction (axis) of the plate or angle. The coupons were standard ASTM tensile specimens for plates, shapes, and flats.[3] These coupons had a gage length of 8 in., a width at the reduced section of 1.5 in., and the thickness was that of the material as rolled.

(c) YIELD STRENGTH

The method selected for determining the yield strength of these coupons is essentially the "set method" described by the Section on Elastic Strength of Materials of the Technical Committee on Mechanical Testing of the American Society for Testing Materials.[4] The yield strength was taken as the stress for which the strain was 0.002 greater than the strain computed from the stress and the Young's modulus of elasticity.

(d) EXTENSOMETER

The strains in some coupons were measured by the use of a Ewing extensometer having a gage length of 8 in. One division on the scale of this instrument corresponded to a strain of 0.000025 in the coupon. The readings were estimated to 0.1 division. For the coupons of carbon-manganese steel upon which a Ewing extensometer was not used, the strains were measured by the use of a Berry strain gage having a gage length of 8 in. The yield strength was determined graphically by a method which gave values approximating closely those obtained by the use of the Ewing extensometer.

(e) TESTING MACHINE

The coupons were tested in a screw-power, beam-and-poise machine having a capacity of 100 kips.

(f) SPEED OF THE MOVABLE PLATEN

For the coupons on which a Ewing extensometer was used, the speed of the movable platen of the testing machine under no load was 0.04 in./min and this speed was maintained until the stress was

[3] Figure 1, Stand. Am. Soc. Testing Materials [1] 68 (1933).
[4] Proc. Am. Soc. Testing Materials [1] 31, 602 (1931).

about three-quarters of the yield strength. For higher stresses the speed was 0.01 in./min. After the extensometer was removed the speed was 0.4 in./min until the coupon ruptured.

For the coupons on which a Ewing extensometer was not used, the speed was 0.04 in./min until the yield strength was observed. For higher stresses the speed was 0.4 in./min.

III. RESULTS FOR THE COUPONS

1. TENSILE TESTS

The results of the tensile tests of the coupons are given in table 2. The properties of the material are average values for the longitudinal members of the same size and shape.

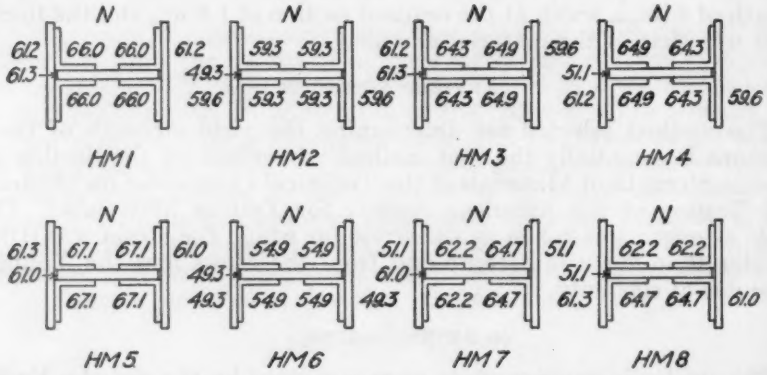

FIGURE 3.—*Average yield strength, in kips per square inch, of the coupons representing each longitudinal piece of the columns.*

A typical Ewing stress-strain graph for the carbon-manganese steel is shown in figure 9 of Research Paper RP 831.

The speed of the movable head of the testing machine was much lower than is customarily used when determining the yield strength. For these coupons the rate at which the stress was increased is more nearly the rate for the columns than the rate customarily used for coupons.

2. CHEMICAL COMPOSITION

Chemical analyses were made of samples from coupons having the highest and the lowest tensile strength for each thickness and each shape. The results are given in table 3.

IV. RESULTS FOR THE COLUMNS

1. YIELD STRENGTH OF THE LONGITUDINAL PIECES

The average yield strength of the material for each longitudinal piece of the column is shown in figure 3.

TABLE 2.—*Results of the tensile tests of columns*

COLUMN HM1—CARBON-MANGANESE

Column material		Yield strength (average)	Tensile strength (average)	Elongation in 8 inches (average)	Reduction of area (average)
Shape	Nominal size				
	In.	*kips/in.²*	*kips/in.²*	*Percent*	*Percent*
1 plate	20 by 1.5	61.2	106.3	18.5	42.4
1 plate	20 by 1.5	61.2	106.3	18.5	42.4
1 plate	20 by 1.25	61.3	107.5	17.6	37.5
2 angles	8 by 8 by 1	66.0	97.5	20.0	49.8
2 angles	8 by 8 by 1	66.0	97.5	20.0	49.8
Weighted average		63.2	102.9	19.0	44.6

COLUMN HM2—CARBON-MANGANESE

1 plate	20 by 1.5	59.6	104.0	19.0	41.8
1 plate	20 by 1.5	59.6	104.0	19.0	41.8
1 plate	20 by 1.25	49.3	88.3	26.0	56.1
2 angles	8 by 8 by 1	59.3	97.4	19.0	39.7
2 angles	8 by 8 by 1	59.3	97.4	19.0	39.7
Weighted average		57.7	98.5	20.2	43.4

COLUMN HM3—CARBON-MANGANESE

1 plate	20 by 1.5	61.2	106.3	18.5	42.4
1 plate	20 by 1.5	59.6	104.0	19.0	41.8
1 plate	20 by 1.25	61.3	107.5	17.6	37.5
2 angles	8 by 8 by 1	64.3	100.2	18.2	43.8
2 angles	8 by 8 by 1	64.9	97.0	19.7	48.9
Weighted average		62.3	102.8	18.6	43.1

COLUMN HM4—CARBON-MANGANESE

1 plate	20 by 1.5	61.2	106.3	18.5	42.4
1 plate	20 by 1.5	59.6	104.0	19.0	41.8
1 plate	20 by 1.25	51.1	93.3	22.2	56.1
2 angles	8 by 8 by 1	64.9	97.0	19.7	48.9
2 angles	8 by 8 by 1	64.3	100.2	18.2	43.8
Weighted average		60.5	100.4	19.4	46.3

COLUMN HM5—CARBON-MANGANESE

1 plate	20 by 1.25	61.3	107.5	17.6	37.5
1 plate	20 by 1.25	61.0	104.9	19.0	42.6
1 plate	20 by 1.25	61.0	104.9	19.0	42.6
2 angles	8 by 8 by 1	67.1	97.2	18.5	46.4
2 angles	8 by 8 by 1	67.1	97.2	18.5	46.4
Weighted average		63.8	101.9	18.5	43.3

COLUMN HM6—CARBON-MANGANESE

1 plate	20 by 1.25	49.3	88.3	26.0	56.1
1 plate	20 by 1.25	49.3	88.3	26.0	56.1
1 plate	20 by 1.25	49.3	88.3	26.0	56.1
2 angles	8 by 8 by 1	54.9	93.3	21.7	50.6
2 angles	8 by 8 by 1	54.9	93.3	21.7	50.6
Weighted average		51.8	90.5	24.1	53.6

TABLE 2.—*Results of the tensile tests of columns*—Continued

COLUMN HM7—CARBON-MANGANESE

Column material		Yield strength (average)	Tensile strength (average)	Elongation in 8 inches (average)	Reduction of area (average)
Shape	Nominal size				
	In.	*kips/in.²*	*kips/in.²*	*Percent*	*Percent*
1 plate	20 by 1.25	51.1	93.3	22.2	56.1
1 plate	20 by 1.25	51.1	93.3	22.2	56.1
1 plate	20 by 1.25	61.0	104.9	19.0	42.6
2 angles	8 by 8 by 1	62.2	96.9	21.0	49.7
2 angles	8 by 8 by 1	64.7	96.9	19.5	51.8
Weighted average		58.4	97.0	20.7	51.2

COLUMN HM8—CARBON-MANGANESE

1 plate	20 by 1.25	61.3	107.5	17.6	37.5
1 plate	20 by 1.25	61.0	104.9	19.0	42.6
1 plate	20 by 1.25	51.1	93.3	22.2	56.1
2 angles	8 by 8 by 1	64.7	96.9	19.5	51.8
2 angles	8 by 8 by 1	62.2	96.9	21.0	49.7
Weighted average		60.3	99.7	19.9	47.8

TABLE 3.—*Chemical composition of the carbon-manganese steel*

Description of samples			Chemical composition				
Thickness	Shape	Tensile strength	Carbon	Manganese	Phosphorus	Sulphur	Silicon
In.		kips/in.²	*Percent*	*Percent*	*Percent*	*Percent*	*Percent*
1	Angle	93.3	0.31	1.55	0.029	0.015	0.20
1	do	100.2	.33	1.70	.020	.021	.17
1.25	Plate	86.0	.30	1.49	.034	.029	.17
1.25	do	109.3	.39	1.88	.024	.024	.17
1.5	do	101.2	.32	1.91	.024	.022	.18
1.5	do	108.5	.37	1.95	.027	.024	.19

2. SHORTENING

Typical graphs of average column stress plotted against the strain for each compressometer on column HM6 are shown in figure 4. The curves were all drawn parallel. These graphs are typical of those for the other columns. A comparison of these graphs with those for a tower column shown in figure 10 of Research Paper RP831 indicates that the loads on these H-shaped columns were somewhat more eccentric than those on the tower columns.

For each load, also, the average strain for each column was computed from the values for the four compressometers. These average strains were used for the average stress-strain graphs for each column shown in figure 5.

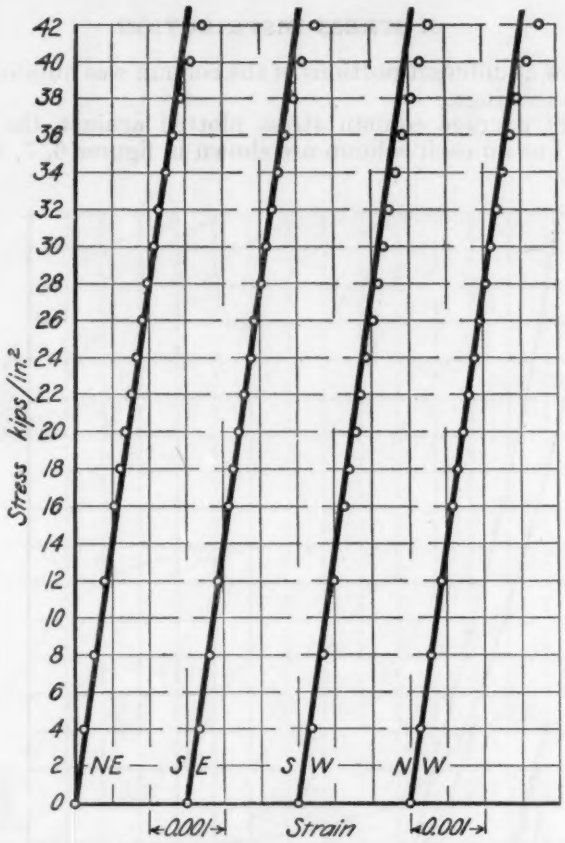

FIGURE 4.—*Typical graphs of average column stress plotted against the stress for each compressometer on column* HM6.

The properties of the columns are given in table 4.

TABLE 4.—*Properties of the columns*

Column	Young's modulus of elasticity	Proportional limit [1]	Weighted yield strength of material	Column yield strength	Column efficiency (based on column yield strength)	Column was loaded to		Remarks
						Load	Stress	
	kips/in.²	kips/in.²	kips/in.²	kips/in.²	*Percent*	kips	kips/in.²	
HM1	29,000	28	63.2	60.5	95.7	10,005	69.0	
HM2	27,150	28	57.7	54.5	94.5	10,005	69.0	
HM3	28,300	32	62.3	59.5	95.5	10,005	69.0	
HM4	29,000	24	60.5	57.0	94.2	10,005	69.0	
Average					95.0			
HM5	28,200	32	63.8	60.5	94.8	9,990	74.0	
HM6	27,600	28	51.8	50.5	97.5	9,940	73.6	Final maximum.
HM7	28,800	34	58.4	56.5	96.7	9,990	74.0	
HM8	28,100	28	60.3	58.5	97.0	9,990	74.0	
Average					96.5			

[1] Determined as the stress for which the average compressometer strain was 0.000012 greater than the strain computed by the use of the Young's modulus of elasticity.

3. STRESS DISTRIBUTION

The strain at different portions of the column was obtained from the strain-gage readings.

Graphs of average column stress plotted against the strain for each gage line on each column are shown in figures 6, 7, 8, 9, 10, 11, 12, and 13.

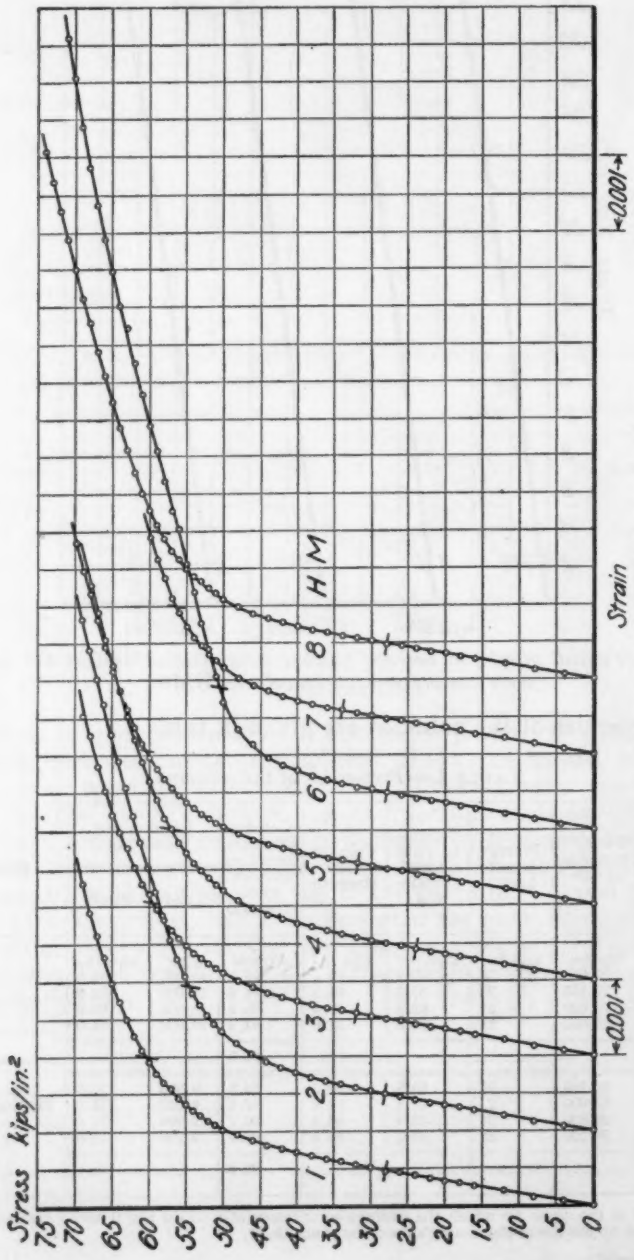

FIGURE 5.—*Stress-strain graphs for each column.*

(The strains are the average of the values for the four compressometers.)

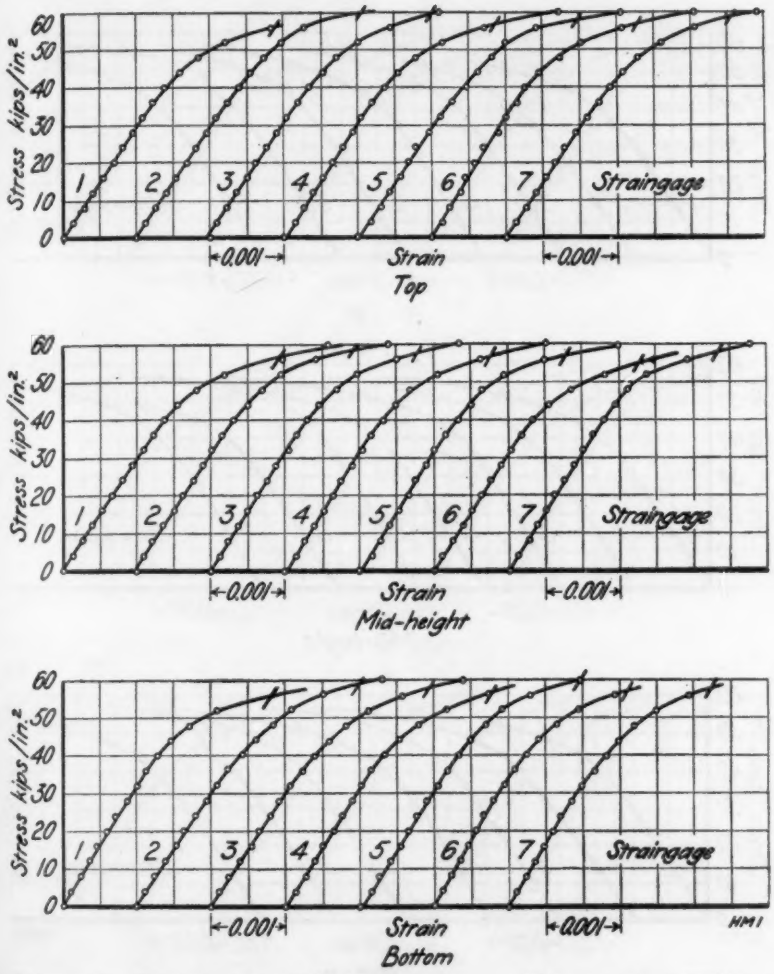

FIGURE 6.—*Stress-strain graphs for the strain-gage lines on column* HM1.

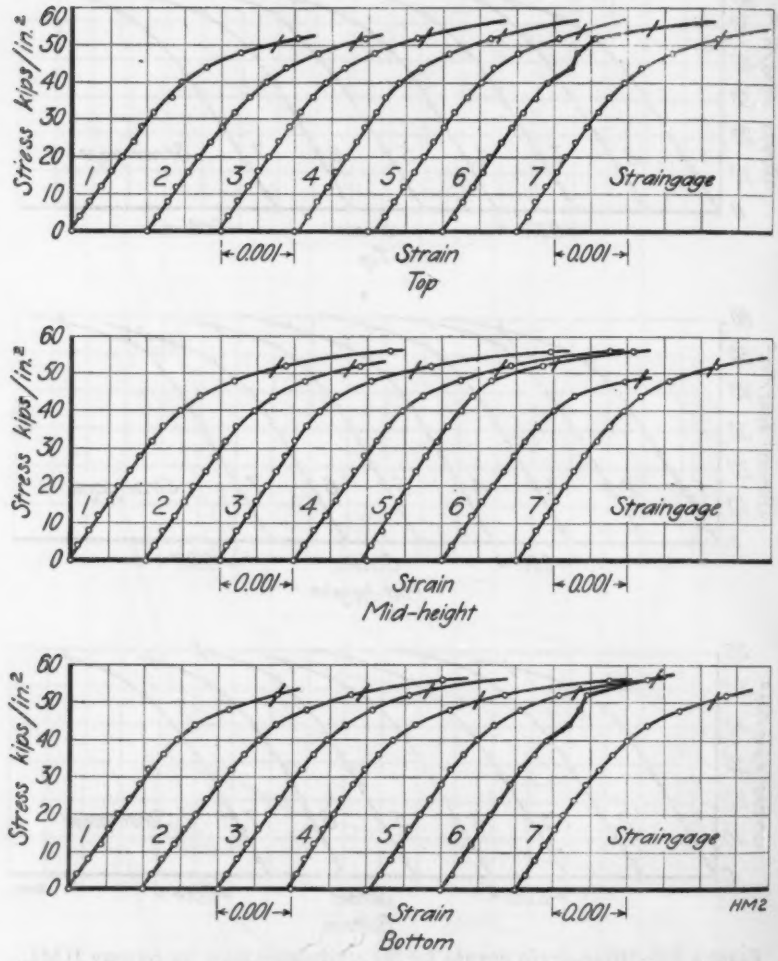

FIGURE 7.—*Stress-strain graphs for the strain-gage lines on column* HM2.

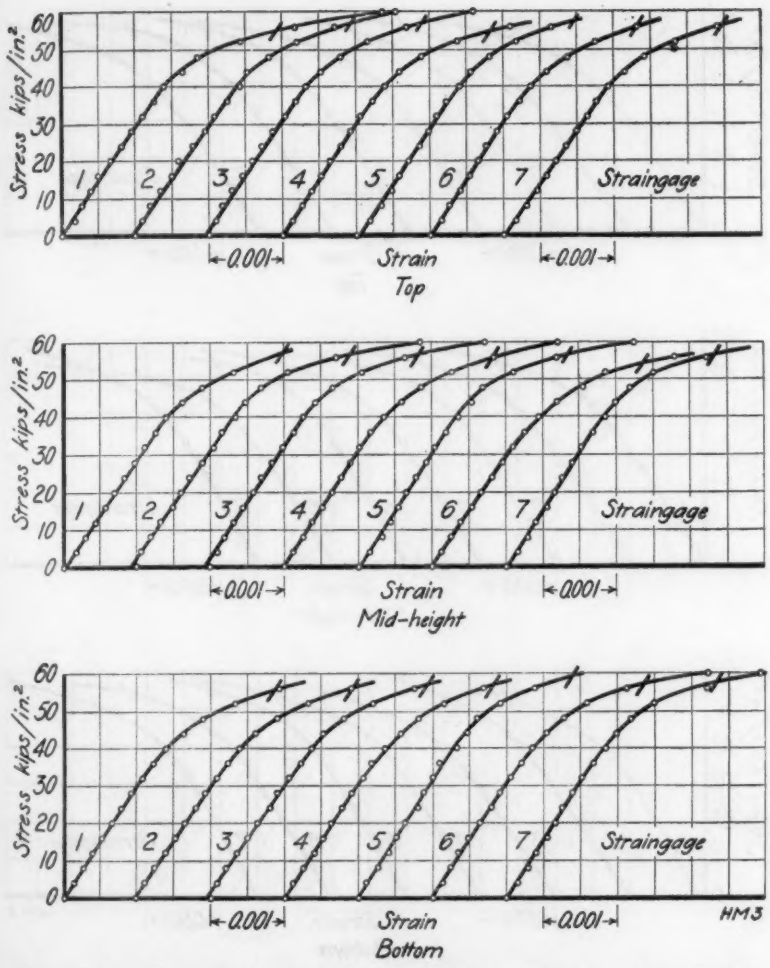

FIGURE 8.—*Stress-strain graphs for the strain-gage lines on column* HM3.

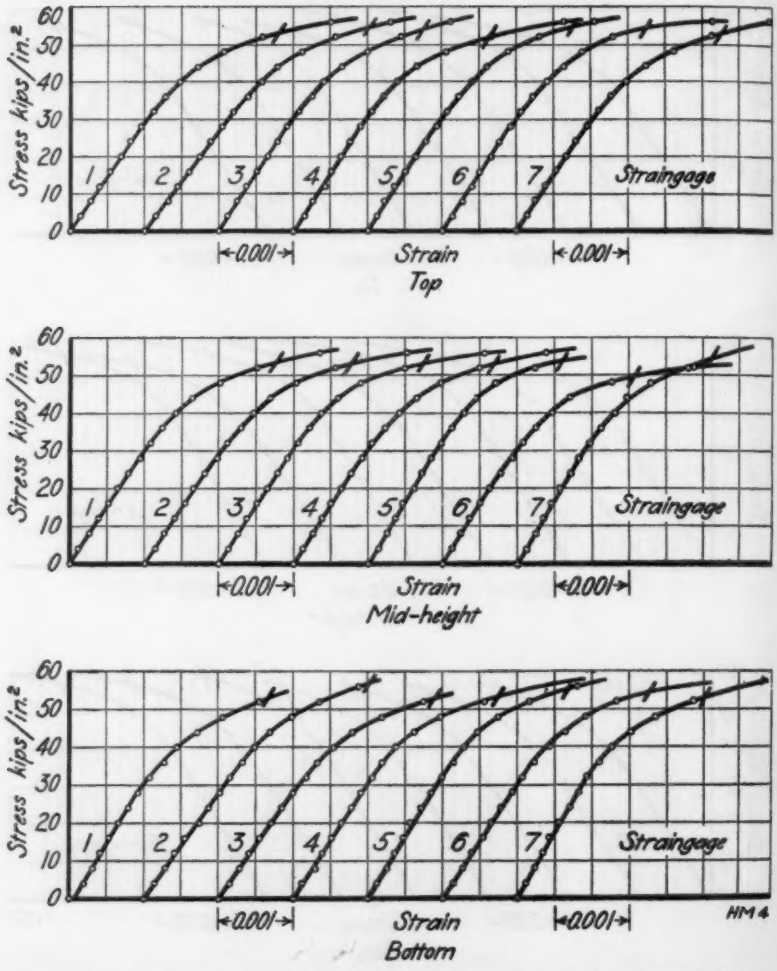

FIGURE 9.—*Stress-strain graphs for the strain-gage lines on column* HM4.

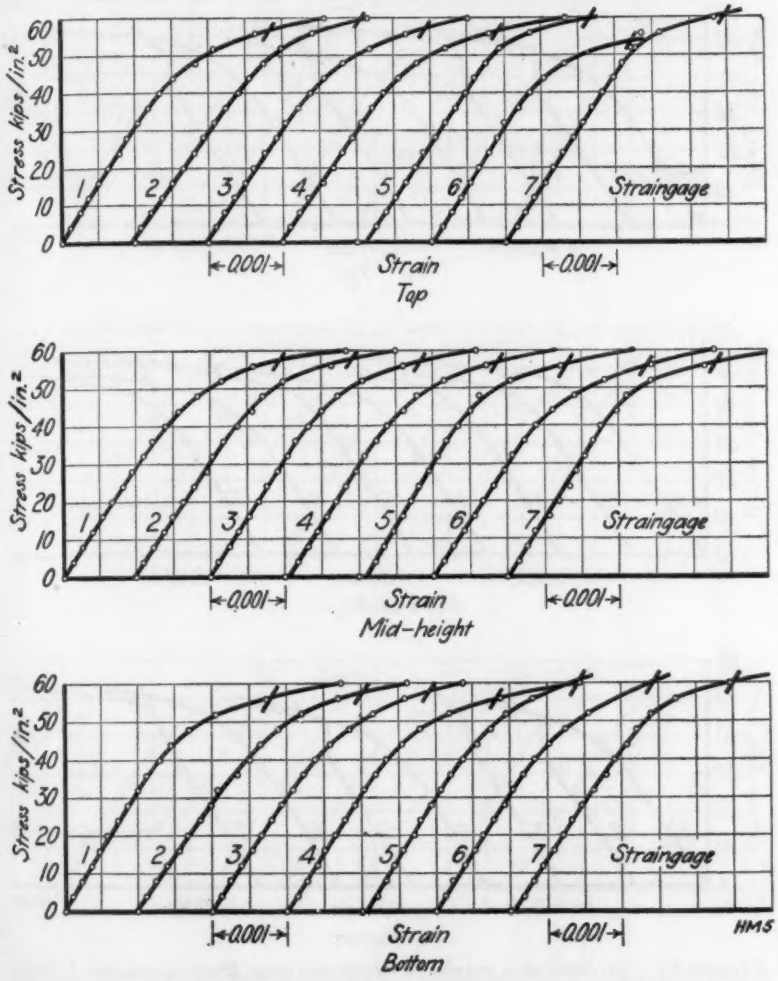

FIGURE 10.—*Stress-strain graphs for the strain-gage lines on column* HM5.

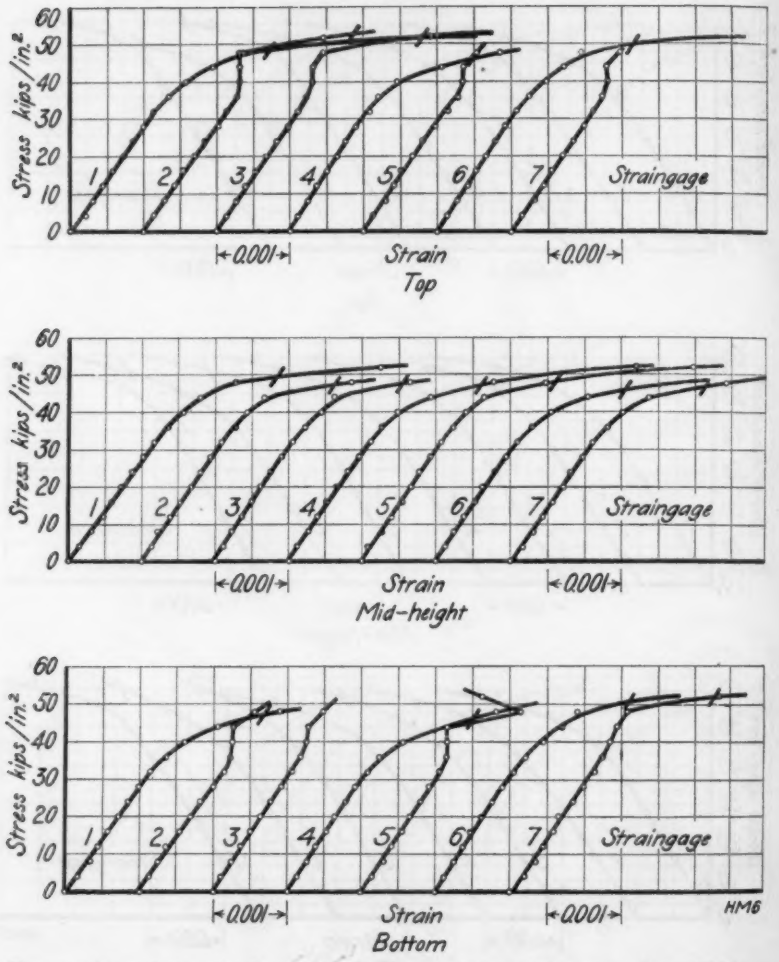

FIGURE 11.—*Stress-strain graphs for the strain-gage lines on column* HM6.

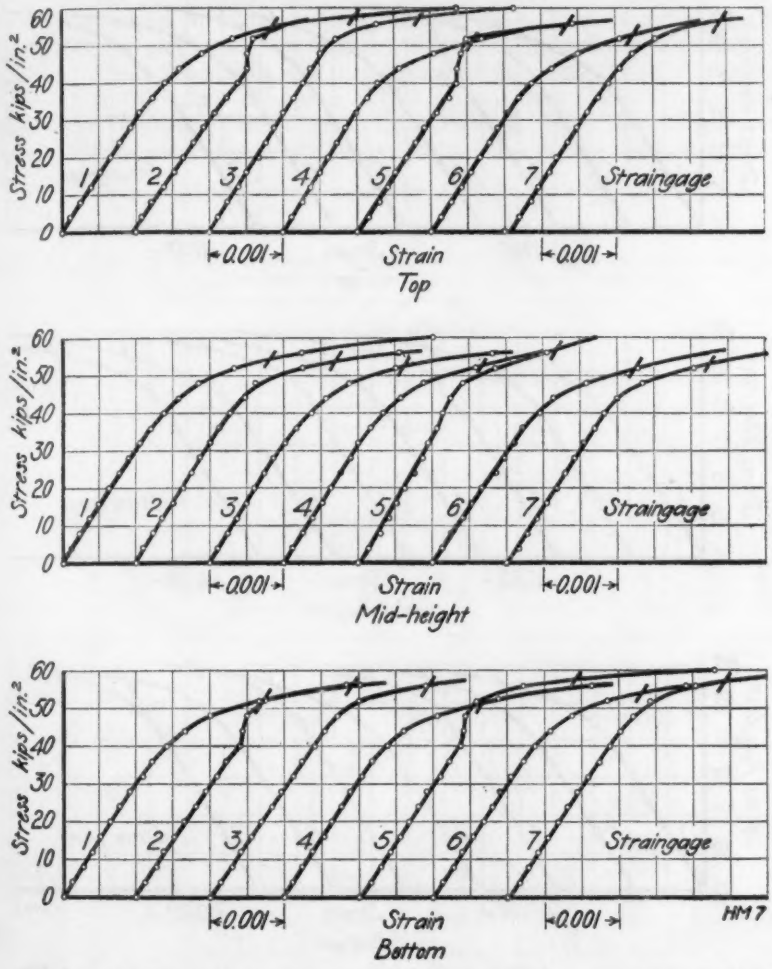

FIGURE 12.—*Stress-strain graphs for the strain-gage lines on column* HM7.

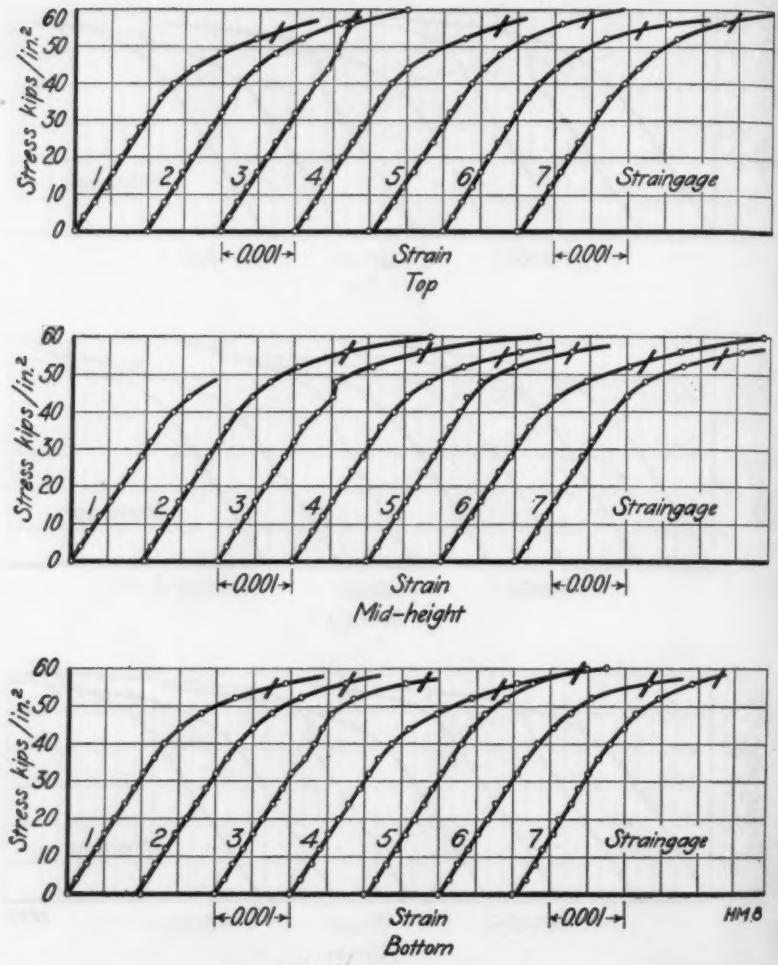

FIGURE 13.—*Stress-strain graphs for the strain-gage lines on column* HM8.

The differences in the slope of the curves below 30 kips/in.^{2} are, in all probability, not caused by differences in the Young's modulus of elasticity for the material at the gage line but by the shortness of the gage length (2 in.), the unavoidable errors in the strain-gage readings, and especially the fact that the stress may not have been uniformly distributed over the cross section of the column as assumed when plotting the graphs. The strain-gage readings were discontinued before the strain at the gage lines was sufficient to allow the yield strength to be determined in the same way as for the column yield strength. The yield strength for the strain-gage lines was, therefore, taken as the stress for which the strain was 0.001 greater than the strain computed by using the Young's modulus. The yield strengths were obtained graphically from the stress-strain graphs. Some of the values were obtained from the extrapolated portion of the curve. The values are given in table 5.

TABLE 5.—*Yield strengths for the strain-gage lines on the columns*

[These yield strengths are the stresses for which the strain was 0.001 greater than the strain computed using Young's Modulus. They were obtained graphically from the stress-strain graphs]

Column	Yield strength, kips/in.^{2}											
	Strain gage 1			Strain gage 2			Strain gage 3			Strain gage 4		
	Top	Middle	Bottom	Top	Middle	Bottom	Top	Middle	Bottom	Top	Middle	Bottom
HM1	56.0	57.0	(56.0)	(60.0)	58.5	59.0	59.5	58.0	58.0	57.0	57.0	57.0
HM2	50.5	51.5	52.0	51.0	51.5	52.5	(52.5)	51.0	(53.0)	(52.5)	51.0	50.5
HM3	55.0	(57.5)	55.5	57.0	57.0	56.0	57.0	57.0	(57.0)	55.0	55.5	(57.5)
HM4	53.0	53.5	(53.0)	54.5	53.0	(57.0)	54.0	52.5	(53.0)	52.0	53.0	(53.5)
HM5	56.5	58.0	56.5	59.5	58.0	58.0	57.0	57.0	58.0	56.5	(57.0)	56.0
HM6	[1](48.5)	49.5	47.0	(53.0)	47.5	-------	52.0	47.5	-------	46.0	47.5	46.5
HM7	(55.0)	54.5	52.0	58.0	54.0	56.0	57.5	52.5	(56.0)	51.0	(52.5)	51.5
HM8	(54.0)	-------	55.5	(57.0)	56.5	(56.5)	-------	56.0	(57.0)	(56.0)	55.0	54.5

Column	Yield strength, kips/in.^{2}									Average
	Strain gage 5			Strain gage 6			Strain gage 7			
	Top	Middle	Bottom	Top	Middle	Bottom	Top	Middle	Bottom	
HM1	58.0	57.0	60.0	57.0	(55.0)	(57.0)	58.5	58.0	(58.0)	57.7
HM2	(54.0)	53.0	(53.0)	(54.5)	(48.5)	(56.5)	(52.0)	51.5	51.0	52.1
HM3	(57.5)	56.5	(59.5)	56.0	54.0	57.5	(56.5)	(56.5)	58.0	56.6
HM4	55.0	(54.0)	55.5	54.5	49.5	(54.0)	53.0	(54.0)	(53.0)	53.5
HM5	(59.5)	(56.5)	(61.0)	53.5	56.0	(60.5)	(61.0)	(56.5)	(60.0)	57.7
HM6	-------	48.0	-------	(50.0)	46.0	51.0	-------	47.0	52.5	48.7
HM7	55.5	(57.0)	57.5	(53.0)	52.0	54.0	(57.0)	(53.0)	(57.0)	54.6
HM8	(58.0)	56.0	59.0	54.5	54.0	56.0	(57.0)	55.0	(58.5)	55.7

[1] Values in parentheses throughout this table are extrapolated values.

The average tensile yield strength of all the angles was 5.7 kips/in.^{2} greater than that for all the plates. There were no strain-gage lines on the angles; therefore no stress-strain graphs were drawn for the angles. For stresses greater than about 40 kips/in.^{2}, however, it is probable that the angles carried more than the proportion of the load computed from the ratio of their cross-sectional area to the total cross-sectional area.

The average ratio of the yield strength of the plates (cover plates and web) at the strain-gage lines to the tensile yield strength of the coupons was about 90 percent and, in general, was less for the webs than for the cover plates.

There were irregularities in some of the stress-strain graphs, particularly strain gage 6, top and bottom, column HM2 (fig. 7); strain gages 2, 3, 5, and 7, top and bottom, columns HM6 (fig. 11); strain gages 2 and 5, top and bottom, column HM7 (fig. 12); and strain gage 3, top, middle, and bottom, column HM8 (fig. 13).

Because these irregularities appear only for the strain-gage lines at the top and bottom (except for column HM8) it seemed probable that they were caused, at least in part, by a nonuniform distribution of the stress over the cross section of the column.

A study of the stress-strain graphs showing irregularities and the values of the yield strength shown in figure 3 indicates that the irregularities occurred in members having a lower yield strength than that of the other members of the column, and it seems probable that the irregularities were caused by a greater proportion of the load being carried by the adjacent members. The strain in a member having an appreciably lower yield strength than adjacent members would be expected to be about the same as the average strain for the adjacent members.

For column HM2 the yield strength of the coupons from the web was about 10 kips/in.^{2} less than that for the cover plates and the angles. For column HM6 the irregularities occurred in the edges of the cover plates at each of the four corners. The web and the cover plates had the same coupon yield strength, but the yield strength of the angles was about 6 kips/in.^{2} greater. Apparently the edges of the cover plates behaved somewhat differently from either the middle of the cover plates or the web, because these edges received less support from the angles. For column HM7 the yield strengths of the coupons from the angles and the web were about 10 kips/in.^{2} greater than those from the cover plates. As for column HM6 the irregularities occurred in two of the edges of the cover plates but at diagonally opposite corners, the northwest and the southeast. Because the yield strength of the coupons from the two angles adjacent to the west cover plate was less than that for the two angles adjacent to the east cover plate irregularities might be expected for strain gages 2 and 7 instead of 2 and 5.

For column HM8 irregularities occurred only for strain gage 3 on the north edge of the east cover plate. This was the only column showing irregularities for the top, middle, and bottom strain gage lines. The yield strength of the coupons from the web was almost 10 kips/in.^{2} lower than that of the east cover plate, but irregularities did not occur in the web as they did for column HM2, perhaps because in column HM8 the yield strength of the angles was several kips/in.^{2} greater than that of the cover plates.

The yield strength of the coupons from the east cover plate was slightly less than that of the west cover plate, and the yield strength of the north angles 2.5 kips/in.^{2} less than that of the south angles, which may account for the irregularities occurring only in the edge of the cover plate, at the northeast corner of the column.

These graphs may be compared with the stress-strain graphs for four steel columns fabricated by riveting from a web plate and four angles shown on pages 85 to 106, Tests of Metals, Watertown Arsenal, Mass., 1912. The strain-gage readings for two additional columns are given on page 51 of the Tests of Metals, 1913. For those columns the gage lines extended the entire length of the edges of the four flanges.

The stress-strain graphs may be misleading because the average stress for the column was used as ordinate. The actual stress at a particular strain-gage line may be considerably greater or less than the average value. In order to show the strains in the column more clearly, at the suggestion of W. R. Osgood the graphs were plotted on a perspective outline of the cross section of the column. The strains are shown in figures 14, 15, 16, 17, 18, 19, 20, and 21.

In general, the strain in the outer edges of the flanges for a given stress greater than about 48 kips/in.^{2} was less than the strain at the middle of the cover plates. Also the strain in the middle of the web was less than the strain at the middle of the cover plates for the top and bottom of the column but greater than the strain at the middle of the cover plates at the midheight of the column.

Apparently there are greater differences in the strains for columns HM5, HM6, HM7, and HM8 having cover plates 1.25 in. thick than for columns HM1, HM2, HM3, and HM4 having cover plates 1.5 in. thick.

In general, the strains appear to be more nearly the same for the columns with webs and cover plates having about the same yield strength.

The stress-strain graphs showing irregularities correspond to perspective graphs which show little or no increase in strain for an increase in stress. Because each column was fabricated from a number of longitudinal pieces, it did not behave as a unit under load.

Whether the maximum load on the columns which behaved erratically was affected by this behavior is an interesting question. If the maximum load could have been determined on all of the columns the results might have thrown some light on this subject. It seems advisable in the future when obtaining strain-gage measurements for the purpose of determining the distribution of strain in fabricated steel columns, to obtain such measurements on all of the longitudinal pieces, including the angles of H-shaped columns. This would be especially desirable for columns fabricated by welding to determine the effect of stress-relieving heat treatment.

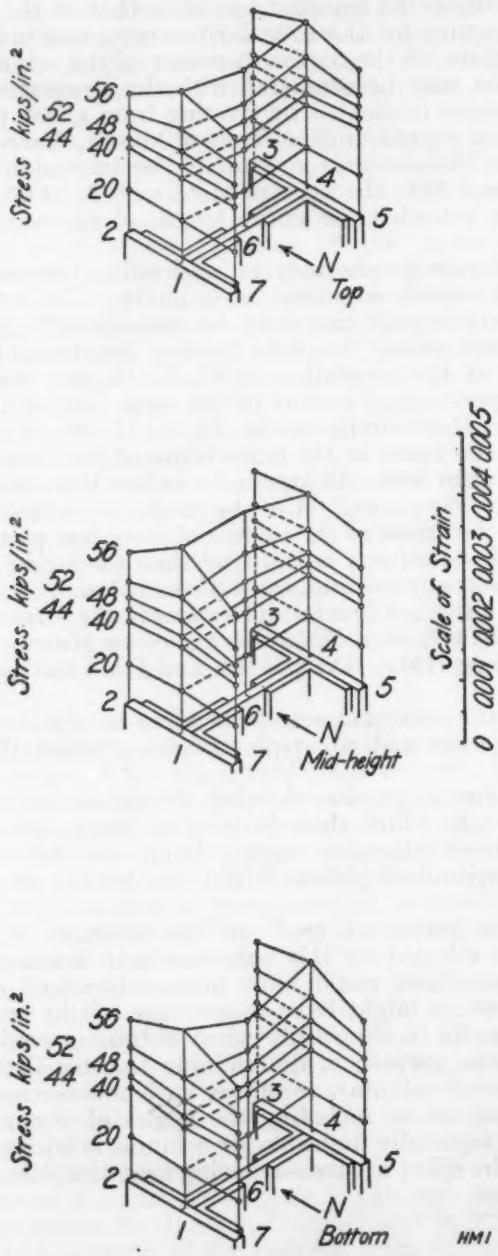

FIGURE 14.—*Strains in column* HM1.

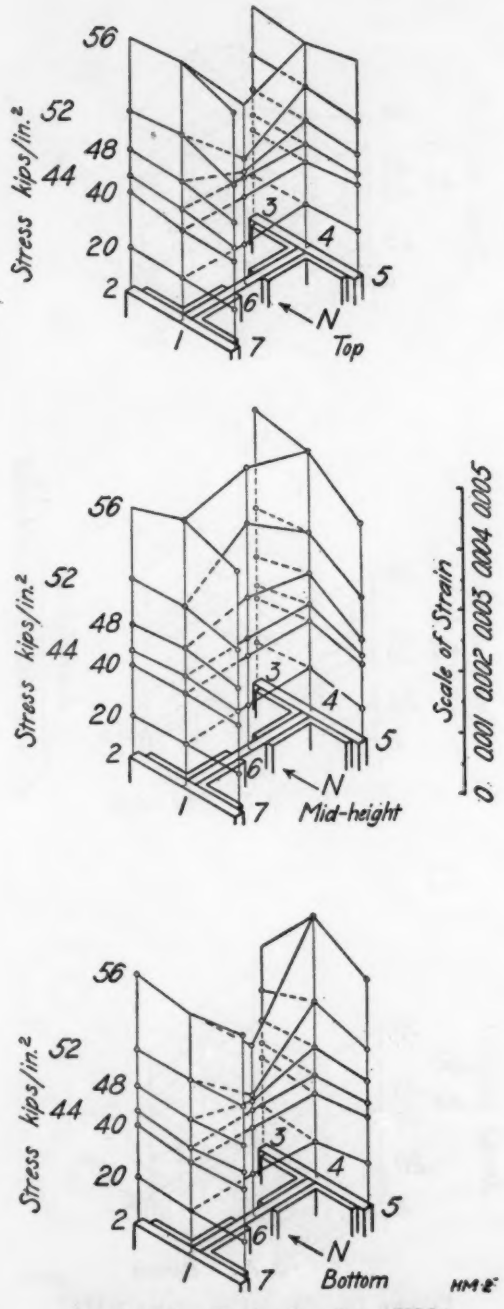

FIGURE 15.—*Strains in column* HM2.

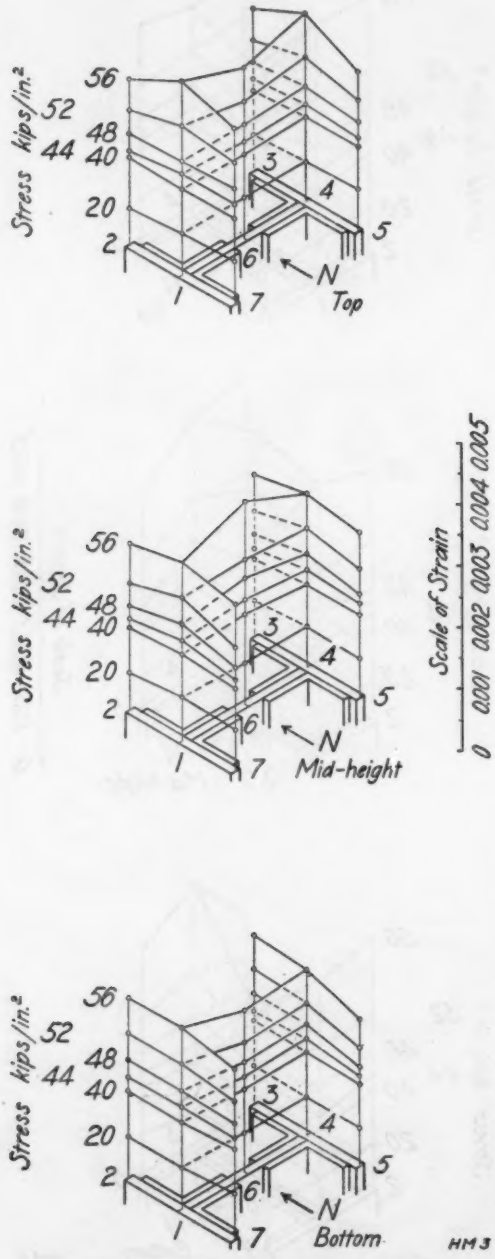

FIGURE 16.—*Strains in column* HM3.

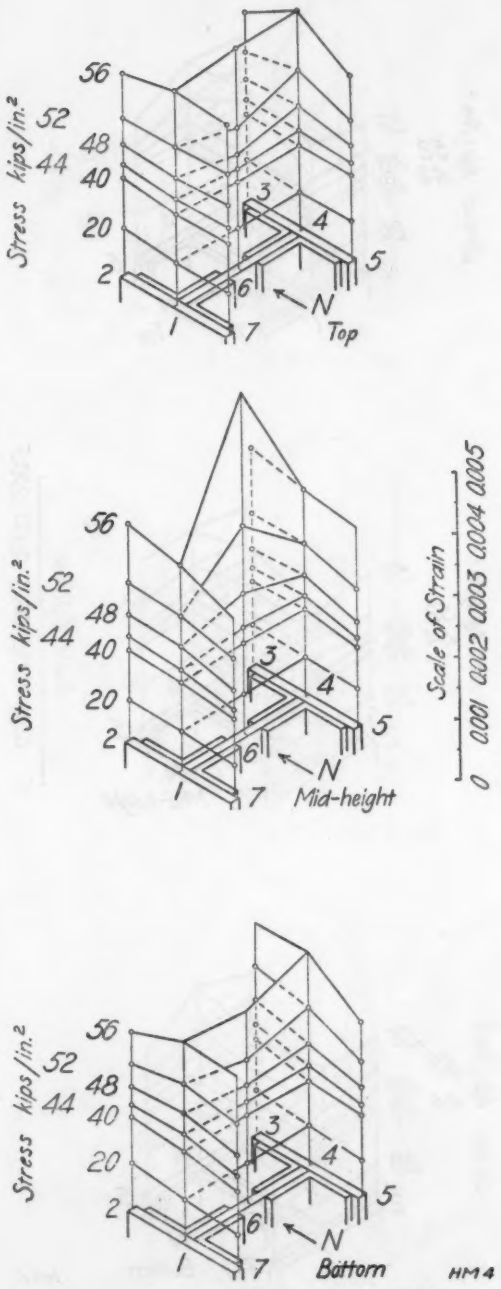

FIGURE 17.—*Strains in column* HM4.

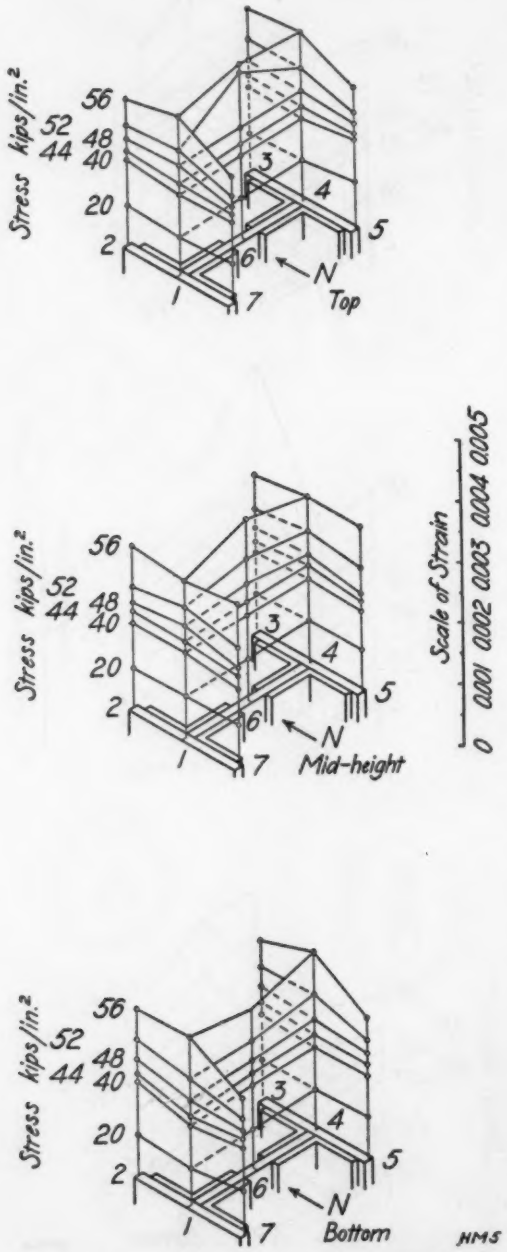

FIGURE 18.—*Strains in column* HM5.

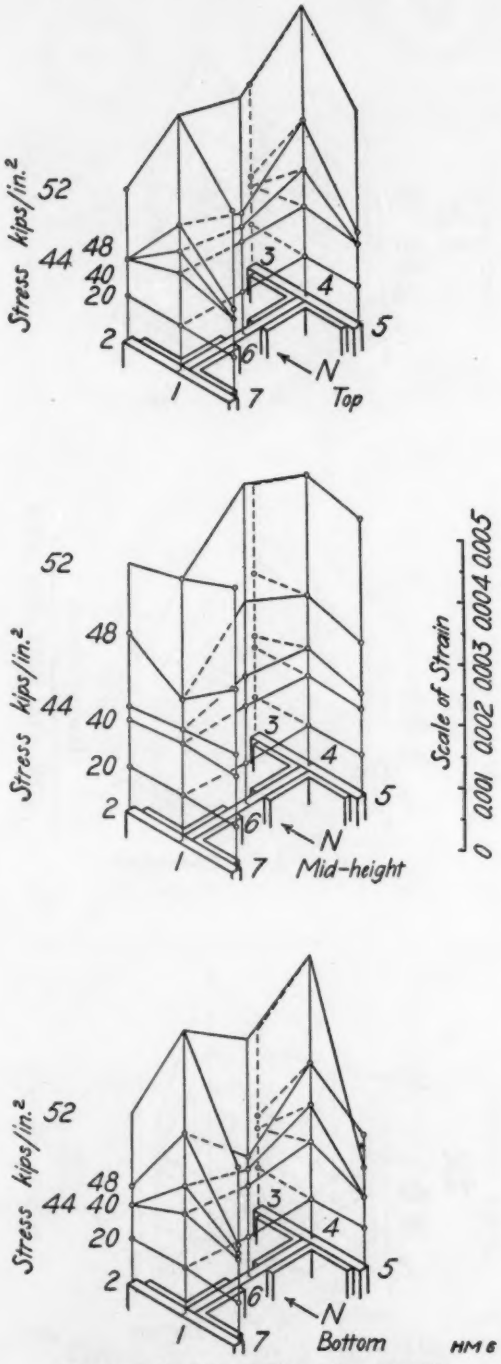

FIGURE 19.—*Strains in column* HM6.

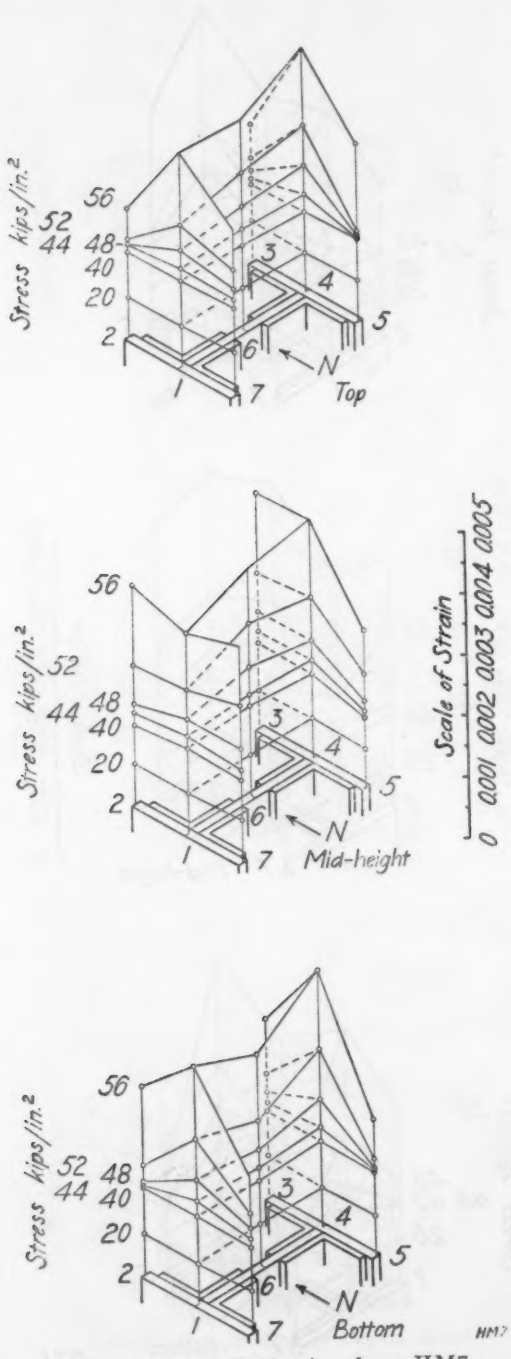

FIGURE 20.—*Strains in column* HM7.

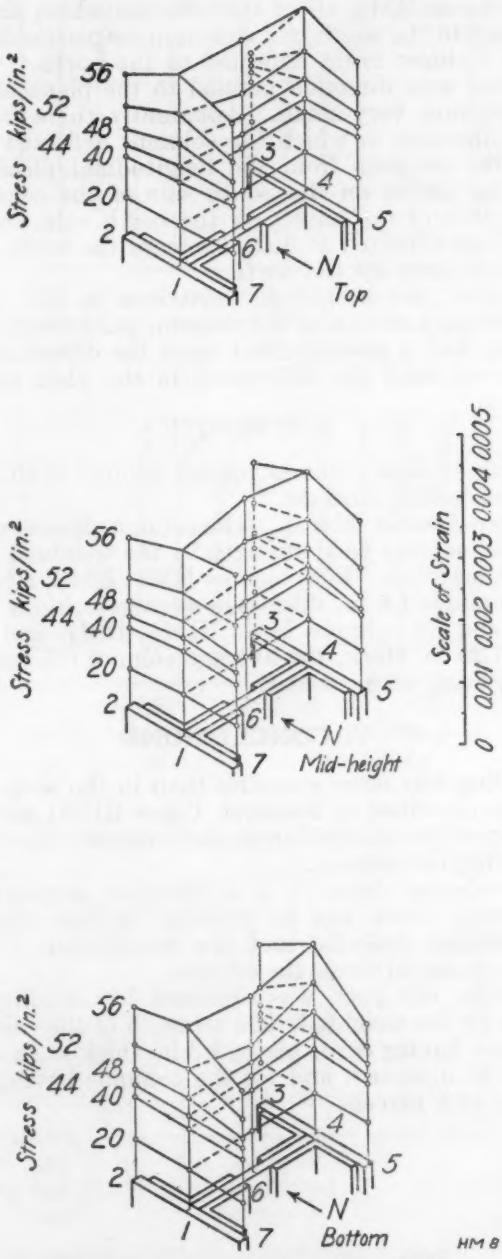

FIGURE 21.—*Strains in column* HM8.

4. LATERAL DEFLECTION

The lateral deflections of the columns are shown in figure 22. Except for column HM8, all of the columns which deflected appreciably deflected to the south in a direction perpendicular to the plane of the web. Column HM8 deflected to the north. The deflection in the east and west direction parallel to the plane of the web was for all the columns very small. Apparently there was no relation between the direction in which the columns deflected and the yield strength of the coupons from the longitudinal pieces. The yield strength of the angles on the south side of the column HM8 was greater than that of the angles on the north side and the column might have been expected to deflect toward the south. However, it actually deflected toward the north.

It is probable that accidental variations in the distribution of stress over the cross section of the column, particularly near the ends of the column, had a greater effect upon the direction in which the column deflected than the differences in the yield strength of the main members.

5. STRENGTH

The strength of these columns, except column HM6, exceeded the capacity of the testing machine.

The loads are given in table 4. The column efficiency was obtained by dividing the column yield strength by the weighted yield strength of the column material. For columns HM1, HM2, HM3, and HM4, having cover plates 1.5 in. thick, the average column efficiency was 95.0 percent and for columns HM5, HM6, HM7, and HM8 having cover plates 1.25 in. thick, the average column efficiency was somewhat greater, being 96.5 percent.

V. CONCLUSIONS

1. The loading was more eccentric than in the tests of tower and chord columns described in Research Paper RP831 and RP897.

2. For seven of the eight columns the strength exceeded the capacity of the testing machine.

3. All the columns deflected in a direction perpendicular to the web. Apparently there was no relation between the direction in which the columns deflected and the distribution of tensile yield strength of the material across the column.

4. The column efficiency was obtained by dividing the column yield strength by the weighted yield strength of the column material. For the columns having cover plates 1.5 in. thick the average column efficiency was 95.0 percent and for the columns having cover plates 1.25 in. thick, 96.5 percent.

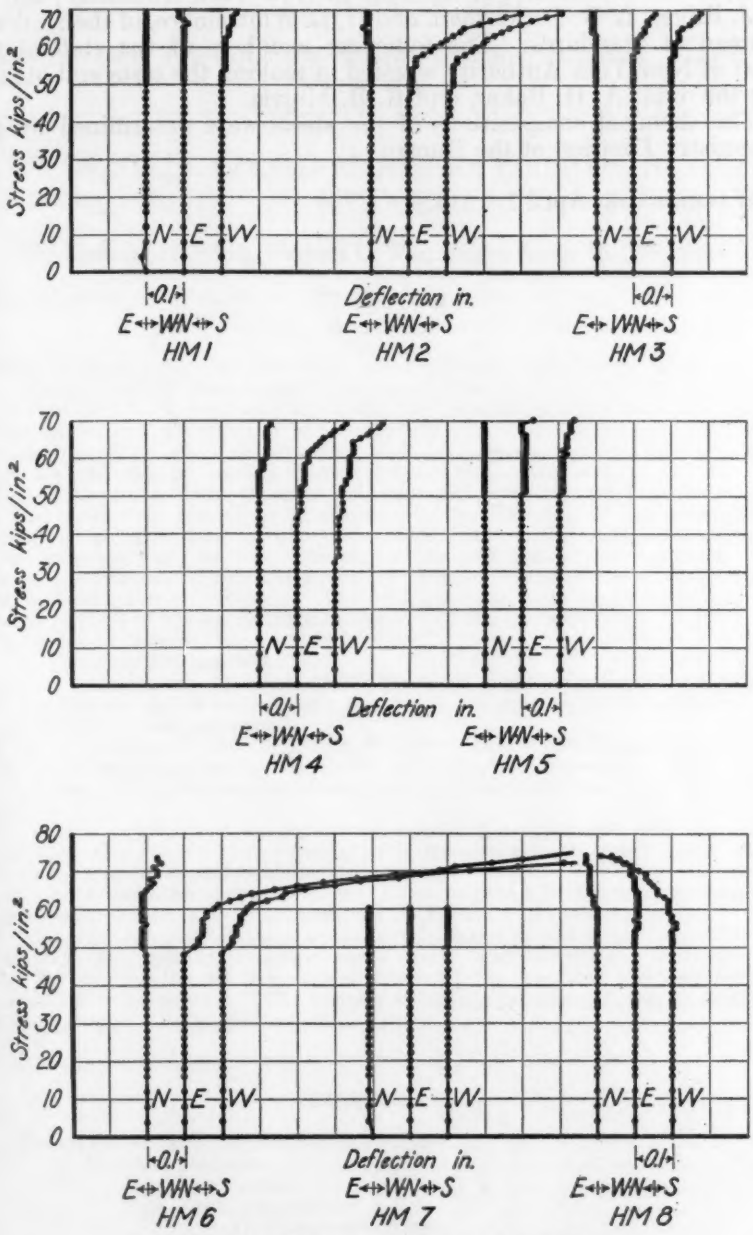

FIGURE 22.—*The lateral deflections of the columns.*

The program and testing procedure were prepared by O. H. Ammann chief engineer; L. S. Moisseiff, consulting engineer; and R. S. Johnston, research engineer, of the Port of New York Authority; and by L. J. Briggs, L. B. Tuckerman, and H. L. Whittemore, of the National Bureau of Standards. The following members of the staff of the Port of New York Authority assisted in making the tests and obtaining the data: A. H. Baker, and R. B. Morris.

The chemical compositions of the steels were determined by the Chemistry Division of the Bureau.

WASHINGTON, April 7, 1936.

U. S. Department of Commerce National Bureau of Standards

RESEARCH PAPER RP897

Part of Journal of Research of the National Bureau of Standards, Volume 16, June 1936

TESTS OF STEEL CHORD MEMBERS FOR THE BAYONNE BRIDGE

By Ambrose H. Stang, Herbert L. Whittemore, Leroy R. Sweetman

ABSTRACT

While designing the Bayonne (Kill van Kull) steel-arch bridge, which crosses from Port Richmond, Staten Island, to Bayonne, N. J., the Bridge Department of the Port of New York Authority requested the cooperation of the National Bureau of Standards in an investigation of the strength and other properties of the lower-chord members. These members were made of carbon-manganese steel and were of the double-box type, having diaphragms and continuous walls.

Because the ratio of the width of the cover plates to their thickness was large, the Port Authority wished to determine whether buckling of the cover plates would cause failure of the members under loads less than their estimated strength.

Two columns were tested. The shortening and the lateral deflection were measured. The tensile properties and the chemical composition of the material were determined from coupons. The test columns were made dimensionally one-half the size of the actual chord members of the bridge.

It was found that—

1. The loading was nearly axial.
2. The Young's modulus of elasticity increased slightly for repeated loadings.
3. For stresses which were nearly the maximum stresses in the columns, the lateral deflection was very small.
4. Under a stress of about 38 kips/in.^{2} the two cover plates began to buckle for their entire length and the buckles increased as the load increased. The ratio of the distance between the nearest lines of rivets to the thickness of the cover plate was 45.

The results on these two columns are in substantial agreement with the values obtained by the use of Bryan's formula for the compressive stress under which wide plates may be expected to buckle.

After these tests the chord members of the Bayonne Bridge were re-designed so as to prevent failure of these members by buckling of the cover plates.

5. The yield strength of these columns was taken as the stress for which the strain was 0.002 greater than the elastic strain, and the column efficiency obtained by dividing the column yield strength by the weighted yield strength of the material in the column. The average column yield strength was 57 kips/in.^{2}, and the average column efficiency 97.4 percent.

CONTENTS

	Page
I. The specimens and the method of testing	628
1. The test columns	628
(a) Description	628
(b) Testing procedure	630
(1) Compressometers	630
(2) Lateral deflection	630
(3) Loading	630

I. The specimens and the method of testing—Continued. Page
2. Method of determining the properties of the columns 630
(a) Young's modulus 630
(b) Proportional limit 631
(c) Column yield strength 631
(d) Weighted yield strength of the material 631
(e) Column efficiency 631
3. Coupons 631
(a) General 631
(b) Shape and size 631
(c) Yield strength 631
(d) Extensometer 632
(e) Testing machine 632
(f) Speed of the movable platen 632
II. Results for the coupons 632
1. Tensile tests 632
2. Chemical composition 633
III. Results for the columns 633
1. Shortening 633
2. Lateral deflection 634
3. Maximum load 634
(a) Strength 634
(b) Description of the failure 635
IV. Conclusions 637

NOTE.—The bridge department of the Port of New York Authority designed and built the Kill van Kull Bridge,[1] between Port Richmond, Staten Island, N. Y., and Bayonne, N. J. The bridge is a two-hinged steel arch, having a span of 1,675 feet. The lower chords of this bridge are carbon-manganese steel. At the time, this was a new type of alloy steel which had heretofore not been used in any large structure, and its behavior in heavy fabricated compression members was unpredictable on the basis of any existing tests. Because of this, and the relative importance of these principal load-carrying members in the bridge, the Port of New York Authority asked the National Bureau of Standards to cooperate in tests to determine their actual strength and behavior under load. In the design, the lower chord members were made constant in depth back to back of chord angles, and the cross-sectional areas were varied to meet the stress requirements by changing the thicknesses of the material. The restriction imposed by proportioning in this manner, and by using the customary limiting minimum thicknesses of material, resulted, for economic reasons, in the use of cover plates having width-to-thickness ratios somewhat larger than conventionally allowed. It was felt that a test of the section designed on this basis would also give valuable data on the buckling strength of these cover plates and the effect of this upon the strength of the member as a whole. The investigation was completed before the final design of the bridge.

I. THE SPECIMENS AND THE METHOD OF TESTING

1. THE TEST COLUMNS

(a) DESCRIPTION

The two carbon-manganese test columns, designated CM1 and CM2, were fabricated by riveting. The dimensions are shown in figures 1 and 2, and the nominal dimensions and properties are given in table 1. Column CM1, after test, is shown in figure 3.

[1] Pap. Discuss. Am. Soc. Civ. Eng. **56**, 487 (1930); Pap. Discuss. Am. Soc. Civ. Eng. **56**, 500 (1930). Pap. L. S. Moisseiff, J. Franklin Inst. **213**, no. 5, 491 (1932).

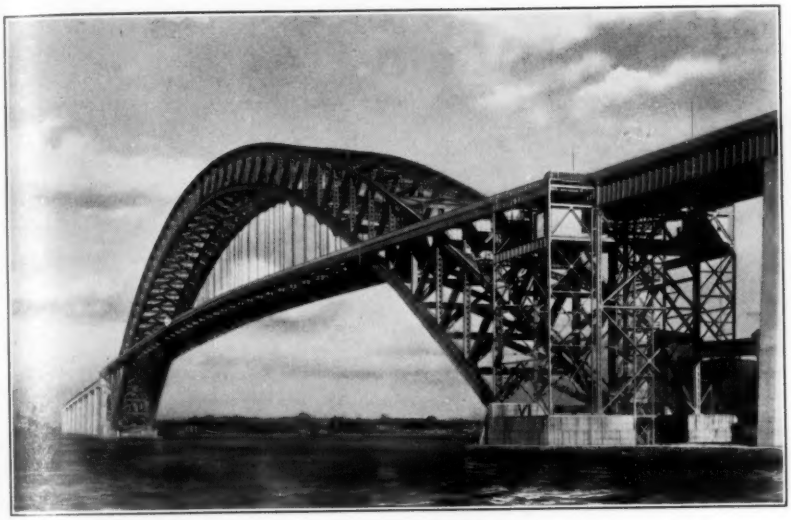

The Bayonne Bridge.

Steel-arch bridge which crosses the Kill van Kull from Port Richmond, Staten Island, N. Y., to Bayonne, N. J.

TABLE 1.—*Nominal dimensions and properties of the test columns*

Number of columns tested	Symbol	Kind of steel	Cross-sectional area of steel	Length		Moment of inertia		Radius of gyration		Slenderness ratio	
						I_{x-x}	I_{y-y}	r_{x-x}	r_{y-y}	$x-x$	$y-y$
			in.²	ft	in.	in.⁴	in.⁴	in.	in.		
2	CM1, CM2	Carbon-manganese.	155.2	20	9	31,043	17,259	14.14	10.54	17.6	23.6

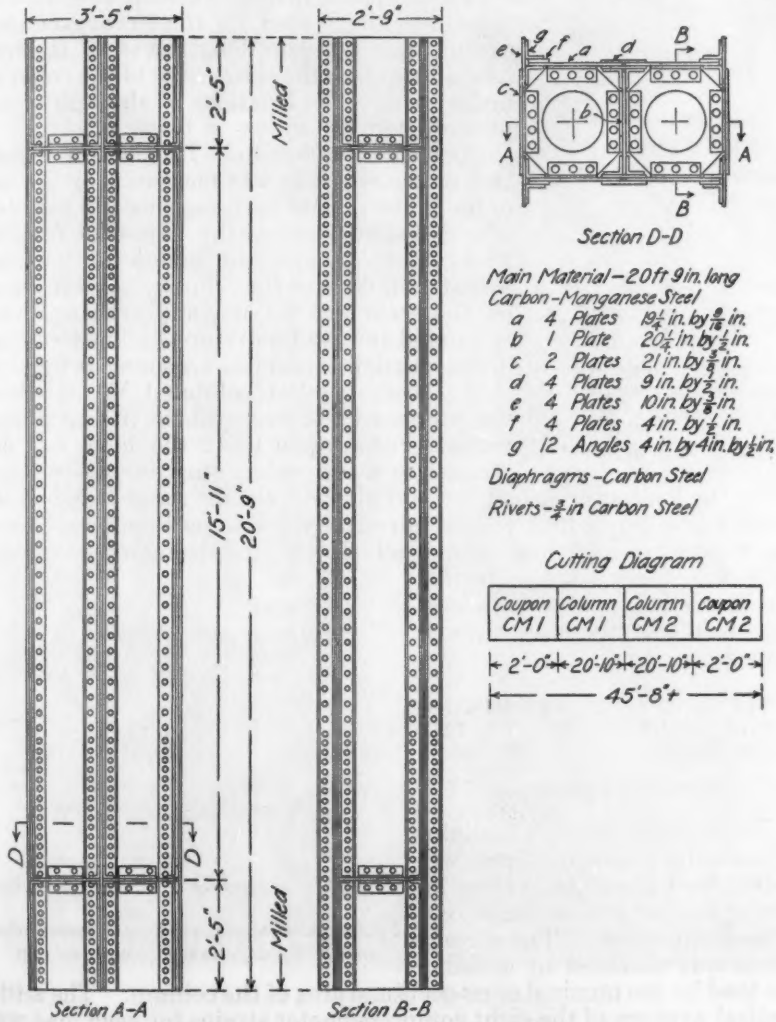

FIGURE 1.—*Dimensions of the test columns.*

The dimensions of the cover plates of the test columns and of those for the Bayonne Bridge as originally designed are shown in figure 2.

The longitudinal pieces of each column, that is the longitudinal plates and angles, were cut as shown in the cutting diagram in

figure 1. Each longitudinal piece of the column was match-marked to correspond with a coupon cut from the same plate or angle, and its location in the column was recorded.

(b) TESTING PROCEDURE

Both columns were tested as flat-end columns by the use of the equipment and methods described in National Bureau of Standards Research Paper RP831, Tests of Steel Tower Columns for the George Washington Bridge.[2]

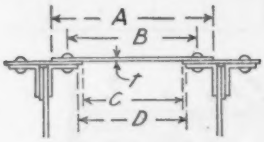

Cover Plate	Kill van Kull Bridge	Test Column
Width, A	42 in.	21 in.
thickness, t	$\frac{3}{4}$ in.	$\frac{3}{8}$ in.
B	$31\frac{1}{4}$ in.	$16\frac{1}{8}$ in.
C	$25\frac{7}{8}$ in.	13 in.
D	$27\frac{3}{4}$ in.	$13\frac{7}{8}$ in.
Ratio $\frac{B}{t}$	41.6	45.0
" $\frac{C}{t}$	34.5	34.7
" $\frac{D}{t}$	37.0	37.0

FIGURE 2.—*Dimensions of the cover plates of the test columns and of those for the Kill van Kull Bridge, as originally designed.*

(1) *Compressometers.*—Compressometers similar to those used for the tower columns, except that the gage length was 15 ft, were used to measure the shortening of the columns under load. The locations of the eight compressometers are shown in figure 4.

(2) *Lateral deflection.*—The lateral deflection of the columns was measured by the use of the taut-wire and mirror-scale deflectometer. The distance between the supports for the wire was 15 ft, and the middle of the wire was at midheight of the column. One division on the scale was 0.1 in., and readings were estimated to 0.1 of a division. The locations of the four deflectometers are shown in figure 4.

(3) *Loading.*—For column CM1 the load was increased by increments to the maximum value. For column CM2 the load was decreased to a low value, then increased, once when the load approached the end of the "elastic range" and again when the column had yielded plastically. For both columns, after the maximum load had been reached, the load decreased so rapidly that the beam of the testing machine could not be balanced. The test was therefore discontinued.

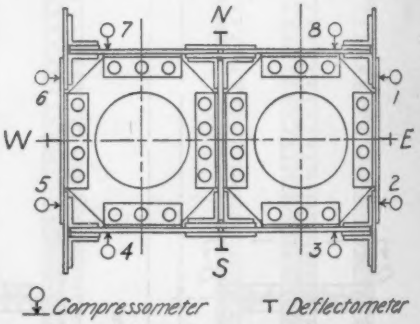

FIGURE 4.—*Locations of the compressometers and of the deflectometers on a column.*

2. METHOD OF DETERMINING THE PROPERTIES OF THE COLUMNS

(a) YOUNG'S MODULUS

The average Young's modulus of elasticity for each column was determined from the values of average stress and average compressometer strain. The average stress was obtained by dividing the load by the nominal cross-sectional area of the column. The arithmetical average of the eight compressometer strains for each load was taken as the average compressometer strain. The computed strains obtained by dividing the average stresses in the elastic range by a trial

[2] J. Research NBS 15, 3 (1935) RP831.

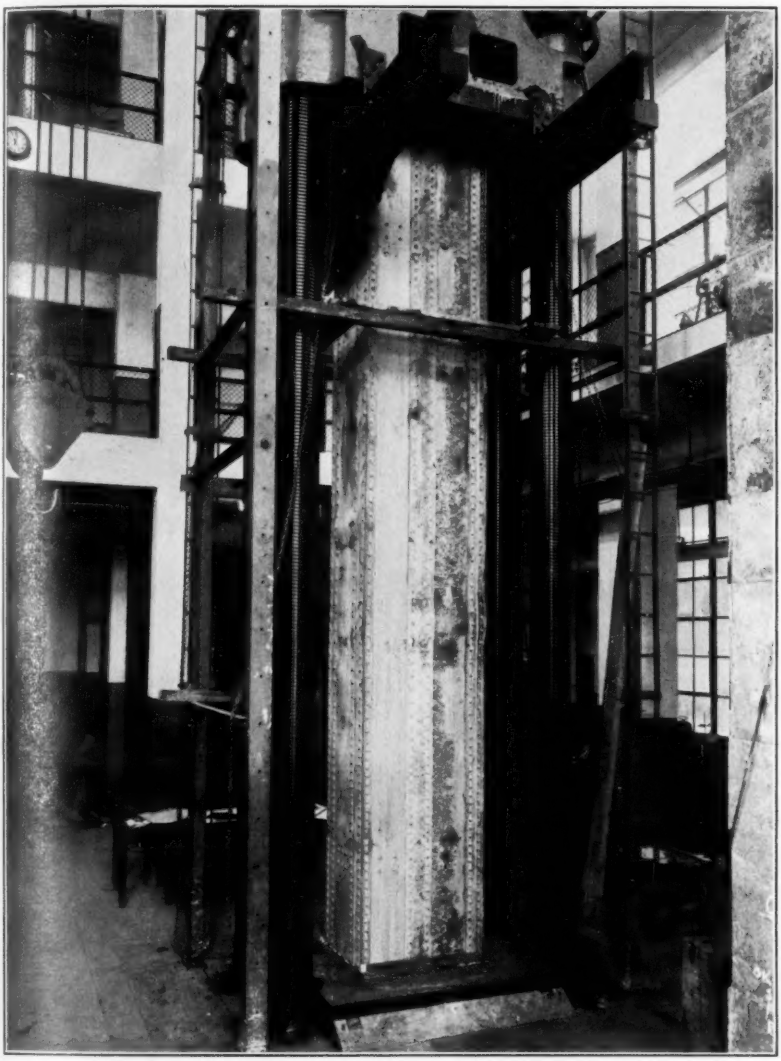

FIGURE 3.—*Column* CM1 *after test.*

UNIV. OF MICH.

modulus were compared with the average compressometer strains. The trial modulus for which the computed strains agreed most closely with the compressometer strains for loads within the elastic range was taken as the Young's modulus of elasticity of the column.

(b) PROPORTIONAL LIMIT

A proportional limit for each column was determined as the stress for which the average compressometer strain was 0.000012 greater than the strain computed by using Young's modulus.

(c) COLUMN YIELD STRENGTH

For reasons discussed later, the yield strength of the column was taken as the stress for which the average compressometer strain was 0.002 greater than the strain computed by using Young's modulus. The value for each column was obtained graphically from the stress-strain graph for the column.

(d) WEIGHTED YIELD STRENGTH OF THE MATERIAL

The weighted average tensile yield strength of the material in the column was obtained from the yield strengths of coupons by weighting them in the ratio of the cross-sectional area of the main member which they represented to the total nominal cross-sectional area of the column.

(e) COLUMN EFFICIENCY

The column efficiency was obtained by dividing the column yield strength by the weighted yield strength of the material in the column.

3. COUPONS

(a) GENERAL

The coupons were machined from the piece marked "coupon" in the cutting diagram in figure 1. This diagram shows the relation of the coupons to the longitudinal pieces used in fabricating each column. For the plates, one coupon was taken at the middle of the plate. For the angles, one coupon was taken at the middle of one of the legs of the angle.

(b) SHAPE AND SIZE

The axis of each coupon was parallel to the rolling direction (axis) of the plate or angle. The coupons were standard ASTM tensile specimens for plates, shapes, and flats.[3] These coupons had a gage length of 8 in., a width at the reduced section of 1.5 in., and the thickness was that of the material as rolled.

(c) YIELD STRENGTH

The method selected for determining the yield strength of these coupons is essentially the "set method" described by the Section on Elastic Strength of Material of the Technical Committee on Mechanical Testing of the American Society for Testing Materials.[4] The yield strength was taken as the stress for which the strain was 0.002 greater than the strain computed from the stress and the Young's modulus of elasticity.

[3] Figure 1, Stand. Am. Soc. Testing Materials [I] 68, (1933).
[4] Proc. Am. Soc. Testing Materials [I] 31, 602 (1931).

(d) EXTENSOMETER

The strains in some coupons were measured by the use of a Ewing extensometer having a gage length of 8 in. One division on the scale of this instrument corresponded to a strain of 0.000025 in the coupon. The readings were estimated to 0.1 division. For the coupons upon which a Ewing extensometer was not used, the strains were measured by the use of a Berry strain gage having a gage length of 8 in. The yield strength was determined graphically by a method which gave values approximating closely those obtained by the use of the Ewing extensometer.

(e) TESTING MACHINE

The coupons were tested in a screw-power, beam-and-poise machine having a capacity of 100 kips.[5]

(f) SPEED OF THE MOVABLE PLATEN

For the coupons on which a Ewing extensometer was used, the speed of the movable platen of the testing machine under no load was 0.04 in./min, and this speed was maintained until the stress was about three-quarters of the yield strength. For higher stresses the speed was 0.01 in./min. After the extensometer was removed the speed was 0.4 in./min until the coupon ruptured.

For the coupons on which a Ewing extensometer was not used, the speed was 0.04 in./min until the yield strength was observed. For higher stresses the speed was 0.4 in./min.

II. RESULTS FOR THE COUPONS

1. TENSILE TESTS

The results of the tensile tests of the coupons are given in table 2. The properties of the material are average values for the longitudinal members of the same size and shape.

TABLE 2.—*Results of the tensile tests of coupons*

Column material		Number of coupons tested	Yield strength (average)	Tensile strength (average)	Elongation in 8 in. (average)	Reduction of area (average)
Shape	Nominal size					
	in.		kips/in.[2]	kips/in.[2]	*Percent*	*Percent*
COLUMN CM1—CARBON-MANGANESE STEEL						
4 plates	19¼ by 9/16	4	59.8	101.0	17.8	48.1
1 plate	20¼ by ½	1	61.9	104.2	16.4	40.1
2 plates	21 by 3/8	2	63.2	105.2	17.2	45.9
4 plates	9 by ½	4	54.8	94.5	19.6	48.7
4 plates	10 by 3/8	4	56.3	91.6	21.6	54.8
4 plates	4 by ½	4	56.4	92.5	20.0	47.0
12 angles	4 by 4 by ½	12	56.6	93.7	20.3	49.8
Weighted average			58.3	97.4	19.1	48.5
COLUMN CM2—CARBON-MANGANESE STEEL						
4 plates	19¼ by 9/16	4	60.0	98.2	18.8	46.5
1 plate	20¼ by ½	1	60.0	101.4	20.2	41.0
2 plates	21 by 3/8	2	63.0	105.1	16.4	40.8
4 plates	9 by ½	4	55.4	96.2	18.5	46.6
4 plates	10 by 3/8	4	56.2	94.6	20.4	51.0
4 plates	4 by ½	4	55.6	91.8	20.7	55.7
12 angles	4 by 4 by ½	12	56.4	93.4	19.8	50.8
Weighted average			58.1	96.8	19.2	47.7

[5] 1 kip=1,000 lb.

A typical Ewing stress-strain graph for the carbon-manganese steel is shown in figure 9 of Research Paper 831.

The speed of the movable head of the testing machine was much lower than is customarily used when determining the yield strength. For these coupons the rate at which the stress was increased is more nearly the rate for the columns than the rate customarily used for coupons.

2. CHEMICAL COMPOSITION

The Bureau's Chemistry Division made chemical analyses of samples from coupons having the highest and the lowest tensile strength for each thickness and each shape. The results are given in table 3.

TABLE 3.—*Chemical composition of the carbon-manganese steel*

Description of samples			Chemical composition				
Thickness	Shape	Tensile strength	Carbon	Manganese	Phosphorus	Sulphur	Silicon
in.		kips/in.²	*Percent*	*Percent*	*Percent*	*Percent*	*Percent*
½	Angle	88.9	0.31	1.54	0.025	0.020	0.17
½	do	99.1	.33	1.59	.031	.021	.17
⅜	Plate	90.8	.31	1.54	.025	.018	.17
⅜	do	105.3	.36	1.71	.027	.026	.19
½	do	90.5	.31	1.53	.027	.014	.17
½	do	104.2	.35	1.72	.024	.018	.18
9/16	do	88.2	.30	1.53	.036	.018	.15
9/16	do	111.0	.37	1.86	.019	.018	.20

III. RESULTS FOR THE COLUMNS

1. SHORTENING

For loads which did not exceed the proportional limit the strain was almost the same for each of the compressometers. The average of the values for the eight compressometers was used for the stress-strain graphs shown in figure 5. The elastic properties of the columns are given in table 4. For column CM2, on which the load was released, the Young's modulus of elasticity was slightly greater for the second and the third loading than for the first loading. For this column the proportional limit for the second and the third loadings equaled or

TABLE 4.—*Elastic properties of the test columns*

Column	Maximum stress			Young's modulus of elasticity			Proportional limit			Set after—	
	First loading	Second loading	Third loading	First loading	Second loading	Third loading	First loading	Second loading	Third loading	First loading	Second loading
	kips/in.²	kips/in.²	kips/in.²	kips/in.²	kips/in.²	kips/in.²	kips/in.²	kips/in.²	kips/in.²		
CM1	[b] 59.0			28,100			28.0				
CM2	28.0	40.0	[b] 58.6	28,200	28,350	28,450	26.0	32.0	40.0	0.000030	0.000130

[a] Determined as the stress for which the average compressometer strain was 0.000012 greater than the strain computed by the use of Young's modulus of elasticity.
[b] Final maximum stress, preceding failure.

exceeded the stress applied in the previous loading. Although the stress for the first loading exceeded the initial proportional limit by 2 kips/in.², the permanent set was small after this load was released.

After the second loading, the permanent set of column CM2 was slightly less than that for tower column TM2 (carbon-manganese steel) after the second loading. (See table 5, Research Paper 831.) The maximum stress for the second loading was 40 kips/in.^{2} for both of these columns.

2. LATERAL DEFLECTION

The deflections for each side of the column are shown in figure 6. For both columns the lateral deflections were small until the final maximum load was approached.

3. MAXIMUM LOAD

(a) STRENGTH

The column strengths given in Technologic Paper 328 were the values of the first maximum stress. It was stated that "the practically definite first maximum stress, occurring before any appreciable lateral deflection of the column, and fairly reproducible when the column material and test conditions are reproduced, should furnish a good measure of the strength of the column in practical use. This justifies the practice followed in this report of recording the first maximum stress observed in a column test as the 'column strength' under the given test conditions. However, as was previously pointed out, this would not be justified in case no maximum were observed before the column was badly deformed."

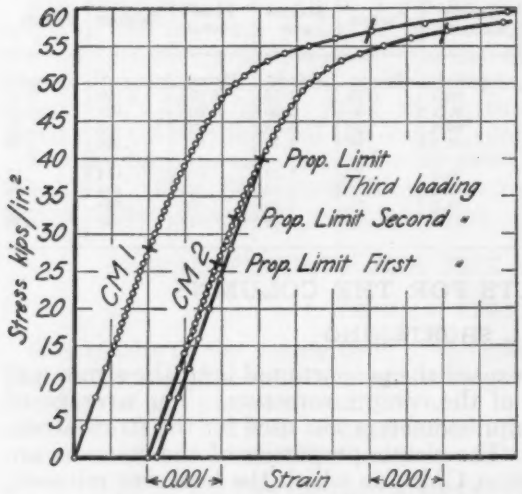

FIGURE 5.—*Stress-strain graphs for the columns.*

With regard to the procedure that should be followed when no maximum is observed before the column is badly deformed, it was stated that "the best criterion could only be determined by a series of tests on columns in this range, in which the stress deformation curves were carefully determined."

In tensile tests of steels which do not show a definite yield point, it has become customary to define a yield strength in terms of the stress necessary to produce a definite strain (usually 0.002) in the coupon in excess of the computed elastic strain. It seemed probable that a similar definition of a column yield strength would be satisfactory for columns for which no definite first maximum load is observed, and for this reason the column yield strengths in Research Paper 831 were computed on this basis.

The Bayonne test columns did show a definite first maximum stress, after which the stress decreased rapidly. This first maximum

stress could therefore have been used when computing the column efficiency as in Technologic Paper 328. However, the method adopted in Research Paper 831 was followed, the column efficiency being determined by dividing the column yield strength by the weighted yield strength of the material in the column.

The strengths of the test columns are given in table 5. The average column efficiency was 97.4 percent. This value is slightly less than the column efficiency of tower columns TM1 and TM2 of carbon-manganese steel, which had a greater slenderness ratio (tower columns 28.9, chord columns 17.6).

The final maximum stress was on the average 3.3 percent greater than the column yield strength.

(b) DESCRIPTION OF THE FAILURE

The failures of the chord columns have been described by R. S. Johnston.[6]

Neither of these columns showed either "pick-up" or "hang-on",[7] probably because the longitudinal pieces in the column were relatively thin.

TABLE 5.—*Strength and efficiency of the test columns*

Column	First and final maximum load	Weighted yield strength of material	Column yield strength [a]	First and final maximum stress	Column efficiency (based on column yield strength)
	kips	kips/in.^{2}	kips/in.^{2}	kips/in.^{2}	*Percent*
CM1	9,156	58.7	57.0	59.0	97.1
CM2	9,102	58.1	56.8	58.6	97.8
Average	9,129	58.4	56.9	58.8	97.4

[a] Stress for which the strain was 0.002 greater than the elastic strain.

Column CM2 was tested before column CM1. At the greater loads column CM2 scaled on all four sides. Under a stress of 53 kips/in.^{2} the two cover plates, c in figure 1, were definitely buckled over their entire length. Under the maximum load, buckles appeared suddenly in the adjacent sides just above mid-height as shown in figures 7 and 8.

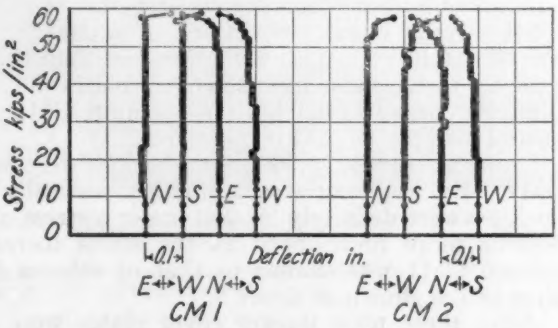

FIGURE 6.—*Lateral deflections for the columns.*

The ratio of the distance between the nearest lines of rivets to the thickness of the cover plate was 45, as given in figure 2. This ratio is limited to a maximum of 40 in some specifications for carbon steel.[8] For alloy steels a ratio not exceeding 36 is allowed. Although the ratio for the

[6] Eng. News-Rec. **103,** 909 (1929).
[7] Tech. Pap. BS **21,** (1926) T328 (particularly p. 57–60).
[8] Bul. Am. Railway Eng. Assn., no. 374 (1935) Report Com. Iron and Steel Structures.

cover plates of the chord columns somewhat exceeded this specification value, it was expected that the cover plate would be restrained sufficiently by the angles to prevent failure of the column by buckling of the cover plates.

The buckling of wide plates in ships under compressive loads was discussed mathematically by Bryan.[9] His results lead to the following equation for the stress at which plates simply supported at the lateral edges buckle elastically:

$$S=3.5\frac{Et^2}{b^2},$$

in which

S=stress at which plate buckles, lb/in.^{2}
E=Young's modulus of elasticity, lb/in.^{2}
t=thickness of plate, in.
b=width of plate, in.

The constant 3.5 depends upon the assumption that the Poisson's ratio for the plate is 0.25. It is also assumed that the plate is infinitely long and that the proportional limit of the plate is greater than the buckling stress.

The average value of the Young's modulus of elasticity for the coupons from the cover plates of the chord columns was 29,100,000 lb/in.^{2} for column CM1 and 28,800,000 lb/in.^{2} for column CM2. Bryan shows that the distance from crest to crest of the buckles measured longitudinally along the plate, is equal to the effective width of the plate. The distance from crest to crest on column CM2, after the test, was 19.7 inches. This is greater than the distance between rivet lines (16.88 in.), but less than the width of the cover plate (21 in.). Apparently the cover plates were restrained by the angles so that the effective width was less than the actual width but greater than the distance between the nearest rivet lines. The ratio of this effective width to the thickness of the cover plate was 52.4. The buckling stress for the cover plates of column CM2, computed by the use of Bryan's equation for an effective width of 19.7 inches, was 36,600 lb/in.^{2} This value was less than the average proportional limit for the coupons from the cover plates (39,500 lb/in.^{2}) but greater than the proportional limit of column CM2 for the first and the second loading, as shown by figure 5.

Under a stress of 36,600 lb/in.^{2} buckles were not apparent in column CM1. By applying a straightedge vertically to the cover plates, buckless were definitely located under a stress of 38,000 lb/in.^{2} They became more pronounced as the stress increased. The failure of column CM1 was similar to that of column CM2. Column CM1 after test is shown in figure 8.

After these tests thicker cover plates were used in the Bayonne Bridge to increase resistance to buckling.

Although the results on these two chord columns do not prove that Bryan's formula is correct, they are in substantial agreement with the values obtained by the use of the formula for these columns. For fabricated columns similar to these chord columns, a value of 36 for the ratio of width of plate to thickness may safely be used in design.

[9] Proc. London Math. Soc. 22, 54 (1890).

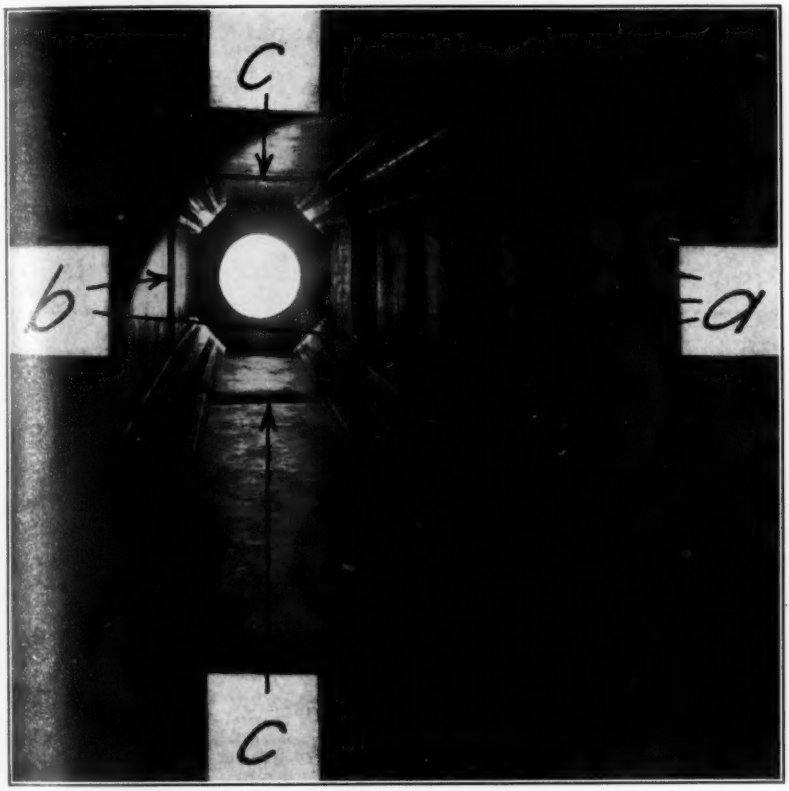

FIGURE 7.—*Buckles in column* CM2, *after test, as they appeared from the bottom of the column.*

The buckles a–a were definite at a stress of 53 kips/in.^{2} Under the maximum load the buckles b–b increased greatly and buckles c–c appeared suddenly.

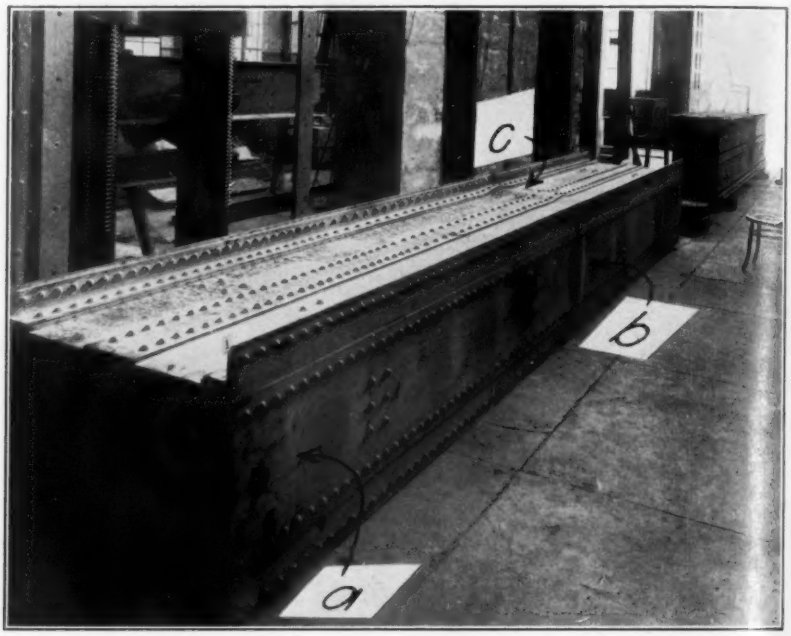

FIGURE 8.—*Chord column* CM1 *after test.*

There were buckles for the entire length of the cover plate a. Under the maximum load the buckle b increased greatly and buckle c appeared suddenly.

IV. CONCLUSIONS

1. The loading was nearly axial.
2. For stresses which were nearly the maximum stresses in the columns the lateral deflection was small.
3. Under a stress of about 38 kips/in.^{2} the two cover plates began to buckle for their entire length, and the buckles increased as the load increased.
4. The yield strength of these columns was taken as the stress for which the strain was 0.002 greater than the elastic strain and the column efficiency obtained by dividing the column yield strength by the weighted yield strength of the material in the column. The average column yield strength was 57 kips/in.^{2}, and the average column efficiency 97.4 percent.

The program and testing procedure were prepared by O. H. Ammann, chief engineer; L. S. Moisseiff, consulting engineer; and R. S. Johnston, research engineer, of the Port of New York Authority; and by L. J. Briggs, L. B. Tuckerman, and H. L. Whittemore, of the National Bureau of Standards. The following members of the staff of the Port of New York Authority assisted in making the tests and obtaining the data: A. H. Baker, F. J. Hinners, S. K. Hoppen, B. A. Lefeve, L. D. Mork, R. B. Morris, and G. A. Woods.

The chemical compositions of the steels were determined by the Chemistry Division of the Bureau.

WASHINGTON, February 27, 1935.

U. S. DEPARTMENT OF COMMERCE NATIONAL BUREAU OF STANDARDS

RESEARCH PAPER RP898

Part of Journal of Research of the National Bureau of Standards, Volume 16, June 1936

THIRD SPECTRUM OF XENON

By C. J. Humphreys

ABSTRACT

The third spectrum of xenon (Xe III) characteristic of doubly ionized xenon atoms (Xe^{++}) appears along with the second spectrum when a Geissler tube containing the gas is operated by an alternating current transformer with condensers and spark gap in the discharge circuit. The partial or complete suppression of lines originating in ions of higher stage than the first by the insertion of varying amounts of inductance in the discharge circuit has been used to distinguish the lines of Xe III from those of the other xenon spectra. Wave-length measurements of xenon spark spectra based mainly on observations with the Rowland grating at the National Bureau of Standards extend from 2200 to 8900 A. The majority of the Xe III lines are in the near ultraviolet region. About 300 lines have been classified arising from 84 levels of Xe III.

The low states of Xe^{++} are ^3P, ^1D, and ^1S, due to the $5s^25p^4$ configuration. The higher excited states are built upon the ^4S, ^2D, and ^2P states of Xe^{+++} by the addition of an *ns*, *np*, or *nd* electron to the normal $5s^25p^3$ configuration. Complete quantum number designations are given for about two-thirds of the levels. A sufficient number of levels are available to account for nearly all the terms belonging to the low and first excited states. Numerous instances of mutual perturbations between terms causing a sharing of combining properties makes an unambiguous assignment of quantum numbers difficult or impossible in such cases. These perturbations apparently are also responsible for frequent and intense intersystem combinations as well as combinations between terms converging to different limits. The fact that all groups of terms are tied together permits an accurate calculation of their relative values. In all cases permitted by the rules governing quantum transitions, the levels of first excited states combine with the low levels giving lines in the extreme ultraviolet region observed by J. C. Boyce. The absolute term values are arrived at from an estimation of the limit of the $5s^25p^3(^4S)nd^3D^\circ$ series. The lowest $4s^24p^4\,^3P_2$ level comes out accordingly 259,089 cm^{-1}, equivalent to an ionization potential of 32.0 volts for Xe^{++}.

CONTENTS

		Page
I.	Introduction	639
II.	Experimental	640
III.	Analysis of the Xe III spectrum	641
	1. Classified lines	641
	2. Theoretical terms	643
	3. General features of the Xe III spectrum	644
	4. Table of terms	645
	5. The (^4S) family of terms; ionization potential	646
	6. Discussion	646

I. INTRODUCTION

The third spectrum or second spark spectrum of an element is characteristic of the doubly ionized atom, as distinguished from the second spectrum or first spark spectrum due to the singly ionized atom,

and the first spectrum or arc spectrum of the neutral atom. These successive spectra are designated by a roman numeral following the chemical symbol which refers to the spectrum and not to the ion. Although the upper limit of excitation may be fixed by controlling the conditions of operation of the light source, it is not possible generally to prevent the simultaneous appearance of spectra from atoms of lower stages of ionization along with those of maximum excitation. For this reason the preliminary sorting of the observed lines so that each is associated with its respective ion source is an essential prerequisite to a term analysis of any spectrum of an element higher than the first.

A discussion of the methods which have been employed successfully to accomplish this selection as well as an account of the early observations of xenon spectra is given in previous publications.[1 2 3 4]

II. EXPERIMENTAL

A complete description of the spark spectra of xenon has been prepared at the National Bureau of Standards over the wave length range 2200 to 8900 A. The spectra were obtained from Geissler tubes operated by a-c transformers in a circuit containing a spark gap and condensers. Except for the region beyond 2575 A in the ultraviolet, the entire spectrum was observed with the 20000 line per inch Rowland grating. One set of observations was made with the 35-ft radius, 30000-line grating at the Massachusetts Institute of Technology. Agreement of various sets of observations indicates that the wave lengths are correct to within 0.01 A for most sharp lines in the range covered by grating observations. The complete list contains about 2000 lines. Probably three-fourths of these are lines of the second spectrum, Xe II, a partial analysis of which has been reported.[5] A list of about 500 lines has been selected which appear to belong to Xe III or spectra still higher, although nearly all are believed to be Xe III. The basis of the selection is the partial or complete suppression of lines originating in ions of higher stage than the first when small amounts of inductance are placed in the circuit. This is the method which was used in the separation of the krypton spectra.[6]

For the xenon tubes used in this investigation a very small amount of inductance was sufficient to suppress the Xe III lines, from 0.00005 to 0.00018 henry being used for most exposures. A comparison was made also with the selection of xenon lines given by L. Bloch, E. Bloch, and G. Déjardin,[7] who observed that there was a radial distribution of ions in an electrodeless discharge tube so that when the slit was illuminated end on, first spark lines appeared as short lines originating in the center of the tube, whereas higher spark lines were long lines whose emitters had greater population near the walls. Comparison of the two methods indicates generally satisfactory agreement, almost perfect in the case of the second spectra of the rare gases. The lines which the Blochs indicate as belonging to the fourth spectrum, however, seem more probably to originate in high energy states of the third.

[1] Wm. F. Meggers, T. L. deBruin, and C. J. Humphreys, BS J. Research **3**, 731 (1929), RP115.
[2] C. J. Humphreys, T. L. deBruin, and W. F. Meggers, BS J. Research **6**, 287 (1931), RP275.
[3] T. L. deBruin, C. J. Humphreys, and Wm. F. Meggers, BS J. Research **11**, 409 (1933), RP599.
[4] C. J. Humphreys, Phys. Rev. **47**, 712 (1935).
[5] C. J. Humphreys, T. L. deBruin, and W. F. Meggers, BS J. Research **6**, 287 (1931), RP275.
[6] C. J. Humphreys, Phys. Rev. **47**, 712 (1935).
[7] L. Bloch, E. Bloch, and G. Déjardin, Ann. Phys. **10**, p. 461 (1924.)

The extreme ultraviolet spectra of xenon, hitherto limited to the description published by Abbink and Dorgelo in 1928,[8] have been observed recently by J. C. Boyce, who includes a list of 128 classified lines of Xe III in a paper just published.[9] These observations were made with the 2-meter vacuum spectrograph of the Carnegie Institution of Washington now set up in the spectroscopy laboratory of the Massachusetts Institute of Technology. Dr. Boyce very generously made these data available to the author previous to publication, and his cooperation while the analysis was in progress is gratefully acknowledged. The connection of the extreme ultraviolet lines with the rest of the observed spectrum will be discussed in connection with the details of the analysis.

III. ANALYSIS OF THE Xe III SPECTRUM

1. CLASSIFIED LINES

Classifications have been obtained for about 300 of the lines ascribed to Xe III. These are assembled in table 1, which gives estimated intensity, wave length in air, wave number in vacuum, and the levels involved in the transition. The intensities are comparable only over short ranges. A letter *h* following the intensity estimate indicates that the line is hazy. Lines marked 1- are very faint, just barely measurable.

TABLE 1.—*Classified lines of* Xe III

Intensity	Wave length (air)	Wave number (vac)	Transition	Intensity	Wave length (air)	Wave number (vac)	Transition
1 h	2235.35	44721.79	$(^3D)6s^3D_1^0-(^3P)6p^3D_2$	3	2658.26	37607.41	$(^4S)5d^3D_3^0-(^4S)6p^3P_1$
1	2303.73	43394.48	$(^4S)5d^3D_2^0-(^2D)6p^3P_1$	1	2661.00	37568.70	$(^4S)5d^3D_3^0-(^2D)6p^3F_2$
1-	2312.29	43233.85	$5s5p^3\,{}^1P_1^0-(^2D)6p^3F_2$	10	2669.00	37456.10	$(^4S)5d^3D_1^0-(^4S)6p^3P_2$
1	2403.76	41588.82	$(^3D)5d^1P_1^0-(^3P)6p^3D_2$	1	2678.54	37322.70	$(^3D)6s^3D_2^0-(^3D)6p^1D_2$
1	2414.52	41403.50	$(^3D)5d^3S_1^0-28_1$	2	2685.58	37224.86	$(^2D)5d^3S_1^0-(^2P)6p^3D_2$
4	2416.73	41365.65	$(^4S)5d^3D_3^0-(^2D)6p^3D_2$	5	2687.03	37204.78	$(^4S)5d^3D_2^0-(^4S)6p^3P_2$
5	2436.48	41030.36	$(^4S)5d^3D_2^0-(^2D)6p^3F_2$	8	2696.50	37074.13	$(^4S)5d^3D_1^0-(^2D)6p^3D_1$
1	2447.64	40843.30	$5s5p^3\,{}^3P_2^0-(^4S)6p^3P_1$	4	2727.22	36656.54	$(^2D)5d^1F_3^0-2_2$
3	2452.62	40760.38	$(^2D)5d^3F_4^0-12_3$	4	2728.22	36643.11	$(^4S)6s^3S_1^0-(^2D)6p^3F_2$
1	2463.02	40588.28	$(^2D)5d^1D_2^0-36$	12	2740.80	36474.93	$(^2D)5d^3F_2^0-(^2D)6p^1D_2$
3	2471.28	40452.63	$(^4S)5d^3D_2^0-(^4S)6p^3P_2$	8	2747.88	36380.95	$(^2D)5d^3G_4^0-(^2D)6p^3F_3$
1	2472.34	40435.28	$(^2D)5d^3F_3^0-(^2D)6p^3F_3$	6	2760.76	36211.23	$13_3^0-32_1$
1	2483.43	40254.73	$(^2D)5d^3F_2^0-8_2$	12	2761.60	36200.22	$(^2D)5d^3G_3^0-8_2$ $15_2^0-34_1$
3	2486.69	40201.97	$(^4S)5d^3D_1^0-(^4S)6p^3P_2$	1	2763.00	36181.88	$(^2D)5d^3G_4^0-(^2D)6p^1F_3$
4	2501.04	39971.32	$5s5p^3\,{}^1P_1^0-(^2D)6p^3D_1$	5	2766.20	36140.02	$(^2D)5d^3F_3^0-(^2D)6p^3F_2$
3	2510.52	39820.39	$(^4S)5d^1D_2^0-(^2D)6p^1P_1$	10	2772.41	36059.08	$(^4S)6p^3P_1-(^4S)6d^3D_2^0$
1	2515.14	39747.26	$(^4S)5d^3D_2^0-2_2$	10	2776.96	36000.00	$(^4S)5^3D_3^0-(^3D)6p^3D_2$
1	2524.09	39606.33	$(^4S)5d^3D_1^0-(^4S)6p^3P_2$	5	2779.64	35965.29	$(^2D)5d^3D_2^0-26_1$ $(^4S)6p^3P_2-(^4S)7s^3S_1^0$
2	2533.31	39462.19	$(^4S)5d^3D_3^0-(^2D)6p^3D_2$	12	2783.37	35917.08	$(^2D)6p^3D_2-37^0$
1	2570.26	38894.92	$(^4S)6s^3S_1^0-(^2D)6p^1P_1$	20	2794.86	35769.44	$(^4S)6p^3P_1-(^4S)6d^3D_1^0$
1 h	2572.30	38864.08	$(^2D)5d^1P_1^0-(^2P)6p^3D_1$	20	2800.22	35700.98	**$(^4S)6p^3P_1-(^4S)6d^3D_2^0$**
5	2578.36	38772.74	$(^2D)5d^1F_3^0-(^2D)6p^3F_2$	2	2805.08	35639.13	$15_3^0-32_1$
2	2578.62	38768.83	$(^4S)5d^3D_1^0-(^2D)6p^3D_2$	3	2806.39	35622.49	$(^2D)5d^1P_1^0-(^1D)6p^1D_2$
2	2590.45	38591.80	$(^2D)5d^1F_3^0-8_2$	10	2807.25	35611.58	$2_3-39_2^0$
4	2591.69	38573.34	$(^2D)5d^1F_3^0-(^2D)6p^1F_3$	8	2809.07	35588.51	$(^4S)6p^3P_2-(^4S)6d^3D_1^0$
6	2608.90	38318.90	$(^2D)5d^3F_4^0-2_3$	1	2810.52	35570.15	$(^2D)6p^3D_2-33^0$
1	2624.52	38090.85	13_3^0-36	8	2811.67	35555.60	$(^4S)6p^3P_1-(^4S)7s^3S_2^0$
3	2637.54	37902.83	$(^4S)5d^3D_3^0-(^2D)6p^3D_3$	30	2814.47	35520.23	$(^4S)6p^3P_2-(^4S)6d^3D_3^0$
5	2641.12	37851.46	$(^4S)5d^3D_1^0-(^4S)6p^3P_1$	40	2815.94	35501.69	$(^4S)6p^3P_2-(^4S)6d^3D_2^0$
1	2650.20	37721.78	$(^4S)6p^3P_1-(^4S)7s^3S_1^0$	20	2826.05	35374.69	$(^4S)6p^3P_2-(^4S)7s^3S_1^0$

[8] J. H. Abbink and H. B. Dorgelo, Z. Phys. **47**, 221 (1928).
[9] J. C. Boyce, Phys. Rev. **49**, 730 (1936).

TABLE 1.—*Classified lines of* Xe III—Continued

Intensity	Wave length (air)	Wave number (vac)	Transition
30	2827.45	35357.18	$(^4S)5d^3D^0_3-(^4S)6p^3P_2$
6	2832.95	35288.54	$(^2D)6s^3D^0_3-(^2P)6p^3D_3$
6	2833.18	35285.67	$(^2D)6p^3D_2-31^0_2$
3	2838.85	35215.20	$(^4S)6p^3P_0-(^4S)7s^3S^0_1$
2	2839.57	35206.27	$(^2D)6p^3D_2-29^0_2$
40	2847.66	35106.26	$(^4S)5d^3D^0_3-(^4S)6p^3P_2$
2	2850.25	35074.36	$(^4S)6s^3S^0_1-(^2D)6p^3D_2$
1	2857.81	34981.58	$(^2D)6s^1D^0_2-26_1$
30	2862.41	34925.36	$(^4S)5d^3D^0_2-(^4S)6p^3P_1$
1	2863.86	34907.68	$(^2D)6s^1D^0_2-(^1P)6p^3D_3$
1	2868.42	34852.19	$(^2D)6s^3D^0_1-(^2D)6p^3P_1$
30	2871.68	34812.63	$(^2D)5d^1F^0_3-(^2D)6p^3D_3$
2	2872.73	34799.91	$(^2D)5d^3D^0_2-(^1P)6p^3D_2$
25	2891.71	34571.50	$(^2D)5d^3F^0_3-(^2D)6p^3D_2$
30	2896.63	34512.79	$(^4S)5d^3D^0_1-(^4S)6p^3P_2$
2	2897.69	34500.16	$(^2D)5d^3S^0_1-(^1P)6p^3D_1$
1	2899.57	34477.80	$(^2D)5d^1F^0_3-(^2D)6p^3F_3$
50	2906.56	34394.88	$(^2D)5d^3G^0_4-(^2D)6p^3F_3$
2	2911.47	34336.88	$13^0_1-28_1$
40	2911.90	34331.81	$(^4S)5d^3D^0_1-(^4S)6p^3P_1$
20	2914.12	34305.66	$(^4S)5d^3D^0_2-(^2D)6p^3D_1$
20	2917.59	34264.86	$(^2D)5d^3G^0_5-2_2$
25	2923.51	34195.48	$(^2D)5d^3G^0_4-(^2D)6p^1F_3$
20	2930.29	34116.36	$(^2D)5d^1G^0_4-(^2D)6p^3F_3$
25	2932.74	34087.86	$(^4S)5d^3D^0_3-(^4S)6p^3P_1$
10	2939.13	34013.75	$(^2D)6p^3D_3-37^\circ$
40	2940.22	34001.15	$(^2D)6p^3F_3-33^\circ$
60	2945.25	33943.08	$(^2D)6p^3D_3-35^\circ$
40	2947.53	33916.82	$(^2D)5d^1G^0_4-(^2D)6p^1F_3$
40	2948.06	33910.73	$(^2D)5d^3F^0_3-(^2D)6p^3F_2$
15	2964.98	33717.22	$(^2D)6p^3F_3-31^0_2$
10	2966.97	33694.60	$(^2D)6p^1F_3-39^0_2$
10	2968.56	33676.55	$8_2-39^0_2$
4	2969.45	33666.47	$(^2D)6p^3D_3-33^\circ$
8	2971.24	33646.19	$(^2D)6s^1D^0_1-12_2$
15	2984.63	33495.25	$(^2D)6p^3F_3-39^0_2$
10	2991.25	33421.12	$(^4S)6p^3P_2-(^4S)6d^3D^0_2$
8	2991.45	33418.89	$(^2D)6s^3D^0_2-(^2D)6p^3P_1$
40	2992.91	33402.58	$(^4S)6p^3P_2-(^4S)6d^3D^0_2$
8	2994.69	33382.73	$(^2D)6p^3D_3-31^0_2$
10	3001.85	33303.11	$(^2D)6p^3D_3-29^0_2$
30	3004.32	33275.73	$(^4S)6p^3P_2-(^4S)7s^3S^0_1$
6	3014.18	33166.88	$(^2D)5d^3D^0_2-(^2P)6p^3D_1$
100	3023.80	33061.37	$(^4S)6p^3P_2-(^4S)6d^3D^0_2$ $(^2D)6s^3D^0_1-(^2D)6p^3P_0$
8	3026.52	33031.66	$5s5p^3\,{}^1P^0_1-(^4S)6p^3P_2$
15	3054.49	32729.20	$(^2D)5d^1D^0_2-26_1$
10	3073.49	32526.88	$(^2P)6s^3P^0_1-32_1$
40	3083.54	32420.87	$(^2D)5d^3G^0_5-(^2D)6p^3D_3$
50	3091.06	32342.00	$(^2D)5d^3F^0_2-(^2D)6p^3D_2$
8	3099.91	32249.67	$(^4S)6p^3P_1-(^4S)6d^3D^0_1$
3	3103.47	32212.68	$(^2D)6s^3D^0_2-12_2$
30	3106.33	32183.02	$(^2D)6s^1D^0_2-(^2P)6p^3D_1$
12	3114.46	32099.01	2_2-35°
1	3124.61	31994.75	$(^2P)6s^3P^0_2-36$
20	3150.69	31729.92	$19^0_2-28_1$
10	3151.82	31718.54	$(^2D)5d^1P^0_1-(^2D)6p^3P_1$
8	3152.98	31706.88	$(^2D)6s^3D^0_2-8_2$
2 h	3160.70	31629.44	$(^2P)6s^3P^0_0-28_1$
5 h	3169.82	31538.44	$2_2-31^0_2$
5 h	3177.19	31465.28	$(^2D)6p^1P_1-31^0_2$
40	3185.24	31385.76	$(^2D)6p^1P_1-29^0_2$
25	3196.51	31275.11	$5s5p^3\,{}^1P^0_1-(^4S)6p^3P_1$
4	3199.22	31248.62	$(^2P)6s^1P^0_1-36$
25	3236.84	30885.44	$(^4S)5d^3D^0_1-(^4S)6p^3P_0$
100	3242.86	30828.11	$(^4S)5d^3D^0_2-(^4S)6p^3P_2$
10	3246.84	30790.32	$(^2D)5d^3D^0_2-(^2P)6p^3D_3$
80	3268.96	30581.99	$(^4S)6s^3S^0_1-(^4S)6p^3P_2$
8	3276.39	30512.63	$(^2D)5d^1P^0_1-12_2$
8	3278.48	30493.18	$(^4S)6p^3P_2-(^4S)6d^3D^0_1$
3 h	3284.70	30435.44	$(^2D)5d^3G^0_4-(^2D)6p^3D_3$
10 h	3285.89	30424.42	$(^4S)6p^3P_2-(^4S)6d^3D^0_2$
30	3287.92	30405.64	$(^4S)6p^3P_2-(^4S)6d^3D^0_3$
20	3301.60	30279.66	$(^4S)6p^3P_2-(^4S)7s^3S^0_1$
10	3306.80	30232.04	$13^0_1-26_1$
1	3314.30	30163.63	8_2-35°
10	3314.87	30158.45	$13^0_1-(^2P)6p^3D_3$
2	3317.44	30135.08	$(^4S)5d^3D^0_1-(^4S)6p^3P_2$
2	3319.53	30116.11	$(^1P)6s^3P^0_1-32_1$
40	3331.65	30006.56	$(^2D)5d^1P^0_1-8_2$
1 h	3334.26	29983.07	$(^2D)6p^1F_3-35^\circ$
25	3338.98	29940.69	$(^2D)5d^3D^0_1-(^2D)6p^3P_1$
10	3340.06	29931.00	$(^2D)5d^1D^0_2-(^2P)6p^3D_1$ $(^1P)6s^1P^0_1-34_1$
4 h	3344.97	29887.07	8_2-33°
12	3349.76	29844.34	$(^2D)6s^1D^0_2-(^2D)6p^1P_1$
30	3357.98	29771.28	$(^2D)6s^1D^0_2-2_2$
3 h	3362.81	29728.52	12_2-37°
4	3370.65	29659.38	$15^0_2-26_1$
2 h	3377.09	29602.82	$8_2-31^0_2$
5	3379.02	29585.91	$15^0_2-(^1P)6p^3D_2$
8	3403.89	29369.75	$(^1P)6s^1P^0_1-32_1$
4 h	3435.78	29097.16	$12_2-31^0_2$
60	3444.23	29025.78	$(^2D)6s^3D^0_1-(^2D)6p^1F_3$
70	3454.25	28941.58	$(^2D)6s^1D^0_2-(^2D)6p^1D_2$
25	3467.20	28833.49	$(^2D)5d^3D^0_3-(^2D)6p^1D_2$
40	3468.19	28825.26	$(^4S)6s^3S^0_1-(^4S)6p^3P_1$
1	3479.11	28734.79	$(^2D)5d^3D^0_1-12_2$
4	3497.89	28580.52	$(^2P)6s^1P^0_1-(^1P)6p^3P_0$
80	3522.83	28378.18	$(^4S)5d^3D^0_1-(^4S)6p^3P_1$
20	3539.96	28240.87	$(^1P)6s^3P^0_2-28_1$
50	3542.33	28221.97	$(^2D)6s^3D^0_1-12_2$
50	3552.13	28144.11	$(^2D)5d^1P^0_1-(^2D)6p^1P_1$
40	3561.38	28071.01	$(^2D)5d^1P^0_1-2_2$
100	3579.69	27927.44	$(^2D)6s^1D^0_2-(^2D)6p^1D_2$
80	3583.64	27896.65	$(^2D)6s^1D^0_2-(^2D)6p^1F_3$
5	3592.00	27831.73	$(^4S)5d^3D^0_1-(^4S)6p^1P_1$
6	3601.89	27755.31	$5s5p^3\,{}^1P^0_1-(^4S)6p^3P_1$
40	3607.01	27715.91	$(^2D)6s^1D^0_2-8_2$
20	3609.44	27697.26	$(^2D)6s^1D^0_2-(^2D)6p^1F_3$
4	3618.90	27624.86	$19^0_2-26_1$
40	3623.13	27592.61	$(^2D)6s^1D^0_2-(^2D)6p^1F_3$
600	3624.05	27585.60	$(^4S)6s^3S^0_1-(^4S)6p^3P_2$
3	3628.57	27551.24	$19^0_2-(^1P)6p^3D_2$
20	3632.14	27524.16	$(^2P)6s^1P^0_2-26_1$
3	3636.03	27494.72	$(^2P)6s^1P^0_1-28_1$
15	3641.00	27457.19	$(^2D)6s^1D^0_2-(^2D)6p^3D_3$
5	3644.14	27433.53	$13^0_1-(^1P)6p^3D_1$
3	3653.12	27366.09	$(^4S)5d^3D^0_1-(^4S)6p^3P_2$
20	3654.63	27354.79	$(^2D)5d^3S^0_1-(^2D)6p^3P_1$
50	3676.63	27191.10	$(^4S)6s^3S^0_1-(^4S)6p^3P_0$
4	3708.15	26959.98	23^0_2-36
25	3745.72	26689.58	$(^2D)5d^1D^0_2-(^2D)6p^1D_2$
10	3765.85	26546.91	$(^2P)6s^1P^0_1-26_1$
20	3772.53	26499.91	25^0_2-36
40	3776.30	26473.45	$(^2P)6s^1P^0_1-(^2P)6p^3D_2$
300	3780.98	26440.69	$(^4S)6s^3S^0_1-(^4S)6p^3P_2$
12	3791.67	26366.14	$(^2D)5d^3D^0_2-(^2D)6p^1P_1$
20	3829.77	26103.85	$(^1P)6p^3D_3-39^0_2$
100	3841.52	26024.01	$(^2D)6s^3D^0_1-(^2D)6p^3D_2$
20	3841.88	26021.57	$(^2D)5d^3D^0_3-(^2D)6p^1P_1$
10	3854.30	25937.72	$(^2D)5d^1F^0_3-(^4S)6p^3P_2$

TABLE 1.—*Classified lines of* Xe III—Continued

Intensity	Wave length (air)	Wave number (vac)	Transition
10	3861.05	25892.37	$(^2D)5d^1P_1^\circ-(^2P)6p^3F_2$
200	3877.80	25780.54	$(^3D)6s^3D_3^\circ-2_2$
60	3880.46	25762.86	$(^3D)6s^3D_1^\circ-(^2D)6p^3D_1$
4	3903.70	25609.49	$(^4S)5d^3D_2^\circ-(^4S)6p^3P_1$
4h	3915.30	25533.62	$17_3^\circ-(^2P)6p^3D_3$
500	3922.53	25486.56	$(^4S)6s^5S_2^\circ-(^4S)6p^5P_3$
300	3950.56	25305.73	$(^4S)6s^5S_2^\circ-(^4S)6p^5P_1$
4	3969.91	25182.39	$25_1^\circ-34_1$
8	3985.96	25080.99	$23_2^\circ-32_1$
20	3992.85	25037.71	$(^3D)6s^1D_2^\circ-(^3D)6p^3P_1$
4	4021.62	24858.60	$(^4S)5d^3D_1^\circ-(^4S)6p^5P_1$
10	4028.58	24815.65	$(^3D)5d^3D_3^\circ-12_2$
20	4043.21	24725.86	$(^2P)6s^3P_0^\circ-(^2P)6p^3D_1$
200	4050.05	24684.10	$(^4S)6s^3S_1^\circ-(^4S)6p^3P_1$
60	4060.43	24621.00	$25_1^\circ-32_1$
2	4060.88	24618.28	$(^2D)6p^1D_2-37^0$
100	4109.07	24329.56	$(^2D)6s^3D_3^\circ-(^2D)6p^3D_1$
10	4110.06	24323.70	$(^3D)5d^1P_1^\circ-(^2D)6p^3D_2$
1−	4112.34	24310.22	$(^3D)5d^3D_3^\circ-8_2$
3h	4132.42	24192.10	$13_1^\circ-(^2D)6p^1D_2$
10	4142.01	24136.08	$(^2P)6s^3P_2^\circ-26_1$
100	4145.73	24114.43	$(^3D)5d^3D_1^\circ-(^3D)6p^3F_2$
5	4152.03	24077.84	$27_2^\circ-36$
2	4154.65	24062.65	$(^2P)6s^3P_2^\circ-(^2P)6p^3D_2$
1	4167.66	23987.54	$(^2D)6p^1D_2-31_2^\circ$
20	4176.53	23936.60	$(^3D)6s^3D_3^\circ-(^2D)6p^3D_3$
5	4194.88	23831.89	$(^3D)6s^1D_2^\circ-12_2$ / $25_1^\circ-(^2P)6p^3P_0$
10	4203.92	23780.65	$(^3D)5d^3S_1^\circ-(^2D)6p^1P_1$
10	4209.62	23748.45	$(^3P)6s^3P_1^\circ-(^2P)6p^3D_1$
20	4214.04	23723.54	$(^1D)5d^1D_2^\circ-12_2$
10	4216.75	23708.29	$(^3D)5d^3F_3^\circ-(^4S)6p^3P_2$
1−	4232.66	23619.18	$15_2^\circ-(^2D)6p^1D_2$
1	4235.82	23601.56	$(^3D)6s^3D_3^\circ-(^2D)6p^3F_2$
10	4240.24	23576.95	$17_3^\circ-(^3D)6p^1D_2$
20	4272.60	23398.39	$(^1D)5d^3D_3^\circ-(^3D)6p^3F_3$
1	4274.13	23390.01	$(^2P)6s^1P_1^\circ-26_1$
30	4285.89	23325.84	$(^3D)6s^1D_2^\circ-8_2$
2	4305.86	23217.66	$(^1D)5d^3D_3^\circ-8_2$
10	4308.00	23206.12	$23_2^\circ-28_1$
6	4309.33	23198.96	$(^3D)5d^3D_3^\circ-(^2D)6p^1F_3$
1−	4357.66	22941.67	$(^3D)5d^3F_3^\circ-(^4S)6p^5P_3$
4h	4387.52	22785.54	$(^1D)5d^1D_2^\circ-(^2D)6p^3P_1$
4	4395.12	22746.14	$25_1^\circ-28_1$
1−	4417.81	22629.32	$(^3D)5d^1P_1^\circ-(^2D)6p^3D_1$
1−	4425.25	22591.27	$(^2P)6p^3D_3-35^0$
50	4434.16	22545.88	$(^2D)5d^3D_1^\circ-(^2D)6p^3D_2$
8	4453.61	22447.41	$(^2D)5d^3D_2^\circ-(^2D)6p^1P_1$
1	4468.15	22374.37	$(^1D)5d^3D_2^\circ-2_2$
2h	4488.81	22271.39	$(^4S)5d^3D_3^\circ-(^4S)6p^3P_2$
10	4503.46	22198.94	$27_2^\circ-32_1$
1h	4525.67	22090.00	$(^4S)5d^3D_1^\circ-(^4S)6p^5P_1$
30	4537.33	22033.24	$(^1D)6s^3D_3^\circ-(^2D)6p^3D_2$
2	4631.50	21585.25	$19_2^\circ-(^2D)6p^1D_2$
2	4632.68	21579.75	$(^2D)5d^1D_2^\circ-12_2$
1−	4643.63	21528.87	$(^2D)5d^3S_1^\circ-(^2D)6p^3F_2$
9	4657.78	21463.46	$(^2D)6s^1D_2^\circ-(^2D)6p^1P_1$
30	4673.66	21390.54	$(^2D)6s^1D_2^\circ-2_2$
60	4683.53	21345.46	$(^4S)6s^3S_1^\circ-(^4S)6p^3P_2$
1	4685.17	21337.99	$(^2P)6s^3P_2^\circ-(^2P)6p^3D_1$
2	4697.49	21282.03	$(^2D)5d^3D_3^\circ-2_2$
30	4723.57	21164.53	$(^4S)6s^3S_1^\circ-(^4S)6p^3P_1$
4	4743.89	21073.87	$(^1D)5d^1D_2^\circ-8_2$
12	4794.48	20851.51	$(^2D)5d^3D_1^\circ-(^2D)6p^3D_1$
40	4869.47	20530.40	$(^2D)5d^3D_2^\circ-(^2D)6p^3D_3$
3	4927.53	20288.50	$13_1^\circ-(^2D)6p^3P_1$
10	5008.55	19960.31	$(^2D)5d^3S_1^\circ-(^2D)6p^3D_2$
1h	5070.53	19716.32	$15_2^\circ-(^2D)6p^3P_1$
20	5107.38	19574.07	$(^2D)6s^3D_1^\circ-(^4S)6p^3P_0$
1	5114.57	19546.55	$(^2D)6s^1D_2^\circ-(^3D)6p^1D_2$
4	5143.03	19438.39	$(^3D)5d^3D_3^\circ-(^3D)6p^3D_3$
20	5223.66	19138.35	$(^3D)5d^1D_2^\circ-2_2$
3	5233.16	19103.61	$(^3D)5d^3D_2^\circ-(^3D)6p^3F_2$
60	5238.95	19082.50	$13_1^\circ-12_2$
6	5310.99	18823.66	$(^3D)6s^3D_1^\circ-(^4S)6p^3P_2$
30	5367.06	18627.01	$(^3D)5d^3D_2^\circ-(^3D)6p^1D_2$
1	5371.09	18613.03	$(^3D)5d^3F_3^\circ-(^4S)6p^3P_2$
2	5384.17	18567.81	$25_1^\circ-(^2P)6p^1D_2$
50	5401.04	18509.82	$15_2^\circ-12_2$
12	5413.56	18467.01	$17_3^\circ-12_2$
1	5454.30	18329.08	$(^2D)6p^1P_1-(^4S)6d^3D_2^\circ$
1	5510.55	18141.97	$17_3^\circ-(^3D)6p^3F_3$
40	5524.39	18096.53	$(^2P)6s^3P_2^\circ-(^3D)6p^1D_2$
12	5552.83	18003.85	$15_2^\circ-8_2$
2	5566.02	17961.18	$17_3^\circ-8_2$
1	5656.46	17642.82	$(^2D)6s^1D_2^\circ-(^2D)6p^3D_2$
6	5701.31	17534.98	$(^3D)5d^3D_3^\circ-(^2D)6p^3D_2$
12	5748.71	17390.39	$(^3D)6s^3D_3^\circ-(^4S)6p^3P_2$
2h	5761.96	17350.40	$(^2P)6s^1P_1^\circ-(^3D)6p^1D_2$
2	5780.55	17294.61	$(^1D)5d^1D_2^\circ-(^3D)6p^3D_3$
10	5857.61	17067.09	$(^2D)6s^3D_1^\circ-(^4S)6p^3P_1$
25	6221.66	16068.45	$15_2^\circ-2_2$
60	6238.24	16025.74	$17_3^\circ-2_2$
2	6260.16	15969.63	$19_2^\circ-8_2$
2h	6268.30	15948.89	$(^2D)6s^1D_2^\circ-(^2D)6p^3D_1$
1	6371.65	15690.19	$(^2D)5d^1P_1^\circ-(^4S)6p^3P_2$
1	6818.12	14662.76	$(^2D)5d^3D_1^\circ-(^4S)6p^3P_0$
4h	7043.94	14192.69	$(^2P)6s^3P_2^\circ-(^2D)6p^3P_1$
2h	7049.34	14181.82	$17_3^\circ-(^2D)6p^3D_2$
2h	7174.90	13933.64	$(^2D)5d^1P_1^\circ-(^4S)6p^3P_1$
2h	7185.92	13912.27	$(^2D)5d^3D_1^\circ-(^4S)6p^3P_2$
1−	7298.93	13696.87	$(^2D)5d^1D_2^\circ-(^3D)6p^3D_1$
1	7448.9	13421.11	$27_2^\circ-(^2P)6p^3D_1$
5h	7460.82	13399.66	$(^2D)6s^3D_3^\circ-(^4S)6p^3P_2$
1	7653.8	13061.82	$23_2^\circ-(^2D)6p^1D_2$

2. THEORETICAL TERMS

The doubly ionized xenon atom has the same outer electronic structure as neutral oxygen or the neutral atoms of homologous elements in the sixth column of the periodic table. It is isoelectronic with neutral tellurium, singly ionized iodine, or trebly ionized cesium. The Hund [10] theory, predicts for Xe III, the spectrum characteristic of Xe^{++}, an array of terms with the same designations as those belonging to the spectra of the elements mentioned. The most probable electron configurations and resulting spectral terms of Xe^{++} are shown in table 2. The low states of Xe^{++} are ^3P, ^1D, and ^1S due to the $5s^25p^4$ configuration. $5s5p^5$ gives $^3P^\circ$ and $^1P^\circ$. The higher

[10] F. Hund, Linienspektren und periodisches System der Elemente (Julius Springer, Berlin, 1927).

excited states are built upon the ^4S, ^2D, and ^2P states of Xe^{+++} by the addition of an *ns*, *np*, or *nd* electron to the normal $5s^25p^3$ configuration. All the identified levels are explained on the basis of these configurations, but further analysis of this spectrum may require other configurations to account for the remaining uninterpreted levels and unclassified lines.

TABLE 2.—*Electron configurations and spectral terms for* Xe III

Electron configuration			
$5s^25p^4$	^3P	^1D	^1S
$5s5p^5$	$^1P^\circ$ $^3P^\circ$		
	Term limit	*Term limit*	*Term limit*
	$5s^25p^3$ $^4S^\circ$	$5s^25p^3$ $^2D^\circ$	$5s^25p^3$ $^2P^\circ$
$5s^25p^36s$	$^3S^\circ$ $^1S^\circ$	$^1D^\circ$ $^3D^\circ$	$^1P^\circ$ $^3P^\circ$
$5s^25p^36p$	^3P ^1P	^1P ^1D ^1F ^3P ^3D ^3F	^1S ^1P ^1D ^3S ^3P ^3D
$5s^25p^35d$	$^3D^\circ$ $^1D^\circ$	$^1S^\circ$ $^1P^\circ$ $^1D^\circ$ $^1F^\circ$ $^1G^\circ$ $^3S^\circ$ $^3P^\circ$ $^3D^\circ$ $^3F^\circ$ $^3G^\circ$	$^1P^\circ$ $^1D^\circ$ $^1F^\circ$ $^3P^\circ$ $^3D^\circ$ $^3F^\circ$
$5s^25p^37s$	$^3S^\circ$ $^1S^\circ$	$^1D^\circ$ $^3D^\circ$	$^1P^\circ$ $^3P^\circ$
$5s^25p^36d$	^3D $^1D^\circ$	$^1S^\circ$ $^1P^\circ$ $^1D^\circ$ $^1F^\circ$ $^1G^\circ$ $^3S^\circ$ $^3P^\circ$ $^3D^\circ$ $^3F^\circ$ $^3G^\circ$	$^1P^\circ$ $^1D^\circ$ $^1F^\circ$ $^3P^\circ$ $^3D^\circ$ $^3F^\circ$

3. GENERAL FEATURES OF THE XeI III SPECTRUM

The position of xenon in the periodic system leads us to expect a closer approach to *jj* coupling for its spectra than in the case of any of the elements of smaller atomic number which have the same electron configurations. There is no conformity to multiplet interval rules. The intervals are large compared to the term separations so that there is an overlapping in several instances. The intensities are fairly regular for the multiplets of the (^4S) family other than those involving $^3D^\circ$, but very irregular for most of the higher terms converging to (^2D) and (^2P). It is thus indicated that there may be a progressive change in the coupling scheme as one goes to higher terms.

Intersystem combinations are abundant and include several instances of singlet-quintet combinations. Transitions between levels which belong to groups converging to different ion limits are also of frequent occurrence and permit precise calculation of the relative values of all terms. The transitions seem to require only that combining terms be of opposite parity, and conformity to the *j*-selection rule. These facts all indicate that perturbations between terms occur frequently. Further evidence for such perturbations is the occurrence of pairs of terms having the same combining properties. Specific instances will be considered.

Up to the past year no reliable work on the analysis of Xe III had been published. Analysis of the doubly ionized rare-gas spectra by Deb and Dutt[11] is completely wrong. The most intense lines of the (^4S) family have been classified by deBruin.[12] He identified the $6s^5S^\circ - 6p^5P$ and $6s^3S^\circ - 6p^3P$ combinations by extrapolation from Te I[13] and I II[14] and confirmed the identifications by C. J. Bakker's unpublished Zeeman effects. DeBruin also found the (^4S)$6d^5D^\circ$ levels, which are the second members of the series. With

[11] S. C. Deb and A. K. Dutt, Z. Phys. 67, 138 (1931).
[12] T. L. deBruin, Zeeman Verhandelingen, p. 413 (1935).
[13] Bartelt, Z. Phys. 88, 522 (1934).
[14] Lacroute, Ann. phys. 3, 1 (1935).

the exception of one and possibly a second level of this quintet, this analysis is in agreement with deBruin's work.

4. TABLE OF TERMS

All the known terms of Xe III are assembled in table 3. It was suggested by Dr. Boyce that the complete set including the low levels be placed in this paper to avoid the necessity of duplication in printing. For this reason a uniform notation has been adopted. Levels without certain interpretation are given a number, even for even levels, odd for odd levels, the subscript being the probable j value. If the number is followed by a quantum designation, the latter is suggested but not regarded as certain. The table now contains 84 levels. Levels designated 30 and 34 are regarded as of doubtful reality, because some of the combination lines are otherwise classified.

TABLE 3.—Xe III *terms*

Electron configuration						
$5s^25p^4$	$^3P_2$	259089	$^1D_2$	241989	$^1S_0$	221691
	$^3P_1$	249294				
	$^3P_0$	250958				
$5s5p^5$	$^3P_2^1$	160826				
	$^3P_1^1$	155520				
	$^3P_0^1$	149630				
	$^1P_1^1$	140062.72				
	Term limit $5s^2\ 5p^3\ ^4S°$		Term limit $5s^2\ 5p^3\ ^2D°$		Term limit $5s^2\ 5p^3\ ^2P°$	
$5s^25p^36s$	$^3S_2^1$	137613.00	$^3D_3^1$	125854.72	$^3P_2^1$	108583.55
			$^3D_2^1$	124421.51	$^3P_1^1$	107606.40
	$^3S_1^1$	133471.80	$^3D_1^1$	120430.72	$^3P_2^1$	105195.59
			$^1D_2^1$	116040.63	$^1P_1^1$	104449.39
$5s^25p^36p$	$^5P_1$	112307.29	$^3D_1$	100091.90	$^3D_3$	85142.20
	$^5P_2$	112126.40	$^3D_2$	98397.50	$20_1\ ^3D_1$	83857.65
	$^5P_3$	110027.40	$^3D_3$	96494.07	$22_2\ ^3D_2$	81132.93
			$^3F_2$	96828.90		
	$^3P_0$	106280.64	2_2	94650.20	26_1	81059.42
	$^3P_1$	108787.71	$4_1\ ^1P_1$	94577.18	28_1	76954.59
	$^3P_2$	107031.06				
			$^3P_0$	92793.33	$30_0\ ^3P_0$	75868.85
			$6_3\ ^1F_3$	92733.48	32_1	75079.63
			8_2	92714.78	34_1	74518.40
			$10_3\ ^3F_3$	92534.05	36_1 or $_3$	73200.80
			12_2	92208.79		
			$14_1\ ^3P_1$	91002.85		
			$^1D_2$	87099.00		
$5s^25p^35d$	$^5D_1^1$		$1\frac{1}{2}\ ^3F_2^1$	132968.93	13_1^1	111291.36
	$^5D_2^1$	147483.54	$3\frac{1}{2}\ ^1F_3^1$	131306.71	15_2^1	110718.72
	$^5D_3^1$	147232.66	$5\frac{1}{2}\ ^3F_3^1$	130739.49	17_3^1	110675.91
	$^5D_4^1$	146639.15	$7\frac{1}{2}\ ^3G_3^1$	128915.00	19_4^1	108684.32
	$^5D_5^1$	146395.14	$9\frac{1}{2}\ ^3G_4^1$	126928.94	23_3^1	100160.71
			$11\frac{1}{2}\ ^1G_4^1$	126650.41	25_4^1	99700.71
	$^3D_3^1$	137859.15	$^1P_1^1$	122721.35	27_3^1	97278.61
	$^3D_2^1$	134397.28	$^3S_1^1$	118357.77		
	$^3D_1^1$	137165.97				
			$^3D_1^1$	120943.39		
			$^3D_2^1$	117024.51		
			$^3D_3^1$	115932.46		
			$^1D_2^1$	113788.61		
$5s^25p^37s$	$^5S_2^1$	76751.69				
	$^3S_1^1$	71065.72				
$5s^25p^36d$	$^5D_1^1$	76966.03				
	$^5D_2^1$	76624.76				
	$^5D_3^1$	76606.25				
	$^5D_4^1$	76537.87				
	$^5D_5^1$	76248.21				
$5s^25p^36d$ or $7s$			29_3^1	63191.42		
			31_2^1	63111.70		
			33_3^1 or $_2$	62827.70		
			35_2^1 or $_3$	62551.10		
			37_3^1 or $_2$	62480.33		
			39_2^1	59038.63		

5. THE (^{4}S) FAMILY OF TERMS; IONIZATION POTENTIAL

The terms of the (^{4}S) family due to first excited states have all been found with the exception of $5d^5D_4^\circ$. The level is hard to find at best because it is expected to yield only one strong combination. DeBruin's $6d^5D_4^\circ$ may, therefore, be regarded as doubtful. There is better reason for believing that the line at ν33061.37 is $(^2D)6s^3D_1^\circ - (^2D)6p^3P_0$ rather than $(^4S)6p^5P_3 - (^4S)6d^5D_4^\circ$. The $^5D^\circ$ levels are partially inverted in I II, so that $^5D_4^\circ$ is between $^5D_3^\circ$ and $^5D_2^\circ$. The level was not found in Te I. The second series members of the terms of the (^{4}S) family have also been found with the exception of $6d^3D^\circ$. Three series are thus made available on which to base an estimation of the absolute term values and the ionization potential for Xe^{++}. The $^5D^\circ$ series was actually chosen. The values of the limit of the $^5D_2^\circ$ series arrived at directly and from the limits of $^3S^\circ$ and $^5S^\circ$ and known separation of levels are as follows:

$^5D_2^\circ$	147,232 cm^{-1}
$^3S_1^\circ + (^5D_2^\circ - {}^3S_1^\circ)$	147,717 cm^{-1}
$^5S_2^\circ + (^5D_2^\circ - {}^5S_2^\circ)$	141,798 cm^{-1}

The value of $^5D_2^\circ$ obtained through the $^5S^\circ$ series differs from the directly computed limit by 6,000 units. A discrepancy in the same sense and of about the same magnitude was found in Kr III[15], in which spectrum the other series limits were in good agreement.

The choice of 147,232 for the value of the term $5d^5D_2^\circ$ places $^5S_2^\circ$ at 137,613, which was arbitrarily given a whole-number value. All other terms were fixed by their experimentally known relative positions. The value of the lowest $s^2p^4\,^3P_2$ level was calculated through its ultraviolet combinations as 259,089 cm^{-1} giving an ionization potential of 32.0 volts for Xe^{++}. Tate and Smith[16] reported an experimental value of 32.2 ± 0.3 volt. Referring again to the peculiar behavior of the $^5S^\circ$ series, it may be noted that $6s^5S^\circ$ is located between $5d^3D_1^\circ$ and $^3D_3^\circ$ and that $^3D_2^\circ$ is lower. A perturbation of $^5S_2^\circ$ by $^3D_2^\circ$ may be responsible for this state of affairs. The $^3D^\circ$ term is somewhat irregular in all analogous spectra, usually being partially inverted. In Te I it overlaps $^5D^\circ$ and in I II it is lower.

The Moseley diagram for all the terms of the (^{4}S) family except $^3D^\circ$ is shown in figure 1. It is regular in every way. The curves are nearly straight lines, a fact which favors the choice of $^5D^\circ$ for the calculation of the absolute term values rather than $^5S^\circ$ since the latter choice would have increased the curvature. The slopes of the curves are seen to decrease with increasing total quantum number and those related to the same total quantum number are parallel. All this indicates that the terms of the (^{4}S) family are correctly interpreted in all of these iso-electronic spectra. Such a diagram could have been used to predict the terms in Xe III. This was not actually done, since the other evidence was sufficient.

6. DISCUSSION

In the spectra of all the doubly ionized rare gases a very intense multiplet array appears in the extreme ultraviolet owing to the combination of the lowest $s^2p^4\,^3P$ and ^1D terms with $sp^5\,^3P^\circ$ and $^1P^\circ$. The

[15] C. J. Humphreys, Phys. Rev. **47**, 712 (1835).
[16] J. T. Tate and P. T. Smith, Phys. Rev. **46**, 773 (1934).

discovery of this array immediately establishes the intervals between the low terms. When the ultraviolet data are combed with these intervals, the odd levels are found from the s^2p^35d and s^2p^36s configurations which combine not only with the low terms but with the even terms of the first excited states, that is those due to s^2p^36p. For this reason a complete set of data in both the extreme ultraviolet and ordinary optical regions is essential to a satisfactory analysis. In the work on this spectrum, Dr. Boyce had obtained the relative values of most of the odd levels. This was the starting point of the present analysis, which was carried forward by applying the "constant differences" of these odd levels to find the s^2p^36p terms. Complete quantum numbers have been assigned or suggested in all cases where the evidence appears sufficient.

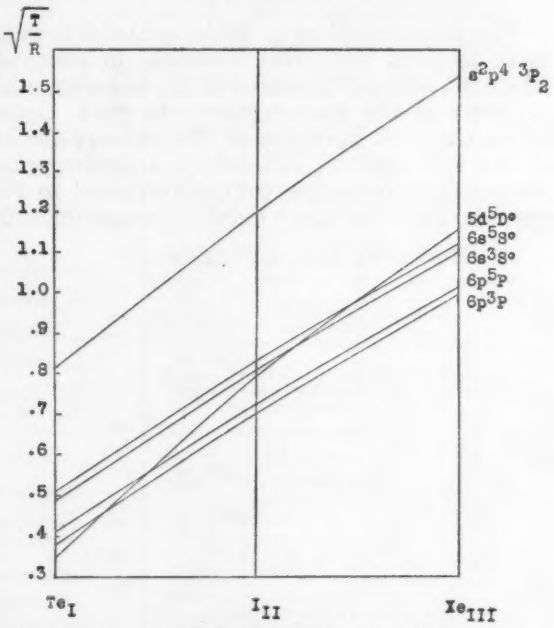

FIGURE 1.—*Moseley diagram for 52 electron-system spectra.*

The strongest multiplet of the (^{2}D) family is the combination $6s^3D^0-6p^3D$, which shows fairly regular intensities. The level designated $6p^3F_2$ behaves similarly to $^3D_2$ so that there is not much basis for a distinction. The designation $^1P_1$ is suggested for the term listed in the table as 4_1, mainly because of its location just above ^3D, where this term is found in analogous spectra, Se I and Kr III. Similarly the highest term in this group 87099.00 is called ^1D. It is similarly located in Se I, Kr III, and I III. There is additional evidence here from the combinations with (^{2}D)$6s^1D^\circ$ and (^{2}D)$5d^1D^\circ$. The levels designated 2_2 and 8_2 show identical combining properties and are evidently perturbing each other. Each combines with (^{2}D)$5d^1P_1^?$, but with no other levels of j-value less than 2. Three levels 6_3, 10_3, and (^{2}P)$6p^3D_3$ show almost identical combining properties but do not combine with levels having j less than three. On the basis of the electron configurations assumed, only one level of j value 4, (^{2}D)$6p^3F_4$, is predicted. We believe it to be missing since in similar spectra it shows only a few combinations, and there may not be enough combinations here to locate it by "constant differences." The interpretations $^1F_3$ and $^3F_3$ are suggested for 6_3 and 10_3, respectively, although it is doubtful if quantum numbers can be assigned unambiguously.

Among levels of the (^{2}P) family, the evidence for positive identifications is insufficient to justify anything more than the assignment of

j values except for the $(^2P)6s\,^3P^\circ$ and $^1P^\circ$ terms. $^3P^\circ$ is a regular term, occurs in the expected position, and gives strong combinations. The identification of $^1P^\circ$ is justified both by its combination with the low ^1D and ^1S terms and strong visible combinations. A few levels have been found which appear to be second series members of odd levels converging to (^2D).

Most of the intense lines of Xe III both classified and unclassified are in the region between 3500 and 4000 A. In the further study of this spectrum, Zeeman effect observations are desirable. It is hoped that such an analysis for both Xe II and Xe III can be undertaken in the near future.

The author wishes to make grateful acknowledgments to all who have assisted with this problem, in particular to Dr. William F. Meggers, who collaborated in the experimental work and in the measurement of the spectrograms; to Prof. George R. Harrison of the Massachusetts Institute of Technology for the use of the facilities of the spectroscopy laboratory, including the 35-ft grating and the wave-length recording comparator; and to Prof. J. C. Boyce, of the same institute for many helpful discussions and the use of his data.

WASHINGTON, March 25, 1936.

INDEX TO VOLUME 16

A

Page

Absorbancy measurements with a Duboscq colorimeter, RP878 349
Acid mixtures, pH curves, RP889 525
Acids, malonic, dissociation constants, RP895 575
Acree, S. F., J. O. Burton and, Calculation of the concentration and dissociation constant of each acid group in a mixture from the pH titration curve, RP889 525
——, *Walter J. Hamer, J. O. Burton and,* Dissociation constants of malonic acid in its sodium-salt solutions at 25° C from electrometric titration measurements, RP895 575
Aging of copper-beryllium alloys, RP890 529
Air permeability of cloth, RP862 139
Alkali degradation of wool protein, RP885 475
Alloys, copper-manganese-aluminum, electrical resistance, RP863 149
Alloys, electrical resistance properties, RP863 149
Alloys, ferrous, soil corrosion, RP883 431
Alloys, thermal expansion of copper-beryllium, RP890 529
Aluminum-manganese-copper alloys, electrical resistance, RP863 149
Antenna, broadcast, radio field-intensity records, RP874 289
Antimony, separation by distillation as chloride, RP871 253
Arabinose, thermal mutarotation, RP892 553
Arc spectrum of columbium, RP881 385
Arsenic, separation by distillation as chloride, RP871 253
Asphalt, accelerated weathering, RP886 481
Atmospheric-exposure tests of zinc and cadmium coatings, RP867 185

B

Barium-flint glasses, X-ray-protective properties, RP870 233
Bars, tool-resisting, magnetic testing, RP894 563
Bayonne Bridge, tests of steel columns for, RP897 627
Beryllium-copper alloys, thermal expansion, RP890 529
Bloom on surfaces, identification, RP879 359
Bluestone tanks, resistance to hypo solution, RP864 161
Blum, William and Abner Brenner, Mesle's chord method for measuring the thickness of metal coatings, RP866 171
——, *Paul W. C. Strausser, and Abner Brenner,* Corrosion-protective value of electrodeposited zinc and cadmium coatings on steel, RP867 185
Boric oxide, determination in glass, RP882 421
Boron in glass, determination, RP882 421
Brenner, Abner, Paul W. C. Strausser, William Blum and, Corrosion-protective value of electrodeposited zinc and cadmium coatings on steel, RP867 185
——, *William Blum and,* Mesle's chord method for measuring the thickness of metal coatings, RP866 171
Brewster, Joseph F., Simplified apparatus for technical sugar colorimetry, RP878 349
Bridge columns, strength tests {RP873 265 / RP897 627}
Broadcast antenna, distance characteristics, RP874 289
Buckling of steel bridge columns, RP897 627
Burton, J. O., and S. F. Acree, Calculation of the concentration and dissociation constant of each acid group in a mixture from the pH titration curve of the mixture, RP889 525

Page

Burton, J. O., Walter J. Hamer, and S. F. Acree, Dissociation constants of malonic acid in its sodium salt solutions at 25° C from electrometric titration measurements, RP895 575

C

Cadmium coatings, corrosion-protective value, RP867 185
Cadmium coatings, measurement of thickness, RP867 185
Calorimeter, heat of solution for cement, RP887 487
Capacitance measurement with Maxwell bridge, RP857 1
Carbon-manganese steel columns, strength tests {RP896 595 / RP897 627}
Cast iron, physical properties, RP880 367
Cast iron, soil corrosion, RP883 431
Cement, determination of silica, RP891 549
Cement, portland, determination of sulphate in, RP893 555
Cement, portland, magnesia in, RP884 467
Cements, effect of prehydration and curing temperatures, RP887 487
Cements, low-heat, properties and preparation, RP887 487
Cesium discharge, RP869 227
Chord column tests, RP897 627
Chord method for thickness measurements, RP866 171
Cleaves, Harold E., John G. Thompson and, A summary of information on the preparation and properties of pure iron, RP860 105
Cloth, cotton, properties {RP861 131 / RP862 139}
Coatings, metal, measurement of thickness, RP866 171
Coblentz, W. W., and R. Stair, A standard source of ultraviolet radiation for calibrating photoelectric dosage-intensity meters, RP858 83
——, *and R. Stair,* Evaluation of ultraviolet solar radiation of short wave lengths, RP877 315
Colorimetry, sugar, RP878 349
Columbium, arc and spark spectra, RP881 385
Columns, H-shaped steel, strength tests, RP896 595
Columns incased in concrete, strength tests, RP873 265
Columns, strength tests of steel, RP897 627
Comparator, alternating-current magnetic, RP804 563
Concrete, effect of prehydration of cement and curing temperatures, RP887 487
Concrete-incased steel columns, RP873 265
Copper-beryllium alloys, thermal expansion, RP890 529
Corrosion of underground structures, RP883 431
Corrosion, protective value of zinc and cadmium, RP867 185
Copper-manganese-aluminum alloys, electrical resistance, RP863 149
Cotton cloth, properties {RP861 131 / RP862 139}
Cover plates for bridge columns, RP897 627
Critical-frequency measurements of ionosphere during solar eclipse, RP868 213
Crowder, J. A., and Milton Harris, Mechanism of the sulfur lability in the alkali degradation of wool protein, RP885 475
Curtis, Harvey L., Charles Moon, and C. Matilda Sparks, An absolute determination of the ohm, RP857 1
Cystine in wool, effect of hydrogen peroxide, RP875 301

D

Deflection measurements of cast-iron test bars, RP880 — 367
d-Galactose, thermal mutarotation, RP892 — 553
Density, copper-beryllium alloys, RP890 — 529
Diffusing surfaces, reflectance measurements, RP872 — 261
Dissociation constants of acid mixtures, RP889 — 525
Distillation and separation of arsenic, antimony, and tin, RP871 — 253
Distinctness-of-image gloss, RP879 — 359
Dosage measurements, X-ray, RP865 — 165
d-Talose, thermal mutarotation, RP892 — 553

E

Eclipse, solar, ionosphere measurements during, RP868 — 213
Electrical-resistance alloys, properties, RP863 — 149
Electrical standards, international, RP857 — 1
Electrodeposition of zinc and cadmium on steel, RP867 — 185
Electrodeposits, measuring thickness, RP866 — 171
Expansion, thermal, copper-beryllium alloys, RP890 — 529

F

Fabric assistance, effect of number of yarns and yarn twist, RP861 — 131; RP862 — 139
Fading, radio, from broadcast antenna, RP874 — 289
Felt, asphalt-saturated, weathering, RP886 — 481
Felt roofing, weathering, RP888 — 511
Field-intensity records, radio, RP874 — 289
Filters, spectral, for measuring absorbancy in sugar solutions, RP878 — 349
Finn, A. N., Francis W. Glaze and, Routine determination of boron in glass, RP882 — 421
Flint glasses, X-ray-protective properties, RP870 — 233

G

Galactose, thermal mutarotation, RP892 — 553
Gases, rare, spectra of, RP898 — 639
Geib, Martin N. V., Charles G. Weber and, Treatment of offset papers for optimum register, RP859 — 93
Gibson, Kasson S., Deane B. Judd and, Note on the effect of a cover glass in reflectance measurements, RP872 — 261
Gilliland, Theodore R., Elbert B. Judson, Samuel S. Kirby and, Ionosphere studies during partial solar eclipse of February 3, 1935, RP868 — 213
Glass, cover, effect on reflectance measurements, RP872 — 261
Glass, determination of boron in, RP882 — 421
Glass photometric standards for sugar colorimetry, RP878 — 349
Glass, X-ray protective properties, RP870 — 233
Glaze, Francis W., and A. N. Finn, Routine determination of boron in glass, RP882 — 421
Gloss measurement, RP879 — 359
Grain boundaries in cast iron, RP880 — 367
Graphite, use in molding, RP880 — 367

H

Hamer, Walter J., S. F. Acree, J. O. Burton and, Dissociation constants of malonic acid in its sodium-salt solutions at 25° C from electrometric titration measurements, RP895 — 575
Hardness, copper-beryllium alloys, RP890 — 529
Harris, Milton, Arthur L. Smith and, Oxidation of wool: Effect of hydrogen peroxide on wool, RP875 — 301
——, *Arthur L. Smith and,* Oxidation of wool: The lead acetate test for hydrogen peroxide bleached wool, RP876 — 309
——, *J. A. Crowder and,* Mechanism of the sulfur lability in the alkali degradation of wool protein, RP885 — 475
Heating temperature of liquid cast iron, RP880 — 367
Heats of mutarotation, RP892 — 553
Hidnert, Peter, Thermal expansion of copper-beryllium alloys, RP890 — 529
Hornibrook, F. B., G. L. Kalousek, and C. H. Jumper, Effects of partial prehydration and different curing temperatures on some of the properties of cement and concrete, RP887 — 487
Humphreys, C. J., The third spectrum of xenon, RP898 — 639
Hunter, Richard S., Gloss investigations using reflected images of a target pattern, RP879 — 359
Hydrogen peroxide in wool, RP875 — 301; RP876 — 309
Hypo tanks, resistance to acid attacks, RP864 — 161

I

Immersion test of zinc and cadmium coatings, RP867 — 185
Incased columns, strength, RP873 — 265
Inductance, self-, absolute determination, RP857 — 1
Inductance, self-, construction, RP857 — 1
Inductance, self-, computed value, RP857 — 1
Inductance, self-, Maxwell-Wien bridge for measuring, RP857 — 1
Insley, Herbert and H. F. McMurdie, Studies of the quaternary system $CaO–MgO–2CaO.SiO_2–5CaO.3Al_2O_3$, RP884 — 467
Intensities, radio field, from broadcast antenna, RP874 — 289
Ionic strength of malonate salts, RP895 — 575
Ionization chamber, X-ray, RP865 — 165
Ionization constants of acid mixtures, RP889 — 525
Ionization constants of malonic acid, RP895 — 575
Ionization-density measurements during solar eclipse, RP868 — 213
Ionosphere measurements during solar eclipse, RP868 — 213
Iron, cast, transverse-strength test bars, RP880 — 367
Iron, pure, properties, RP860 — 105
Isbell, Horace S., and W. W. Pigman, Thermal mutarotation of *d*-galactose, *l*-arabinose, and *d*-talose, RP892 — 553

J

Judd, Deane B., and Kasson S. Gibson, Note on the effect of a cover glass in reflectance measurements, RP872 — 261
Judson, Elbert B., Theodore R. Gilliland, Samuel S. Kirby and, Ionosphere studies during partial solar eclipse of February 3, 1935, RP868 — 213
Jumper, C. H., G. L. Kalousek, F. B. Hornibrook and, Effects of partial prehydration and different curing temperatures on some of the properties of cement and concrete, RP887 — 487

K

Kalousek, G. L., C. H. Jumper, F. B. Hornibrook and, Effects of partial prehydration and different curing temperatures on some of the properties of cement and concrete, RP887 — 487
Kessler, Daniel W., Action of "hypo" solution on stone tanks, RP864 — 161
Kill van Kull Bridge, test of steel columns for, RP897 — 627
King, Arthur S., William F. Meggers and, Arc and spark spectra of columbium, RP881 — 385
Kirby, Samuel S., Radio field-intensity and distance characteristics of a high, vertical broadcast antenna, RP874 — 289
——, *Theodore R. Gilliland, and Elbert B. Judson,* Ionosphere studies during partial solar eclipse of February 3, 1935, RP868 — 213
Krynitsky, A. I., and C. M. Saeger, Jr., An improved method for preparing cast-iron transverse test bars, RP880 — 367

L

Page

l-Arabinose, thermal mutarotation, RP892... 553
Lead acetate test for bleached wool, RP876.. 309
Lead-barium glass, absorption of X-rays by, RP870... 233
Liquid-junction potentials of malonic acid and salts, RP895... 575
Lithography, offset, treatment of papers for, RP859... 93
Logan, K. H., Soil-corrosion studies, 1934. Rate of loss of weight and pitting of ferrous specimens, RP883... 431
Loom abrasion, effect on properties of cotton cloth, RP862... 139
Luster identification, RP879... 359

M

McMurdie, H. F., and Herbert Insley, Studies on the quaternary system CaO—MgO—$2CaO.SiO_2$—$5CaO.3Al_2O_3$, RP884... 467
Maczkowske, Edwin E., A rapid method for the determination of silica in portland cement, RP891... 549
Magnesia in portland cements, RP884... 467
Magnetic comparator, alternating-current, RP894... 563
Magnetic testing of tool-resisting prison bars, RP894... 563
Malonic acid, dissociation constants, RP895... 575
Manganese-copper-aluminum alloys, electrical resistance, RP863... 149
Meggers, William F., and Arthur S. King, Arc and spark spectra of columbium, RP881... 385
Melting of cast iron, RP880... 367
Mesle's chord method for measuring thickness of metal coatings, RP866... 171
Metallic coatings, measuring thickness, RP866... 171
Metallic coatings, zinc and cadmium, corrosion-protective value, RP867... 185
Meters, photoelectric dosage-intensity, RP858.. 83
Microstructure of cast iron, RP880... 367
Microstructure of copper-beryllium alloys, RP890... 529
Mohler, Fred L., Reversal temperature and population of excited states in the cesium discharge, RP869... 227
Molding materials, RP880... 367
Moon, Charles, C. Matilda Sparks, Harvey L. Curtis and, An absolute determination of the ohm, RP857... 1
Multiple reflection, RP872... 261

O

Offset papers, treatment and properties, RP859... 93
Offset printing, register, RP859... 93
Ohm, absolute determination, RP857... 1
Ohm, international vs. absolute, RP857... 1
Optical rotation of sugars, RP892... 553
Oxidation of wool {RP875... 301 / RP876... 309

P

Paper, offset, treatment and properties, RP859... 93
Parsons, Douglas E., Herbert L. Whittemore, Ambrose H. Stang and, Some tests of steel columns incased in concrete, RP873... 265
Permeability of cloth, RP862... 139
Phase equilibrium of CaO, MgO, Al_2O_3, SiO_2, RP884... 467
pH curves of acid mixtures, RP889... 525
Photoelectric dosage-intensity meter, RP858.. 83
Photographic tanks, resistance to hypo solution, RP864... 161
Photometric standards, glass, for sugar colorimetry, RP878... 349
Photometry of reflected light, effect of cover glass, RP872... 261
pH titration curves of malonic acid, RP895.. 575

Page

Pigman, W. W., Horace S. Isbell and, Thermal mutarotation of *d*-galactose, *l*-arabinose, and *d*-talose, RP892... 553
Plated coatings, measuring thickness, RP866.. 171
Porter, John W., Daniel H. Taft, Herbert F. Schiefer and, Effect of number of warp and filling yarns per inch and some other elements of construction on the properties of cloth, RP862... 139
Portland cement, determination of silica, RP891... 549
Portland cement, determination of sulphate, RP893... 555
Portland cement, magnesia in, RP884... 467
Preece test, application to electroplated zinc coatings, RP867... 185
Printing, offset, papers for, RP859... 93
Prison bars, tool-resisting, magnetic testing of, RP894... 563
Pouring temperature of cast iron, RP880... 367
Protective value of zinc and cadmium coatings, RP867... 185

Q

Quaternary system CaO—MgO—$2CaO.SiO_2$—$5CaO.3Al_2O_3$, RP884... 467

R

Radiation, solar, ultraviolet, RP877... 315
Radiation standards, RP858... 83
Radio field-intensity records, RP874... 289
Radio, ionosphere measurements, RP868... 213
Reflectance measurements, effect of a cover glass, RP872... 261
Register of offset prints, RP859... 93
Reinforced concrete, strength, RP873... 265
Resistance alloys, electrical, RP863... 149
Resistance, electrical, determination of, RP857... 1
Reversal temperature measurements of cesium discharge, RP869... 227
Riveted columns, strength, RP873... 265
Roofing, asphalt-prepared, weathering, RP886... 481
Roofing felts, weathering, RP888... 511
Rudy, Robert B., Determination of sulphuric anhydride in portland cement by means of the Wagner turbidimeter, RP893... 555

S

Saeger, C. M., Jr., A. I. Krynitzky and, An improved method for preparing cast-iron transverse test bars, RP880... 367
Salt-spray test of zinc and cadmium coatings, RP867... 185
Sanford, Raymond L., An alternating-current magnetic comparator, and the testing of tool-resisting prison bars, RP894... 563
Scherrer, John A., Distillation and separation of arsenic, antimony, and tin, RP871... 253
Schiefer, Herbert F., Daniel H. Taft, and John W. Porter, Effect of number of warp and filling yarns per inch and some other elements of construction on the properties of cloth, RP862... 139
——, *and Daniel H. Taft*, Effect of yarn twist on the properties of cloth, RP861... 131
Silica in cement, rapid method for determination, RP891... 549
Singer, George, Absorption of X-rays by lead glasses and lead-barium glasses, RP870... 233
——, *Lauriston S. Taylor and*, Note on the guarded-field X-ray ionization chamber, RP865... 165
Slate hypo tanks, resistance to hypo solutions, RP864... 161
Smith, Arthur L., and Milton Harris, Oxidation of wool: Effect of hydrogen peroxide on wool, RP875... 301
——, *and Milton Harris*, Oxidation of wool: The lead acetate test for hydrogen peroxide bleached wool, RP876... 309

Page

Snoke, H. R., O. G. Strieter and, A modified accelerated weathering test for asphalts and other materials, RP886 ... 481
Soapstone hypo tanks, resistance to hypo solutions, RP864 ... 161
Soils, corrosiveness, RP883 ... 431
Solar eclipse, ionosphere measurements during, RP868 ... 213
Solar radiation, evaluation of ultraviolet, RP877 ... 315
Solutions, hypo, destructive action on stone, RP864 ... 161
Sparks, C. Matilda, Charles Moon, Harvey L. Curtis and, An absolute determination of the ohm, RP857 ... 1
Spectra of columbium, RP881 ... 385
Spectra of rare gases, RP898 ... 639
Spectroscopic measurement of xenon, RP898 ... 639
Stabilization of copper-beryllium alloys, RP890 ... 529
Stair, R., W. W. Coblentz and, Evaluation of ultraviolet solar radiation of short wave lengths, RP877 ... 315
——, *W. W. Coblentz and,* A standard source of ultraviolet radiation for calibrating photoelectric dosage-intensity meters, RP858 ... 83
Standards, international electrical, RP857 ... 1
Standards, radiation, RP858 ... 83
Stang, Ambrose H., Herbert L. Whittemore, and Douglas E. Parsons, Some tests of steel columns incased in concrete, RP873 ... 265
——, *Herbert L. Whittemore, and Leroy R. Sweetman,* Tests of eight large H-shaped columns fabricated from carbon-manganese steel, RP896 ... 595
——, *Herbert L. Whittemore, and Leroy R. Sweetman,* Tests of steel chord members for the Bayonne Bridge, RP897 ... 627
Steel, columns, strength tests { RP873 ... 265; RP896 ... 595; RP897 ... 627
Steel, protection by zinc and cadmium, RP867 ... 185
Steel, soil corrosion, RP883 ... 431
Stone hypo tanks, resistance to hypo solutions, RP864 ... 161
Strain-gage readings on columns, RP896 ... 595
Strausser, Paul W. C., Abner Brenner, William Blum and, Corrosion-protective value of electrodeposited zinc and cadmium coatings on steel, RP867 ... 185
Strength of cloth { RP861 ... 131; RP862 ... 139
Strength of copper-beryllium alloys, RP890 ... 529
Stress distribution in steel columns, RP896 ... 595
Strieter, O. G., A study of the weathering quality of roofing felts made from various fibers, RP888 ... 511
——, *and H. R. Snoke,* A modified accelerated weathering test for asphalts and other materials, RP886 ... 481
Sugar solutions, light absorbancy, RP878 ... 349
Sugars, thermal mutarotations, RP892 ... 553
Sulfur in wool, RP885 ... 475
Sulphate, determination of, in cement, RP893 ... 555
Sulphuric anhydride, turbidimeter determination of, RP893 ... 555
Surface texture in glass studies, RP879 ... 359
Sweetman, Leroy R., Herbert L. Whittemore, Ambrose H. Stang and, Tests of steel chord columns for the Bayonne Bridge, RP897 ... 627
——, *Herbert L. Whittemore, Ambrose H. Stang and,* Tests of eight large H-shaped columns fabricated from carbon-manganese steel, RP896 ... 595

T

Taft, Daniel H., John W. Porter, Herbert F. Schiefer and, Effect of number of warp and filling yarns per inch and some other elements of construction on the properties of cloth, RP862 ... 139
——, *Herbert F. Schiefer and,* effect of yarn twist on the properties of cloth, RP861 ... 131
Talose, thermal mutarotation, RP892 ... 553
Tanks, stone, resistance to hypo solutions, RP864 ... 161
Taylor, Lauriston S., and George Singer, Note on the guarded-field X-ray ionization chamber, RP865 ... 165
Telemeters for measuring stresses in columns, RP873 ... 265
Temperature measurements during aging of concrete, RP873 ... 265
Temperature, pouring, of cast iron, RP880 ... 367
Textiles, cotton, RP861 ... 131
Textiles, wool, oxidation of { RP875 ... 301; RP876 ... 309; RP885 ... 475
Thermal expansion, copper-beryllium alloys, RP890 ... 529
Thermal mutarotation of *d*-galactose, l-arabinose, and *d*-talose, RP892 ... 553
Thickness, measurements of metal coatings, RP866 ... 171
Thomas, James L., Electrical-resistance alloys of copper, manganese, and aluminum, RP863 ... 149
Thompson, John G., and Harold E. Cleaves, A summary of information on the preparation and properties of pure iron, RP860 ... 105
Tin, separation by distillation as chloride, RP871 ... 233
Turbidimeter, use in sulphate determination, RP893 ... 555
Twist of yarn, effect on properties of cotton cloth { RP861 ... 131; RP862 ... 139

U

Ultraviolet radiation, evaluation for use in medicine, RP877 ... 315
Ultraviolet radiation standard, RP858 ... 83

W

Wagner turbidimeter, use in sulphate determination, RP893 ... 555
Wave lengths of xenon spectra, RP898 ... 639
Weathering of roofing felts, RP888 ... 511
Weathering test for asphalts and other materials, RP886 ... 481
Weave, effect on properties of cloth { RP861 ... 131; RP862 ... 139
Weber, Charles G., and Martin N. V. Geib, Treatment of offset papers for optimum register, RP859 ... 93
Whittemore, Herbert L., Leroy R. Sweetman, Ambrose H. Stang and, Tests of eight large H-shaped columns fabricated from carbon-manganese steel, RP896 ... 595
——, *Leroy R. Sweetman, Ambrose H. Stang and,* Tests of steel chord members for the Bayonne Bridge, RP897 ... 627
——, *Ambrose H. Stang, Douglas E. Parsons and,* Some tests of steel columns incased in concrete, RP873 ... 265
Wool, bleached, lead acetate test, RP876 ... 309
Wool, effect of hydrogen peroxide, RP875 ... 301
Wool protein, alkali degradation, RP885 ... 475
Wrought iron, soil corrosion, RP883 ... 431

X

Xenon spectrum, RP898 ... 639
X-ray dosage measurements, RP865 ... 165
X-ray protective glass, properties, RP870 ... 233

Y

Yarns, effect of number and twist on properties of cotton cloth { RP861 ... 131; RP862 ... 139
Yield strength of steel bridge columns, RP897 ... 627

Z

Zinc coatings, corrosion-protective value, RP867 ... 185
Zinc coatings, measurement of thickness, RP867 ... 185